

NITROGEN GLASSES

A thesis submitted for the degree of
Doctor of Philosophy
of the University of Newcastle upon Tyne

by

Robin Anthony Lynton Drew

The Crystallography Laboratory,
Department of Metallurgy and Engineering Materials
University of Newcastle upon Tyne

September, 1980

To Amanda, for her patience
and endurance.

Contents

	Page
Preface	ii
Acknowledgements	iii
Abstract	iv
Chapter I	<u>Introduction</u>
I.1	Engineering ceramics
I.2	Nitrogen ceramics
Chapter II	<u>Glasses, Silicates and Nitrogen Ceramics</u>
II.1	Introduction
II.2	Glass formation from liquids
II.3	The structure of silicates and aluminosilicates
II.4	Relationship between silicates, aluminosilicates and nitrogen ceramics
Chapter III	<u>Previous Investigations</u>
III.1	Introduction
III.2	The Si-Al-O-N and related systems
III.3	Mg-Si-O-N and Mg-Si-Al-O-N glasses
III.4	Y-Si-Al-O-N glasses
III.5	Other nitrogen glass systems
III.6	Solubility of nitrogen in silicate glasses
III.7	Representation of the Si-Al-O-N system
III.8	M-Si-Al-O-N systems
Chapter IV	<u>Scope of the Present Investigation</u>

		Page
Chapter V	<u>Experimental Methods</u>	27
V.1	Materials specifications	27
V.2	Powder mixing	27
V.3	High-temperature fusion methods	29
V.4	Heat-treatment	33
V.5	X-ray methods	33
V.6	Measurement of glass transition and crystallization temperatures	33
V.7	Viscosity measurement	35
V.8	Refractive index measurement	38
V.9	Microscopy	39
Chapter VI	<u>Nitrogen Glass Formation</u>	41
VI.1	Introduction	41
VI.2	The Mg-Si-Al-O-N system	41
VI.3	The Mg-Si-O-N system	46
VI.4	The Y-Si-Al-O-N system	47
VI.5	The Si-Al-O-N system	50
VI.6	Other glass-forming systems	51
VI.7	Conclusions	53
Chapter VII	<u>Properties of Nitrogen Glasses</u>	54
VII.1	Introduction	54
VII.2	Viscosity	55
VII.3	Crystallization temperature	57
VII.4	Optical properties	61
VII.4.1	Introduction	61
VII.4.2	Infra-red and ultra-violet transmission	62
VII.4.3	Refractive index	63
VII.5	Conclusions	65
Chapter VIII	<u>Devitrification</u>	67
VIII.1	Devitrification of nitrogen glasses	67

		Page
VIII.1.1	Introduction	67
VIII.1.2	Mg-Si-Al-O-N glasses	67
VIII.1.3	Y-Si-Al-O-N glasses	70
VIII.1.4	Ca-Si-Al-O-N glasses	71
VIII.2	Devitrification of vitreous phases present in sintered nitrogen ceramics	72
VIII.2.1	Introduction	72
VIII.2.2	Results of heat-treatments	74
VIII.2.3	Discussion	79
Chapter IX	<u>β''-Magnesium Sialon</u>	81
IX.1	Introduction	81
IX.2	Exploration of the 3M:4X plane close to forsterite	83
IX.3	X-ray and microscopical examination of β''	85
IX.4	Discussion	87
Chapter X	<u>Conclusions and Suggestions for Future Work</u>	92
Appendix	<u>The Dielectric Properties of Selected Nitrogen Glasses</u>	94
	<u>References</u>	99

Preface

This thesis describes original work which has not been submitted for a degree at any other University.

The investigations were carried out in the Crystallography Laboratory, Department of Metallurgy and Engineering Materials at the University of Newcastle upon Tyne during the period October 1977 to September 1980 under the supervision of Professor K.H. Jack.

The thesis describes the investigation of nitrogen glasses occurring in various M-Si-O-N and M-Si-Al-O-N systems. The limits of glass formation are discussed and the changes in physical properties on replacement of oxygen by nitrogen are reported. A new crystalline phase in the Mg-Si-Al-O-N system has been identified as the product of devitrification of a magnesium sialon glass.

Acknowledgements

I wish to thank Professor K.H. Jack for his advice, encouragement and interest during the supervision of this work.

My gratitude is expressed to Dr. S. Hampshire and Dr. D.P. Thompson for their help and invaluable discussions over the past three years.

I also thank:

The Science Research Council and Thermal Syndicate Limited for the award of a CASE studentship;

Mr. J.A. Winterburn and Mr. J. Allen for their help and advice during the period spent at Thermal Syndicate Limited;

Dr. M.H. Battey for his assistance in the measurement of refractive index;

The technical staff of this laboratory;

Many colleagues, past and present, in the Crystallography Laboratory for stimulating discussion and advice and for permission to use their results;

Mrs. A. Rule for typing the script.

Abstract

Nitrogen glasses are prepared in various M-Si-O-N and M-Si-Al-O-N systems (M = Mg, Y, Ca & Nd) by fusing the appropriate metal oxide powders with SiO_2 , Al_2O_3 , Si_3N_4 and AlN at $1600^\circ\text{-}1700^\circ\text{C}$ under a nitrogen atmosphere. The limits of glass formation in some of the nitrogen-containing systems are investigated and properties of the glasses are evaluated.

Nitrogen is incorporated in M-Si-Al-O-N glasses up to 10-12.5 a/o, the highest being in the Y-Si-Al-O-N system. The nitrogen glass-forming regions are extensions of their appropriate M-Si-Al-O-N vitreous regions. Small homogeneous glass regions also form in some M-Si-O-N systems.

Property measurements on both oxide and nitrogen glasses of the same cation composition show that viscosity, refractive index, dielectric constant, and a.c. conductivity all increase with nitrogen incorporation these changes being due to the increased strength, directional character and polarisability of the nitrogen bond compared with oxygen in the glass

network.

Grain-boundary vitreous phases, previously considered to be oxides, occurring in densified silicon nitride and β' -sialons have compositions within the nitrogen glass regions of their appropriate M-Si-O-N or M-Si-Al-O-N systems (where M = Mg or Y), and are therefore shown to be oxynitrides.

A new Mg-Si-Al-O-N phase β'' -magnesium sialon, isostructural with β -Si₃N₄ and with a range of compositions near Mg₂₁Si₁₈Al₃O₄₈N₁₀, is obtained by devitrification of Mg-Si-Al-O-N glasses with a metal:non-metal atom ratio 3M:4X in the presence of undissolved β -Si₃N₄.

I. Introduction

I.1 Engineering ceramics

Over the past twenty years research has been increasingly directed to the production of new engineering materials for a wide variety of applications in the nuclear and aerospace industries and towards energy conservation. Considerable interest has been shown in ceramics for components of gas-turbine engines where their use is expected to increase the operating temperature from 1100°C to 1400°C , thereby achieving higher fuel efficiency and less environmental pollution. An engineering ceramic to withstand such temperatures must combine high strength, oxidation resistance, negligible creep, good thermal shock properties and resistance to corrosive environments.

The useful strength of a material is the stress that it can withstand at small strains usually less than 0.1%. Hence the requirement for a strong ceramic is a high elastic modulus, E . Better still is a high value of elastic modulus divided by specific gravity (the specific modulus), that is a high modulus to weight ratio. Table I.1 lists some high specific modulus materials. High elastic modulus and low density imply that the interatomic bond strength must be high, and that the

Table I.1

Some high specific modulus materials

material	specific modulus 10^4 MNm^{-2}	melting or decomposition temperature $^{\circ}\text{C}$
Si_3N_4	12	1900
SiC	17	2600
Al_2O_3	9	2050
AlN	10	2450
BeO	12	2530
BN	5	2700
C fibre	42	3500
steel		
glass	3	-
wood		
aluminium		

atomic weights and coordination numbers are small, both of which are satisfied by covalent bonding. High decomposition temperatures are also a result of high bond strength.

Of the materials listed, AlN hydrolyses easily, Al_2O_3 has poor thermal shock properties, BeO is toxic, C is readily oxidised and BN is difficult to fabricate. This leaves Si_3N_4 and SiC as leading contenders for high temperature applications and both belong to a group of materials known as "Special Ceramics".

I.2 Nitrogen ceramics

Silicon nitride has been the subject of intensive research since its high strength, wear resistance, high decomposition temperature, oxidation resistance, low coefficient of friction, resistance to corrosive environments and excellent thermal shock properties suggest it should be an ideal high temperature ceramic. However, because silicon nitride is covalently-bonded it has a low self-diffusivity which makes it difficult to sinter to maximum density by firing. Three methods of shaping are employed namely reaction-bonding, hot-pressing and pressureless-sintering.

In reaction bonding the required shape is first

made from compacted silicon powder which is then nitrided at 1400°C , with negligible change in dimensions, to give a product with about 25% porosity. The high porosity has a deleterious effect on oxidation resistance and strength.

Hot-pressing of silicon nitride powder with small amounts (1-2 w/o) of additives such as magnesia, yttria, ceria or zirconia can achieve a fully dense product with high strengths up to 1000°C .

Pressureless-sintered silicon nitride with less than 5 v/o porosity is obtained by using larger amounts of oxide additives (5-10 w/o).

The densification of silicon nitride by either hot-pressing or pressureless-sintering with an oxide additive provides conditions for liquid-phase sintering by solution of $\alpha\text{-Si}_3\text{N}_4$ and reprecipitation of β (Rae et al., 1977). Magnesia, the first widely used additive, reacts with the surface layer of silica that is always present on the nitride to give what was at first thought (Wild et al., 1972a) to be a silicate liquid which cools to give a low softening-temperature glass. The grain-boundary vitreous phase causes the creep resistance of the high-density product to decrease rapidly above 1000°C . It is now well-established that

the liquid phase and the glass that forms from it are oxynitrides (Terwilliger & Lange, 1974; Drew & Lewis, 1974; Jack, 1974).

The Y-Si-O-N liquid formed when hot-pressing silicon nitride with yttria then reacts with more nitride to give highly refractory quaternary oxynitride phases and leads to improved high temperature properties (Gazza, 1975). Impurities are accommodated in the crystalline Y-Si-O-N phases and only a small amount of liquid remains to form a glass (Rae et al., 1975).

It has been argued (Jack, 1974) that densification of even "pure" silicon nitride either with or without an additive can never give a homogeneous, single-phase product because of the silica present on the powder particles. Second phase crystalline inclusions will act as stress-raisers or will initiate cracks because of their differential thermal expansion relative to the matrix while grain-boundary vitreous phases will impair creep resistance.

The field of nitrogen ceramics was further extended by the concurrent discovery in Britain and Japan (Jack & Wilson, 1972; Oyama & Kamigaito, 1971) that it was possible to replace silicon by aluminium and nitrogen by oxygen in silicon nitride without

changing the structure. Silicon nitride is merely the first of what is now known to be a very wide field of nitrogen ceramics formed by "alloying" silicon nitride with alumina and other metal oxides and nitrides. The acronym "sialon" given to phases in the Si-Al-O-N and related systems (Jack, 1973) has become a generic term for materials, vitreous as well as crystalline, that are essentially alumino-silicates in which oxygen is partially or completely replaced by nitrogen.

Bulk nitrogen glasses have been prepared in the Mg-Si-O-N and also the yttrium and magnesium sialon systems (Jack, 1977a). It is clear that these glasses are important because the high temperature strength and creep-resistance of nitrogen ceramics depend markedly on the amount and characteristics of the grain-boundary glass. Nitrogen glasses may also be important in their own right since small concentrations of nitrogen in oxide glasses are reported (Elmer & Nordberg, 1967) to increase their viscosity and resistance to devitrification.

II. Glasses, Silicates and Nitrogen Ceramics

II.1 Introduction

Glass is an amorphous solid and so possesses no long-range order. X-ray diffraction measurements show that glasses are structurally more closely related to liquids than to crystalline solids. They are usually products of fusion formed by continuous cooling of a liquid to a rigid state without the occurrence of crystallization. There are, however, many other techniques for glass formation which do not involve a liquid and so the above statement cannot be taken as a rigid definition of a glass.

The most commercially important group of glass-forming materials are those based on silica and they are the silicates, alumino-silicates and boro-silicates.

II.2 Glass formation from liquids

The tendency to form a glass is determined by the rates of nucleation and growth of crystals from the liquid. Under most circumstances the rate of crystallization of many glass-forming materials is too high for vitrification to occur, with the exception of

silica. The crystallization velocity is reduced drastically when the viscosity of a liquid is high, since structural rearrangement is suppressed. Therefore a material with high viscosity near its melting point is more likely to form a glass.

Bulk crystallization must be preceded by nucleation and the majority of liquids only require a limited amount of supercooling before "critical" nuclei are formed. In viscous liquids the nucleation rate can be reduced by the slow structural mobility and is found to be inversely proportional to the viscosity of the liquid. It is usually found that nucleation rates are more important than crystallization rates in determining whether a liquid will vitrify or not, and if nucleation does not occur when a liquid is cooled it will fail to crystallize and, instead, become a rigid, amorphous solid or glass.

II.3 The structure of silicates and alumino-silicates

In crystalline silicates there is four-fold coordination of oxygen around each silicon and the silicon-oxygen tetrahedron, $[\text{SiO}_4]^{4-}$ is the building unit for all silicate structures. The tetrahedra are joined together by common corners and occur as isolated single units or pairs or may be built

up to form rings, chains, sheets or three-dimensional networks.

The structure of vitreous silica, as proposed by Zachariasen (1932), is a three-dimensional network where each tetrahedron is joined at its vertices to four others but in such a way that the structure is a random network and lacks any long range periodicity. Warren & Bischoe (1938) and Mozzi & Warren (1969) showed that X-ray diffraction data were consistent with the random-network model of Zachariasen. There is a great deal of argument about the structure of vitreous silica and silicates but the random-network model is still widely accepted as the best description of oxide glass structure.

The addition of other oxides, for example of the alkali or alkaline-earth elements (M_2O or MO), to vitreous silica causes the three-dimensional network to break up and results in a reduction of the viscosity because Si-O-Si bonds are broken. Oxides of this type are called "modifiers" and as long as the ratio of M_2O or MO units to the number of SiO_2 units does not exceed one to one then the silicon-oxygen network is preserved because each silicon-oxygen tetrahedron is linked to at least three other tetrahedra and glass formation can still occur. The cation is accommodated in the interstices of the network and thus enables the

charge balance to be maintained. Structurally, silicate glasses are very similar to their crystalline counterparts with the exception that they lack periodicity and are amorphous to X-rays.

Some oxides of the M_2O_3 type, such as alumina, are called "intermediate" oxides because they are neither glass-formers nor modifiers. The aluminium atom may be either four or six coordinated with oxygen giving rise to tetrahedral $[AlO_4]^{5-}$ or octahedral $[AlO_6]^{9-}$ groups. The $[AlO_4]^{5-}$ unit is similar in size to the $[SiO_4]^{4-}$ tetrahedron and therefore can be accommodated in the silicate network provided the necessary charge compensation is made elsewhere in the structure to ensure electroneutrality. The similarity with aluminosilicate minerals can be clearly seen since they are also built up from $[SiO_4]^{4-}$ and $[AlO_4]^{5-}$ tetrahedra.

The addition of alumina to silicate glasses has a fourfold effect:

- (a) increases refractoriness;
- (b) reduces the tendency to crystallize;
- (c) increases the range of glass formation and reduces immiscibility;
- (d) increases chemical resistance and weathering.

II.4 Relationship between silicates, alumino-silicates and nitrogen ceramics

Silicon nitride occurs in two structural modifications (α and β) both of which are built up of SiN_4 tetrahedra. The atomic arrangement of

β - Si_3N_4 is the same as phenacite (Be_2SiO_4) (Hardie & Jack, 1957), whereas α - Si_3N_4 is an alternative way of joining SiN_4 tetrahedra and has approximately twice the cell volume of β . (See Figures II.1(a) & (b)).

α - Si_3N_4 is a defect structure and up to one in thirty nitrogen atoms are replaced by oxygen (Wild et al., 1972b; Hampshire, 1980), whereas β is the stoichiometric form (Si_3N_4).

The similarity between the building units of both silicates and nitrogen ceramics is clearly seen and because of this it was predicted (Wild et al., 1968) that SiN_4 might be replaced by AlO_4 to give a new and wide range of materials both vitreous and crystalline based on the $(\text{Si,Al})(\text{O,N})_4$ tetrahedral building unit.

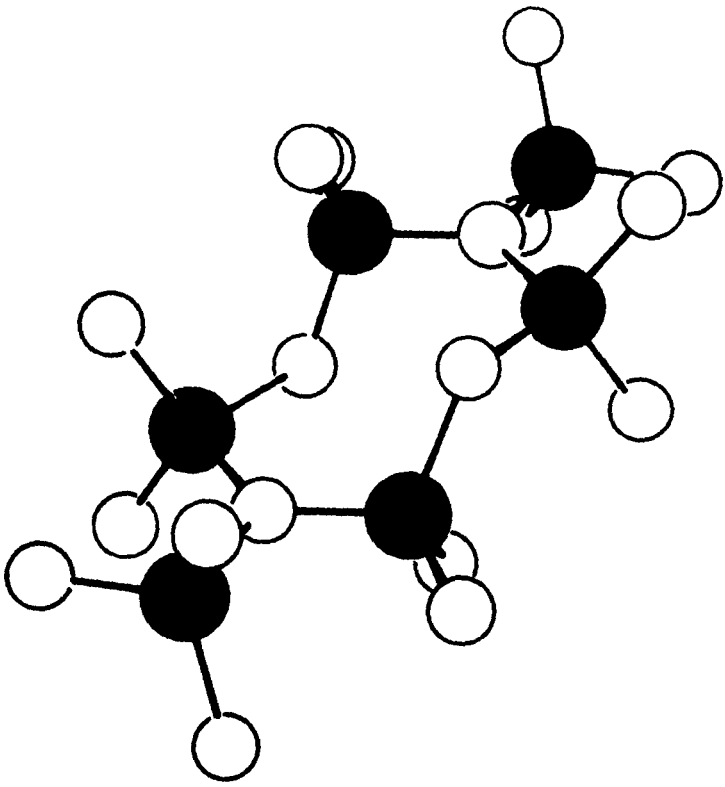
The sialons are essentially alumino-silicates in which oxygen is replaced by nitrogen and if any charge compensation is necessary then other cations are introduced to maintain electroneutrality. The "sialon" tetrahedra can be joined together as networks, sheets, chains or isolated units and are structurally analogous

Figure II.1 The crystal structure of:

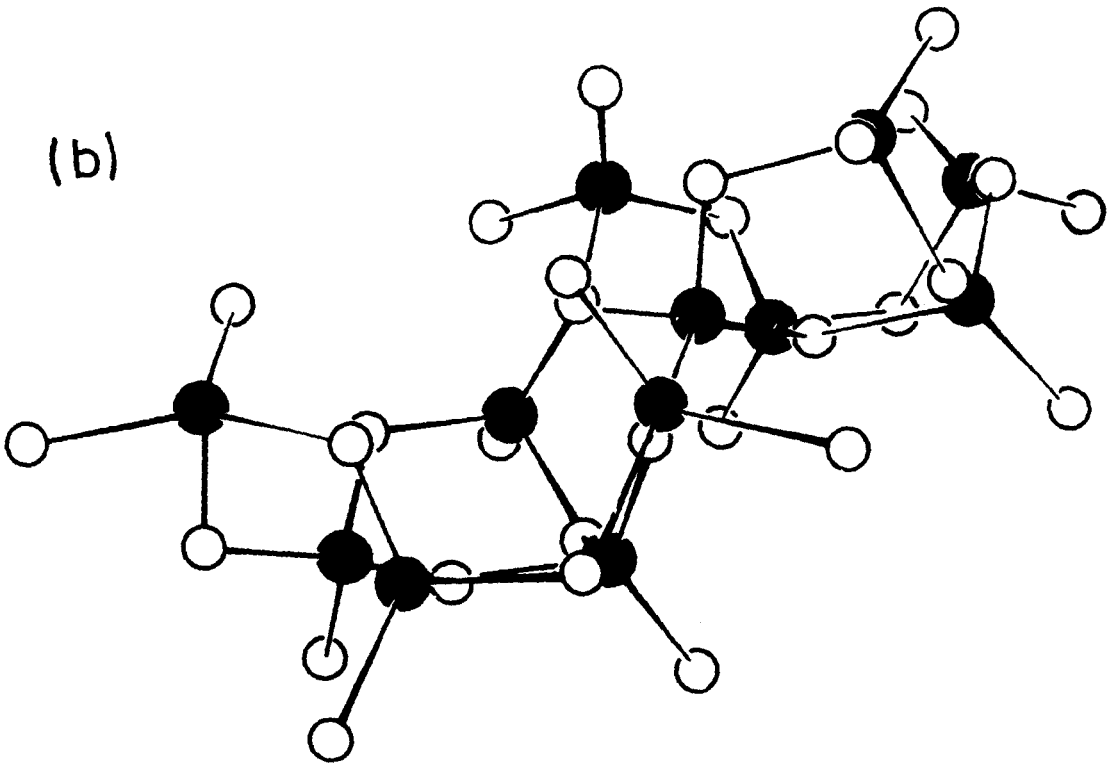
(a) β -silicon nitride, Si_6N_8

(b) α -silicon nitride, $\text{Si}_{12}\text{N}_{16}$

(a)



(b)



to silicates. Other cation additions can either be incorporated in the structural units or become interstitial. Their introduction provides a further degree of freedom and therefore greater structural and chemical diversity. The five-component metal-sialons can also be viewed as metal alumino-silicates where oxygen is replaced by nitrogen. Glass formation occurs in a large number of these ternary oxide systems and it has already been established that some nitrogen can be incorporated in these glasses (Jack, 1977a).

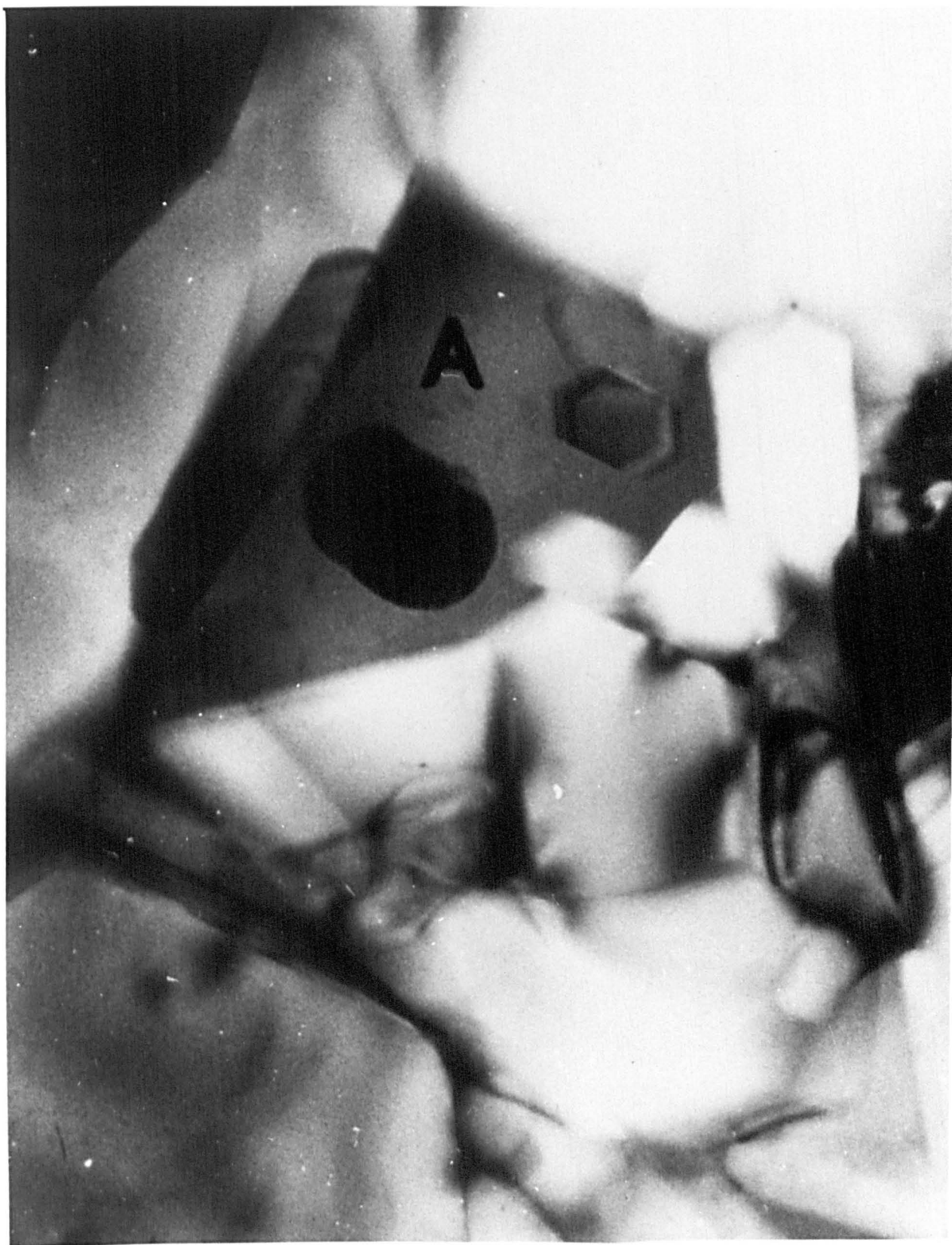
III. Previous Investigations

III.1 Introduction

Silicon nitride was first hot-pressed with 5 w/o MgO to near theoretical density by Deeley et al. (1961). Wild et al. (1972a) studied the role of the MgO and showed that it reacts with the silica that is always present on the surface of the silicon nitride powder particles to give a liquid near the MgSiO_3 - SiO_2 eutectic composition. This cools to give a relatively low softening temperature grain-boundary glass which impairs the strength and creep resistance above 1000°C . Heat-treatment at 1350°C devitrified the glass to give enstatite (MgSiO_3) and silicon oxynitride ($\text{Si}_2\text{N}_2\text{O}$) and so the glass must have contained nitrogen. It was established that the liquid aids densification by liquid-phase sintering and promotes transformation of α to β .

Transmission electron-microscopy of similar material (Nuttall & Thompson, 1974) indicated areas at the junction of silicon nitride grains which showed no diffraction contrast and therefore were amorphous. Some areas even showed hexagonal crystals of β - Si_3N_4 which had grown from the liquid (see Figure III.1).

Figure III.1 Transmission electron-micrograph of Si_3N_4 hot-pressed with MgO showing amorphous region (A) from which has grown a hexagonal β - Si_3N_4 crystal.



Gazza (1975) found that Y_2O_3 produced a dense silicon nitride with good high-temperature properties and attributed this to the formation of refractory grain-boundary phases. Rae et al. (1977) showed that the Y_2O_3 reacts with the surface silica and some nitride to give a liquid which allows densification and transformation from α to β . As the reaction proceeds, the liquid combines with more Si_3N_4 to give one or more quaternary yttrium-silicon oxynitride phases which can accommodate the impurities that would otherwise form a glass on cooling and degrade properties. Some unreacted liquid cools to give a glass but this can be devitrified by suitable heat-treatment thus improving the high-temperature strength. However, the hot-pressed material fails catastrophically at $900^\circ-1200^\circ C$ in an oxidising environment this being due to the oxidation of the grain-boundary Y-Si-O-N phases to give oxides with markedly different specific volumes to that of the starting material.

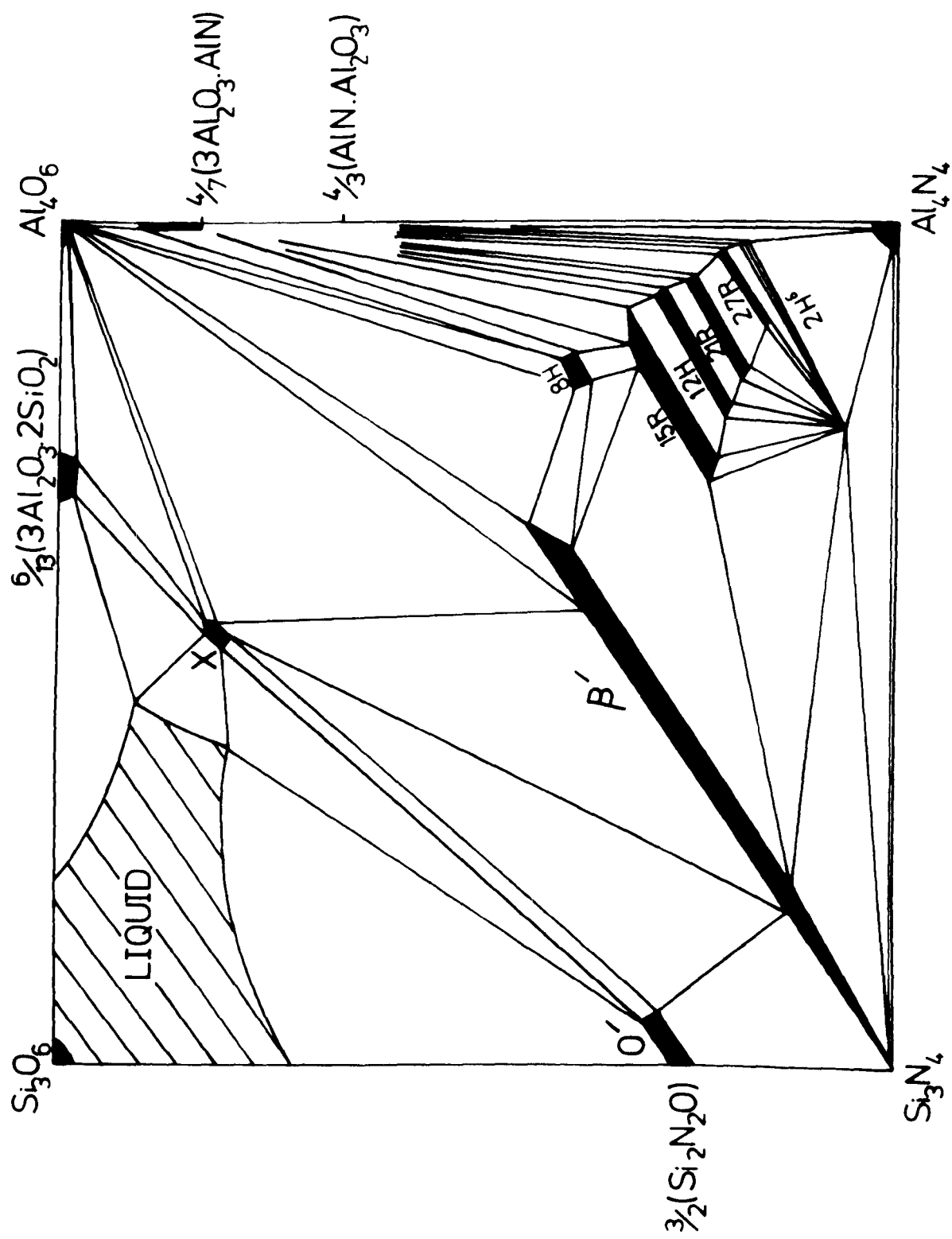
A number of other additives have been explored and include CeO_2 , ZrO_2 , Sc_2O_3 and BeO . The first three of these have been shown to have as good if not superior properties to both Y_2O_3 and MgO (Buang, 1979; Dodsworth, 1980).

III.2 The Si-Al-O-N and related systems

Jack & Wilson (1972) and Oyama & Kamagaito (1971) reacted Si_3N_4 with Al_2O_3 and obtained new materials isostructural with β - Si_3N_4 , and therefore named β' -sialons, but with expanded unit-cell dimensions and containing up to 65 w/o Al_2O_3 . Lumby et al. (1975), Gauckler et al. (1975) and Jack (1976) later showed that the β' phase has a range of homogeneity along the Si_3N_4 - Al_2O_3 -AlN join, and maintains a metal:non-metal ratio of 3:4 according to the formula $\text{Si}_{6-z}\text{Al}_z\text{O}_z\text{N}_{8-z}$ where $0 < z < 4.2$ at 1750°C .

The behaviour diagram of the Si-Al-O-N system is shown in Figure III.2 (Roebuck, 1978). As well as β' -sialon a number of other phases have been observed: X-phase (Jack & Wilson, 1972), which exists in "High-X" and "Low-X" modifications - both with triclinic unit-cells (Jack, 1977b); O' which is $\text{Si}_2\text{N}_2\text{O}$ with partial replacement of Si and N by Al and O (Jack, 1973); and six other phases with ranges of homogeneity extending along lines of constant M:X ratio between β' and AlN (Gauckler et al., 1975). The latter have been fully characterized as a new kind of polytypes related to the wurtzite structure of AlN (Thompson, 1977; Roebuck & Thompson, 1977). The structures are directly related to their compositions M_mX_{m+1} and are described by the Ramsdell symbols

Figure III.2 The Si-Al-O-N behaviour diagram at 1700°C
(after Roebuck, 1978).



8H, 15R, 12H, 21R, 27R and 2H \bar{O} .

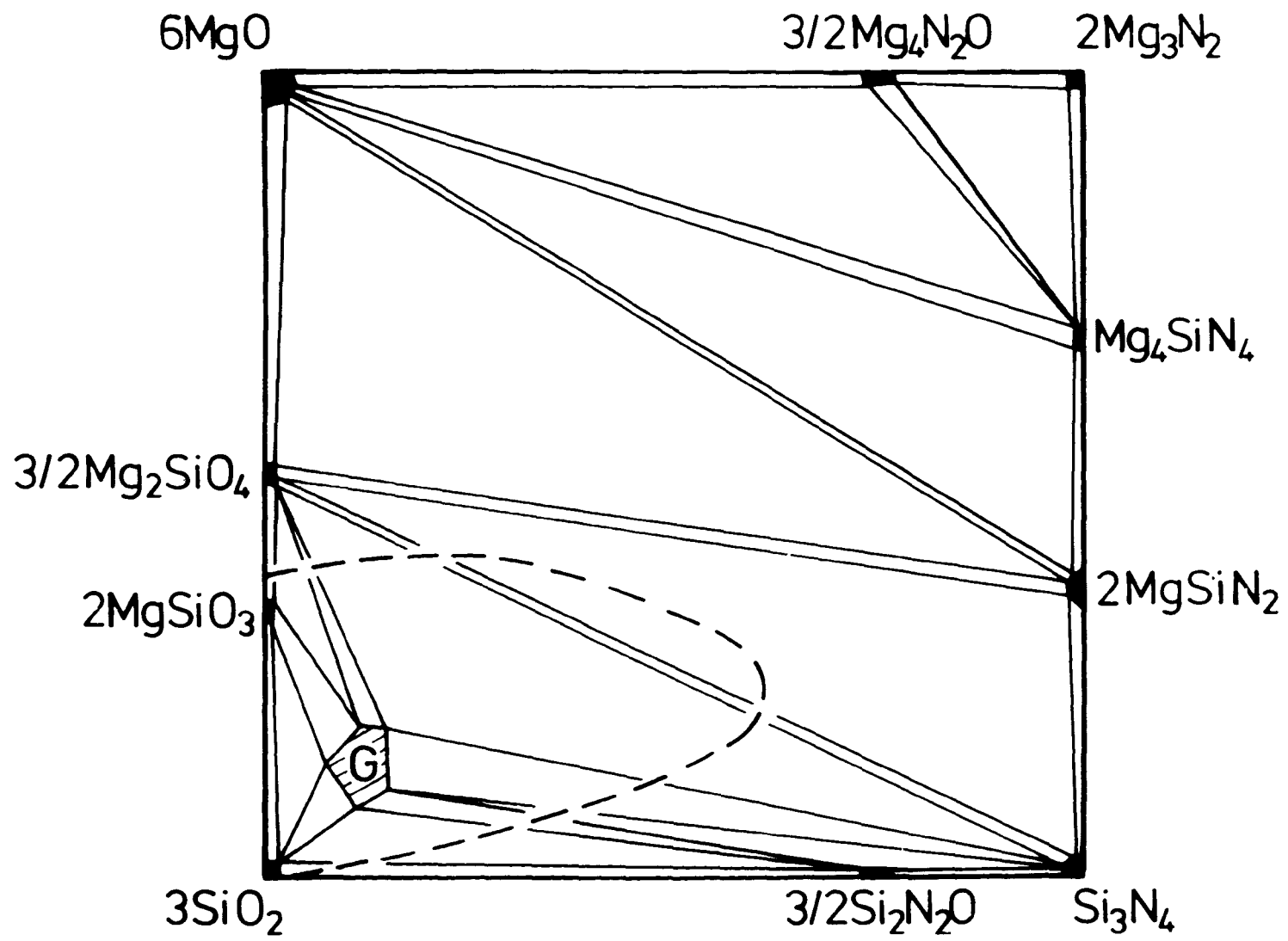
It has been shown that other metals such as Mg, Be and Li can be incorporated in most of the phases of the Si-Al-O-N system with homogeneities extending along appropriate planes of constant M:X ratio in each M-Si-Al-O-N system.

Liquid regions occur in the M-Si-O-N, Si-Al-O-N and more especially the M-Si-Al-O-N systems. It is now well-established that both Si₃N₄ and β' -sialons require an oxide additive for liquid phase densification (Drew & Lewis, 1974; Lewis et al., 1977; Rae et al., 1977). The silicate liquid dissolves some nitrogen and on cooling invariably forms a grain-boundary glass, sometimes in conjunction with other oxynitride or sialon phases. The softening of the glassy-phase above about 1000°C is a major reason for the deterioration in the high-temperature properties of nitrogen ceramics.

III.3 Mg-Si-O-N and Mg-Si-Al-O-N glasses

Perera (1976) observed a large liquid region at 1700°C in the Mg-Si-O-N system (Figure III.3) which also extends into the Mg-Si-Al-O-N system and joins up with the Mg-Si-Al-O liquid region where eutectics occur at 1355°C and 1365°C. The small Mg-Si-O-N

Figure III.3 Mg-Si-O-N behaviour diagram showing the liquid and glass region at 1700°C (after Perera, 1976).



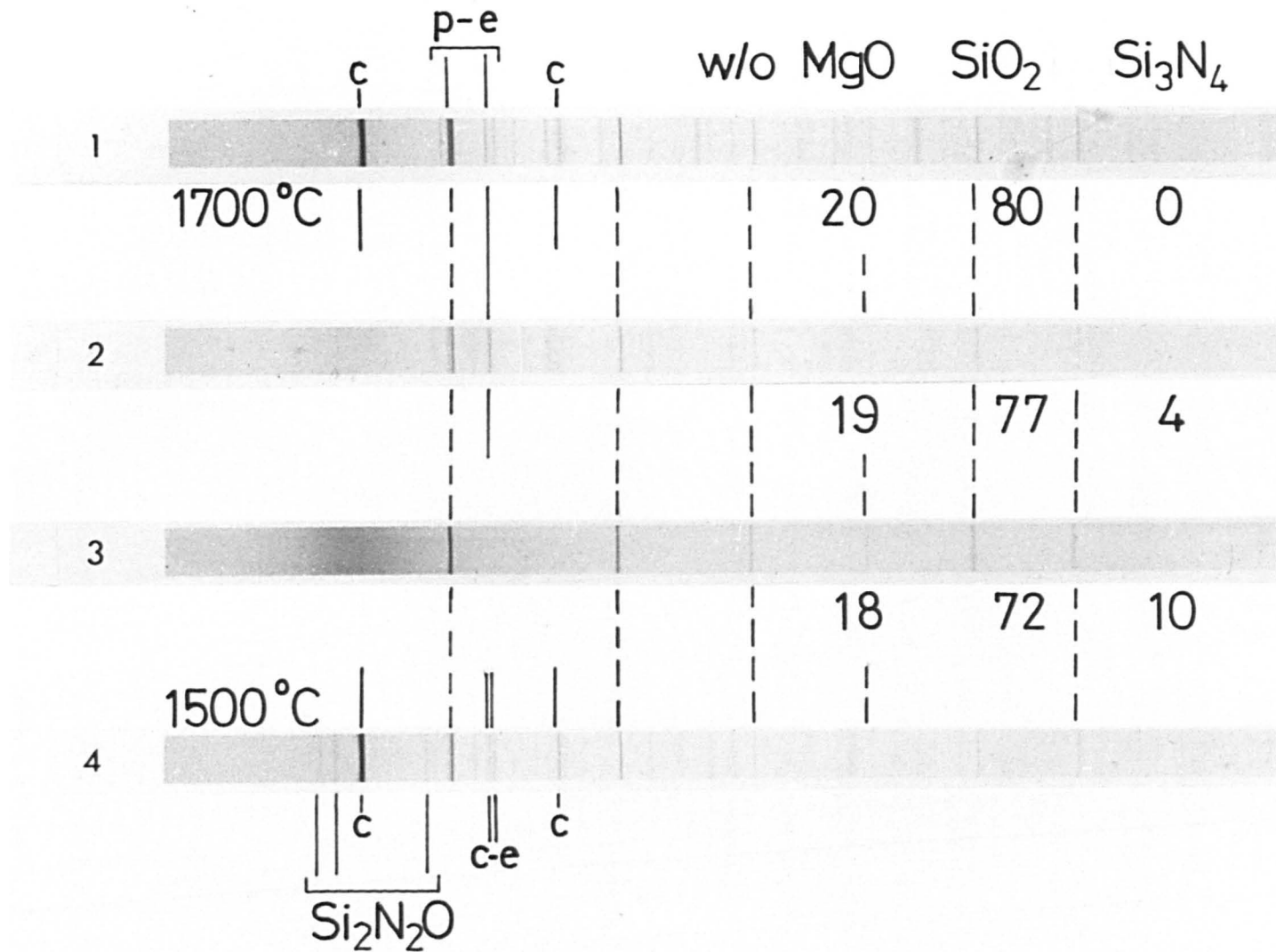
--- Liquid at 1700°C

Figure III.4 X-ray photographs of products obtained by reacting Si_3N_4 with mixtures of MgO and SiO_2 at 1700°C leading to glass formation.

(1) 0 w/o Si_3N_4 (2) 4 w/o Si_3N_4

(3) 10 w/o Si_3N_4 (100% glass)

(4) Devitrification at 1500°C to $\text{Si}_2\text{N}_2\text{O}$, MgSiO_3 (clinoenstatite) and SiO_2 (cristobalite).



--- KCl standard

p-e = protoenstatite

c = cristobalite, SiO₂

c-e = clinoenstatite

glass region explored by Perera (1976) using varying mixtures of MgO , SiO_2 and Si_3N_4 , is also shown in Figure III.3. A typical starting composition was $Mg_{12}Si_{26}O_{56}N_6$ but weight losses up to 10% were reported and attributed to the volatilisation of silicon monoxide and nitrogen. Devitrification of the glass at $1500^{\circ}C$ gave cristobalite, enstatite and silicon oxynitride (see Figure III.4).

Extensive glass formation occurs in the Mg-Si-Al-O system (McMillan, 1964) and additions of aluminium to Mg-Si-O-N compositions extend the vitreous region into the Mg-Si-Al-O-N system (Jack, 1977a). Investigation of the $MgO-SiO_2-AlN$ sub-system (Jack, 1977b) showed that glass containing up to 10 a/o N could be prepared by firing at $1650^{\circ}C$ for 30 minutes (see Figure III.5(a)).

III.4 Y-Si-Al-O-N glasses

A liquid region exists in the Y-Si-O-N system at $1700^{\circ}C$ (see Figure III.6) but no glass-forming region had been reported (Rae, 1976). The Figure also shows the four quaternary phases of this system mentioned previously. A vitreous region exists in the Y-Si-Al-O system (Makishima et al., 1978) and nitrogen glasses have been prepared in the $Y_2O_3-SiO_2-AlN$ sub-system as

shown in Figure III.5(b). Electron-probe microanalysis of one glass sample showed a composition close to that of the starting mix i.e. $Y_9Si_{20}Al_9O_{53}N_9$ and it devitrified at $1200^\circ C$ to give crystalline β - $Y_2Si_2O_7$, $Y_3Al_5O_{12}$ (yttrium-aluminium garnet) and Si_2N_2O . The glass was transparent in this section with a refractive index of 1.76 .

Grain-boundary glass in silicon nitride hot-pressed with relatively small additions of yttria and alumina were found by electron-probe microanalysis to have similar compositions to those just discussed (Jack, 1977b) and, based on the analytical results, a bulk sample of glass with a composition $Y_{11}Si_{12}Al_{16}O_{57}N_4$ was prepared.

III.5 Other nitrogen glass systems

Calcium sialon glasses were also prepared in previous work at Newcastle, a typical composition being $Ca_{11}Si_{18}Al_{11}O_{51}N_9$. Also, in the Si-Al-O-N system without addition of other metals, vitreous phases have been prepared by quenching from $1700^\circ C$ several compositions within the liquid region shown in Figure III.2 (Roebuck, 1978). One composition was $Si_{27}Al_9O_{57}N_7$ and is close to that of X-phase; indeed, the same material slowly cooled gave X-phase, mullite and silicon oxynitride.

Figure III.5 Glass formation in:

(a) the $\text{MgO-SiO}_2\text{-AlN}$ sub-system

(b) the $\text{Y}_2\text{O}_3\text{-SiO}_2\text{-AlN}$ sub-system

(after Jack, 1977b).

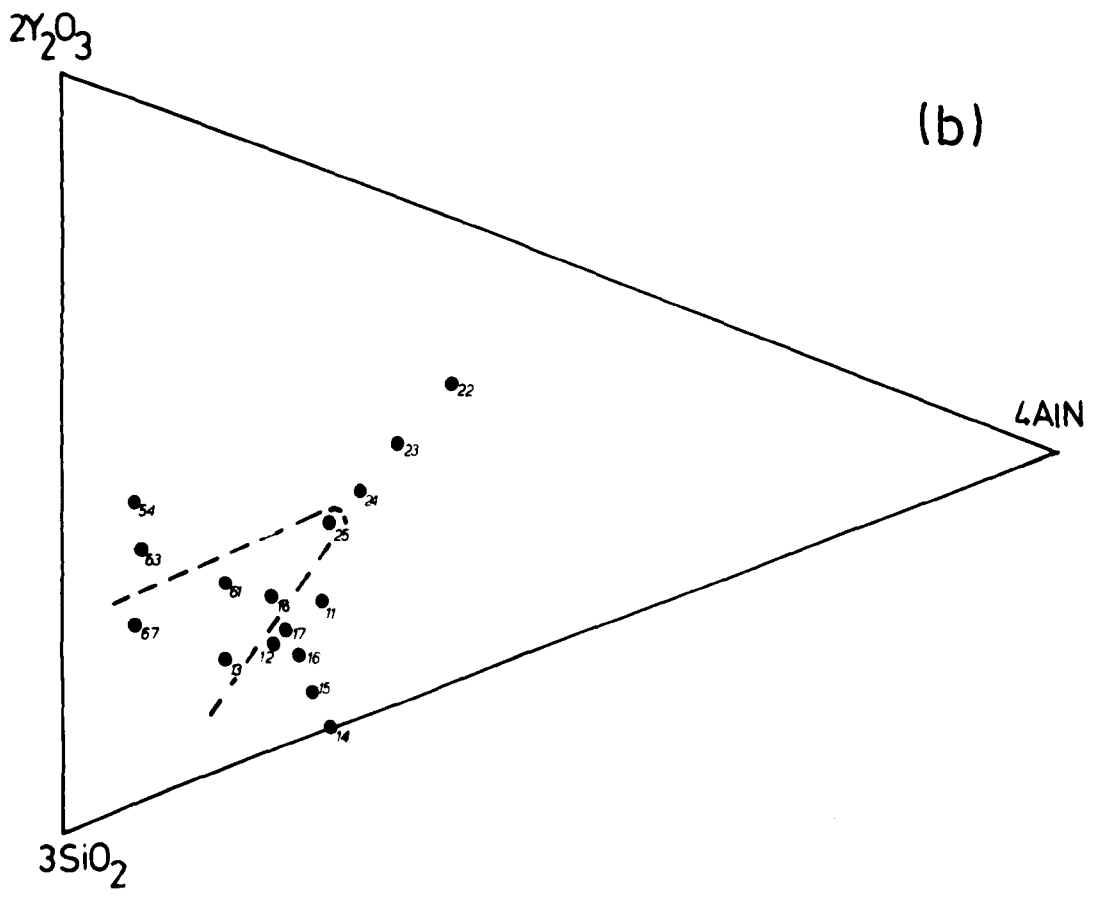
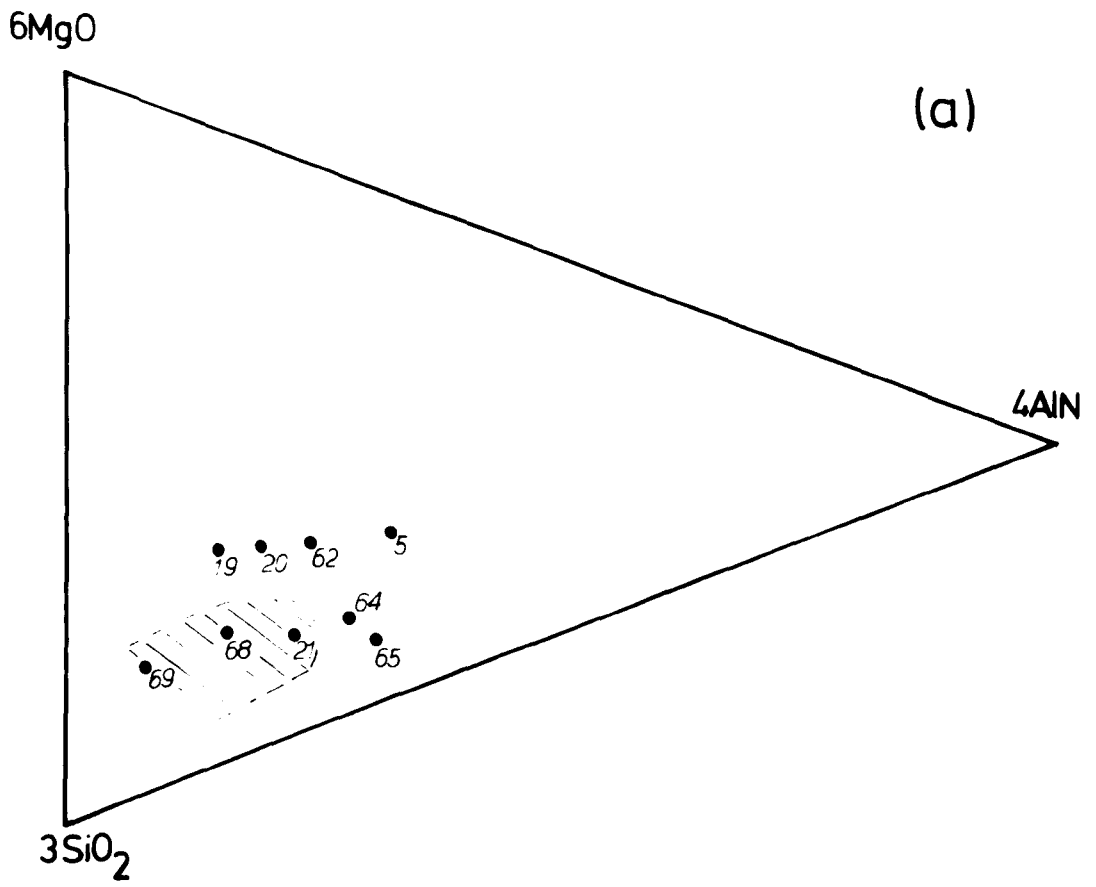
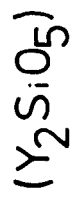
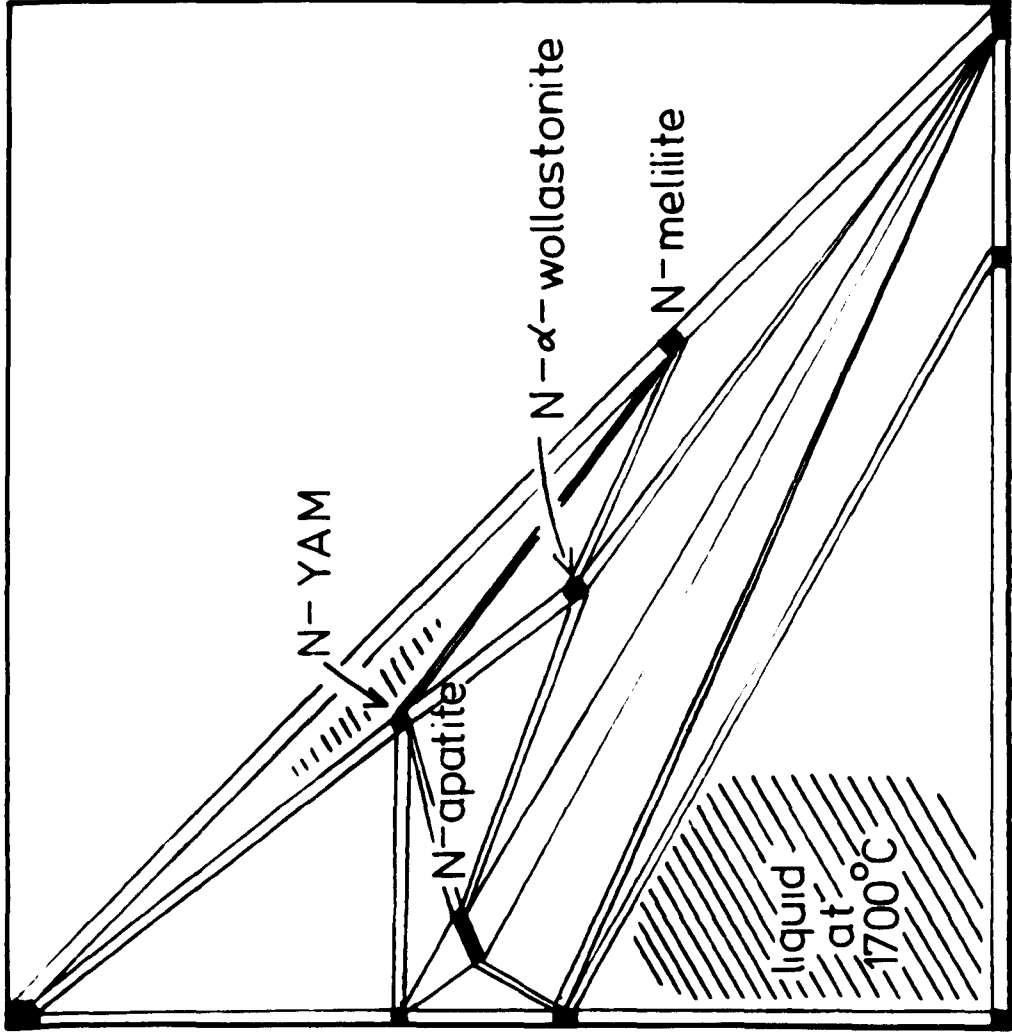
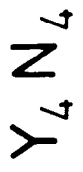


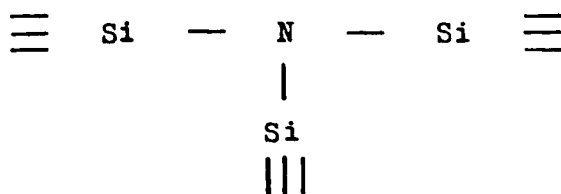
Figure III.6 The Y-Si-O-N behaviour diagram showing the liquid region at 1700°C (after Rae, 1976).



liquid
at
1700°C

III.6 Solubility of nitrogen in silicate glasses

Mulfinger (1966) and Davies & Meherali (1971) showed that the solubility of nitrogen in silicate and alumino-silicate glasses is chemical rather than physical. It was established that molecular nitrogen will react and dissolve chemically only in reducing environments, that is in the presence of carbon, carbon monoxide or hydrogen. It was suggested (Mulfinger & Meyer, 1963) that nitrogen is coordinated with silicon in the structure as follows,



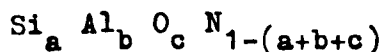
Later work (Kelen & Mulfinger, 1968) indicated that Si_3N_4 dissolves chemically in alkali and alkaline-earth silicate glasses but oxynitride glass formation was followed by decomposition of incorporated nitrogen by reaction with alkali ions in the melt forming volatile nitrides.

Silicon nitride additions to container glass batches was shown by Harding & Ryder (1970) to lower the sulphur and water retention and to increase the softening point of the resultant glass.

The chemical solubility of nitrogen by nitriding with ammonia occurs in silicate glasses (Mulfinger & Franz, 1965) and in reconstructed high-silica glasses (Elmer & Nordberg, 1965). Both investigators detected -NH groups in the glass structure by I.R. spectroscopy and evidence of -NH_2 and -N= was also claimed. Nitriding increased the annealing point, the electrolytical devitrification, and the d.c. resistivity of high-silica glasses and was apparently responsible for the reduction in ultra-violet transmission (Elmer & Nordberg, 1965, 1967).

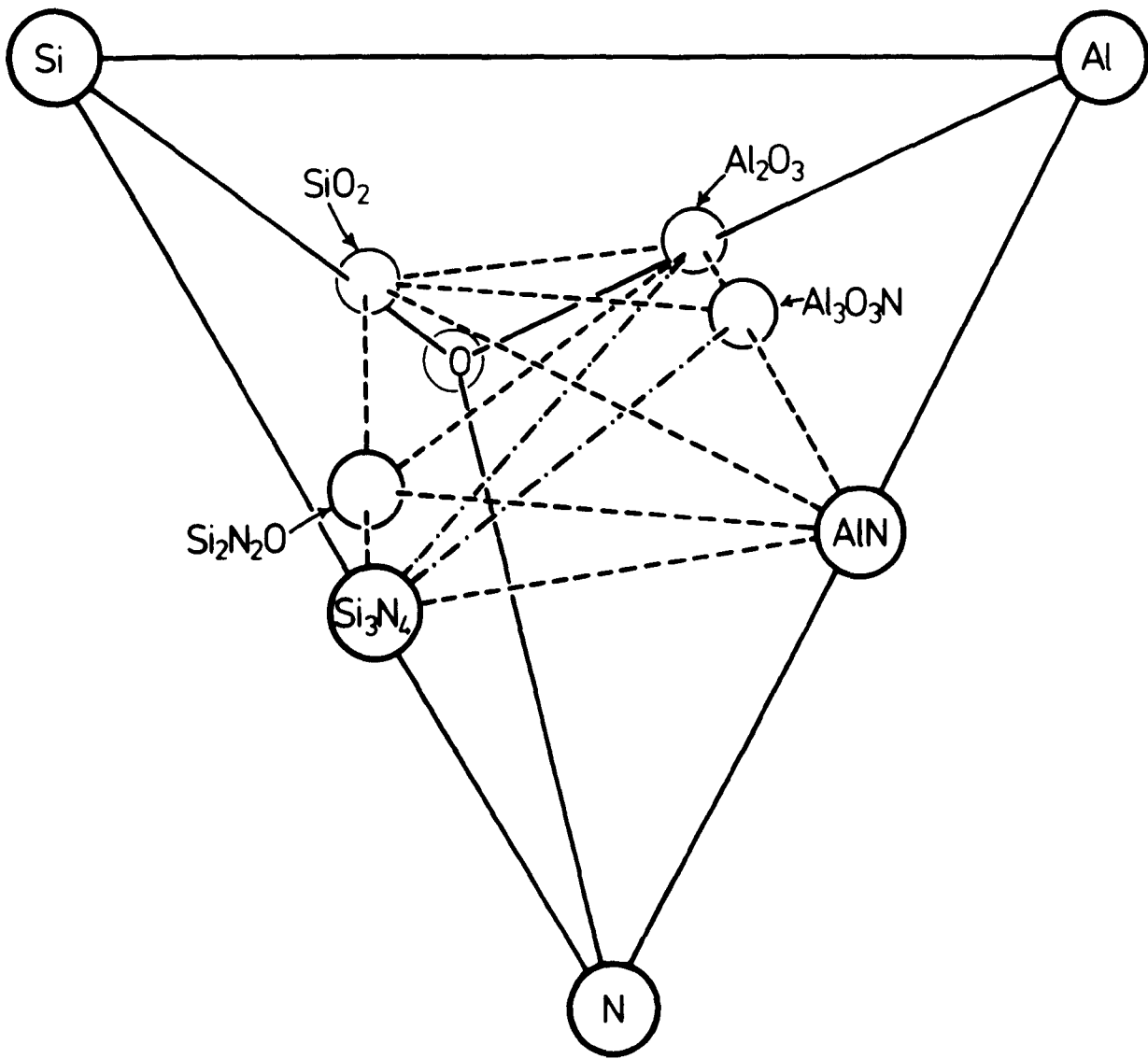
III.7 Representation of the Si-Al-O-N system

The Si-Al-O-N system is apparently four-component and so might be expected to be represented by a regular tetrahedron (see Figure III.7) with each of the vertices representing one atom or one gram-atom of the respective element. A point within the tetrahedron then represents one atom of composition



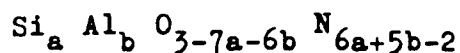
However, since in any phase the elements have fixed valencies Si^{IV} , Al^{III} , O^{II} and N^{III} , one degree of freedom is lost because the sum of the positive valencies must equal the sum of the negative ones,

Figure III.7 The tetrahedral representation
of the Si-Al-O-N system



$$4c + 3b = 2c + 3(1-a-b-c)$$

and so the composition is given by



and the system is pseudo-ternary with compositions given by the two variables a and b . All phases in the system lie on the irregular quadrilateral plane shown in Figure III.8(a) that cuts the edges of the tetrahedron at the compositions $\text{SiO}_2/3$, $\text{Al}_2\text{O}_3/5$, $\text{AlN}/2$ and $\text{Si}_3\text{N}_4/7$. The $[001]$ projection of the quadrilateral is shown in Figure III.9

A simpler representation is obtained by expressing the concentrations in equivalents rather than atoms or gram atoms. Each corner of the Si-Al-O-N tetrahedron is then one equivalent of any element and because one equivalent of an element or compound always reacts with one equivalent of any other species, the compositions of the compounds Si_3N_4 , AlN , Al_2O_3 and SiO_2 (expressed in equivalents) are located at the mid-points of the tetrahedron edges as in Figure III.8(b).

The method of representation is exactly the same as for a reciprocal salt-pair (Zernicke, 1955; Findley, 1927) and involves treating compounds in ionic terms

Figure III.8 Depiction of the tetrahedron in terms of three
orthogonal axes. Corners represent:
in (a) atomic units; in (b) equivalent units.

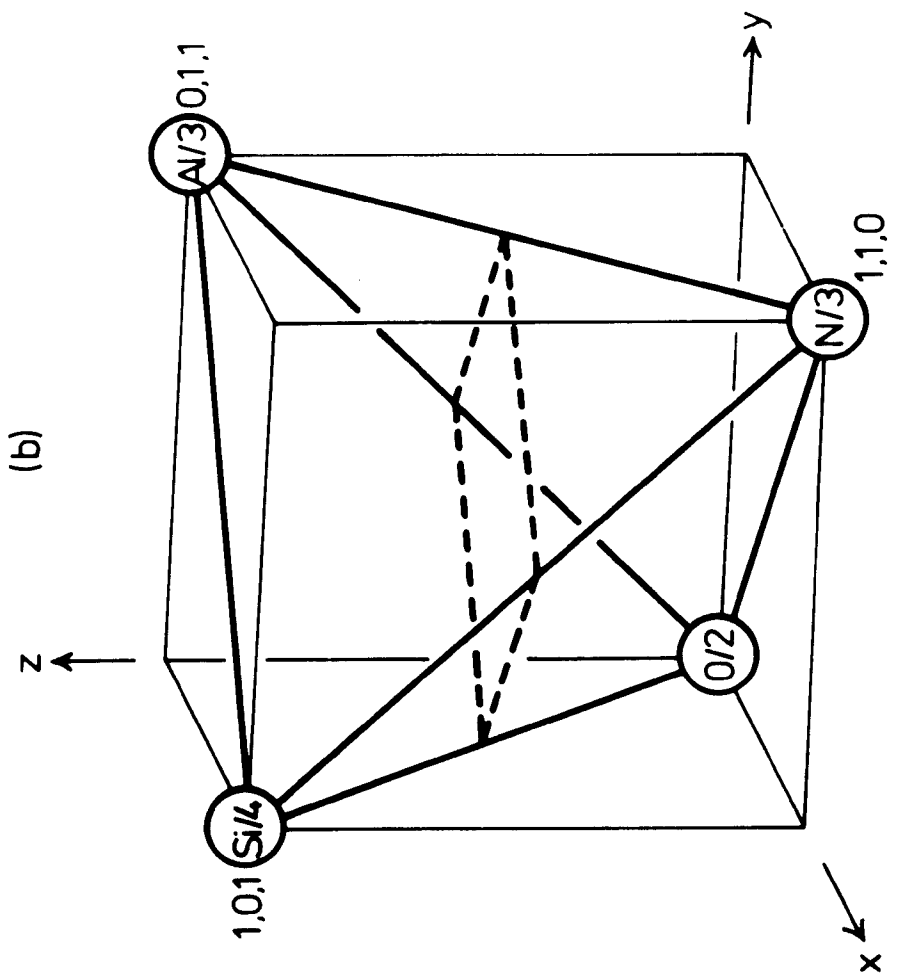
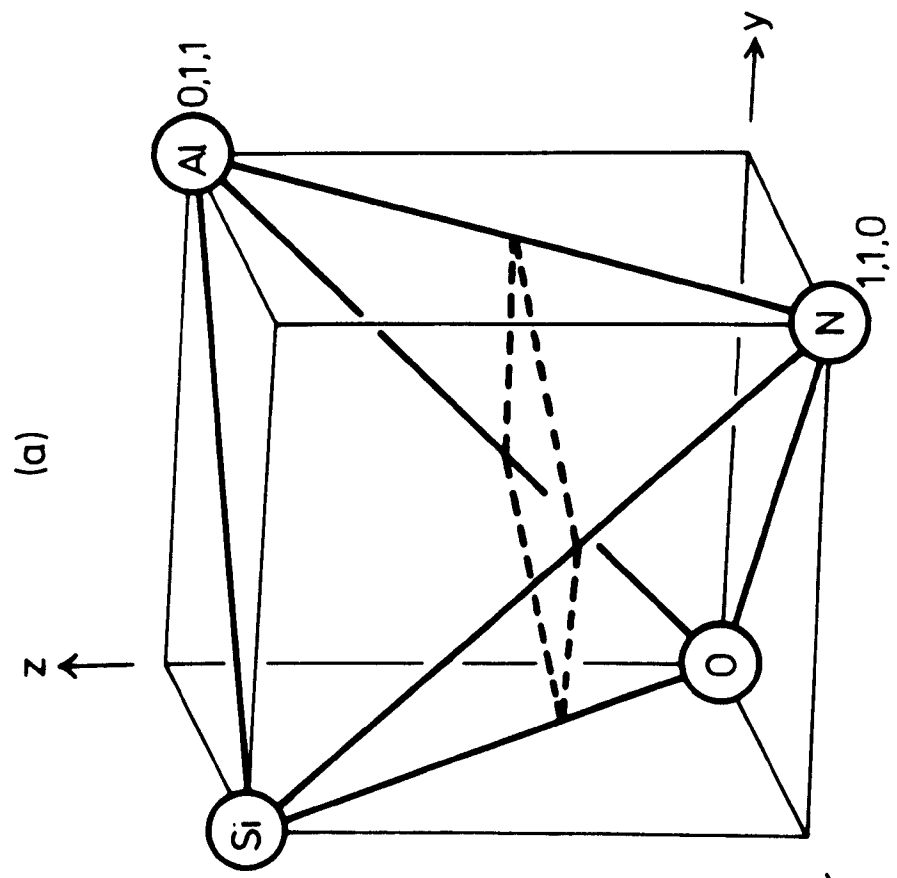
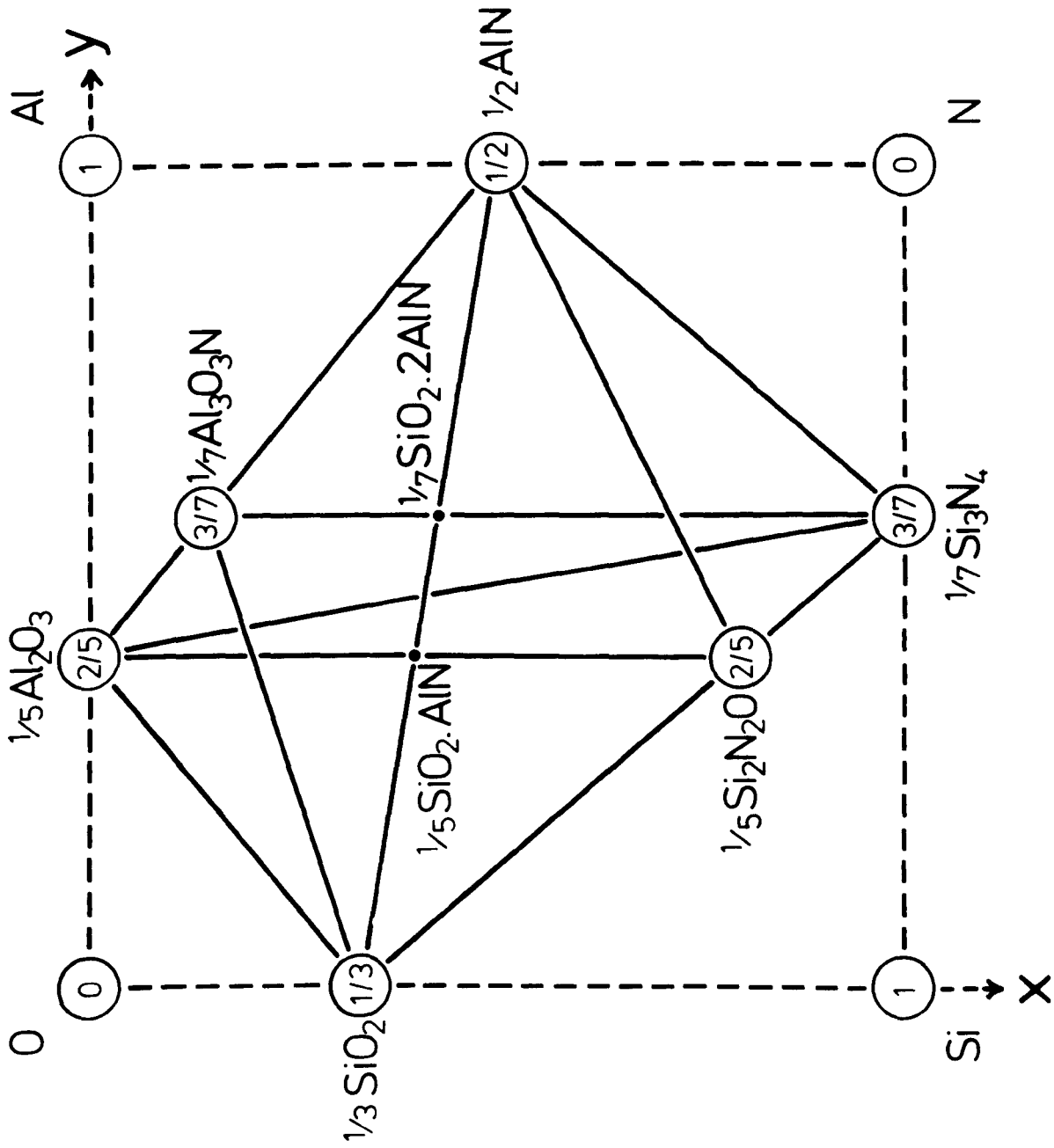


Figure III.9 The irregular quadrilateral plane of the $\text{Si}_3\text{N}_4\text{-AlN-Al}_2\text{O}_3\text{-SiO}_2$ system in atomic units (see Figure III.8(a)). (Heights above the plane of the paper are in the circles.)



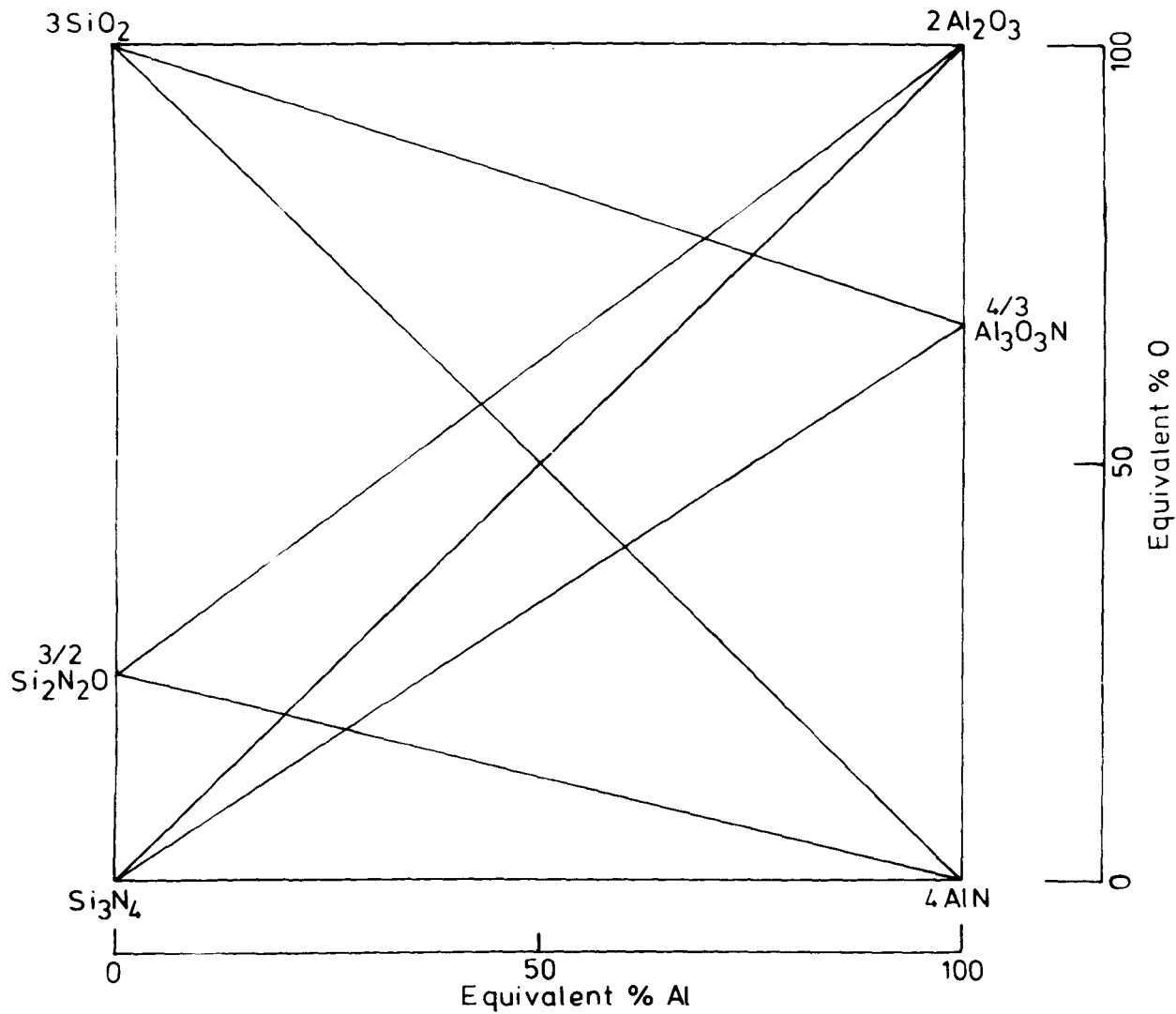
even though the bonding is predominantly covalent. Any composition in the sialon system is defined by the two variables:

$$\frac{\text{Al}/3}{\text{Si}/4 + \text{Al}/3} \quad \text{and} \quad \frac{\text{O}/2}{\text{N}/3 + \text{O}/2}$$

These can be plotted perpendicular to one another and a square is obtained (see Figure III.10).

The bottom left-hand corner conventionally represents one mole of Si_3N_4 and the other three corners then represent Al_4N_4 , Al_4O_6 and Si_3O_6 . All solid phases or mixture of phases within the Si-Al-O-N system fall within the square which is exactly the same as the irregular quadrilateral of Figure III.9 except that concentrations are expressed in equivalents and not atomic units. The representation is very convenient because a composition at any point within the square is a combination of 12+ve and 12-ve valencies; this enables easy plotting of compositions. On moving from left to right 3Si^{4+} are gradually replaced by 4Al^{3+} and similarly from bottom to top 4N^{3-} are replaced by 6O^{2-} . It is clear that although the number of equivalents remain the same, the number of atoms varies.

Figure III.10 The square representing the Si_3N_4 -AlN-Al₂O₃-SiO₂ system in equivalent units (see Figure III.8(b)).



The Square Representation of the Si-Al-O-N System using Equivalent Concentrations

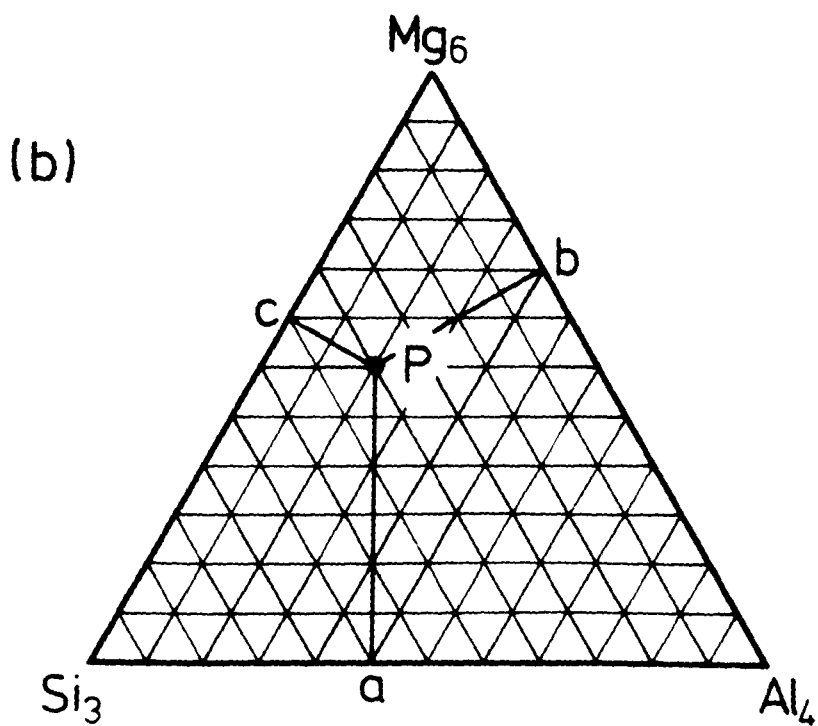
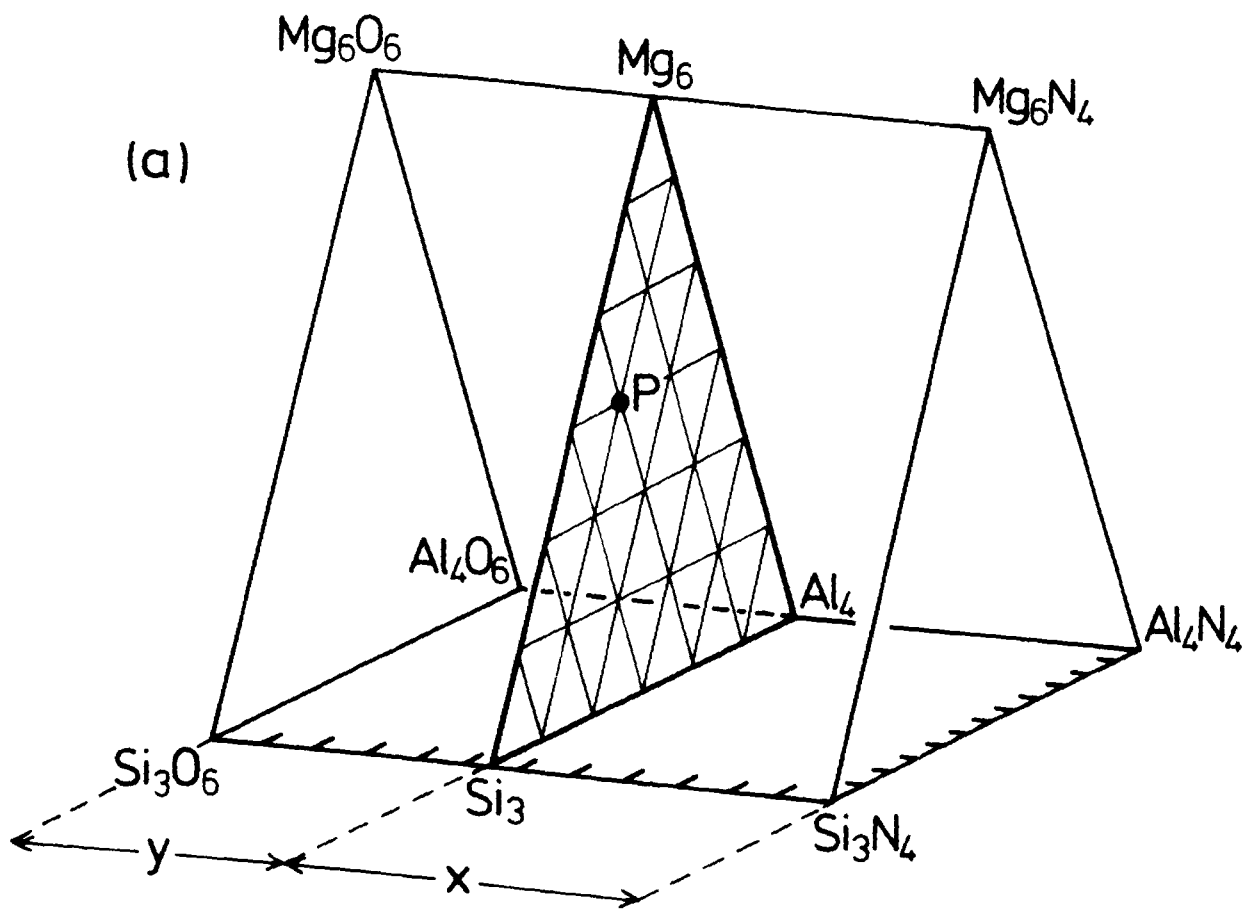
III.8 M-Si-Al-O-N systems

A five-component metal-sialon system is represented in a similar way by Jänecke's triangular prism in which all the edges are equal (Zernicke, 1955). Solid phases must again contain atoms with fixed valencies. The basal plane of the prism is the $\text{Si}_3\text{N}_4 - \text{Al}_4\text{N}_4 - \text{Al}_4\text{O}_6 - \text{Si}_3\text{O}_6$ square of Figure III.10, and the third dimension represents the metal concentration e.g. Mg within the system Mg-Si-Al-O-N (see Figure III.11(a)). The back triangular face represents the ternary oxide system (expressed in equivalents) and the front face that of the nitrides. Any phase, crystalline or vitreous, within the M-Si-Al-O-N system is represented by a region within the Jänecke's prism. Since all edges are equal they may be conveniently divided into twelve parts (one division per valency) or they may be graduated in equivalent percentages (e/o).

Within the prism, vertical triangular planes each represent a constant oxygen:nitrogen ratio as shown in Figure III.11(a). Each plane is parallel to both the oxide and nitride end-faces and 6O^{2-} are replaced by 4N^{3-} on moving from the back to the front face. If the ratio of N:O is fixed (see Figure III.11(b)) then the metal composition (e.g. Mg, Si and Al) can be expressed (in equivalents) by any point, P,

Figure III.11

- (a) Representation of a five-component system (e.g. Mg-Si-Al-O-N) showing the plane of constant N:O ratio within the Jänecke prism.
- (b) Method of representing a cation composition by a point (P) on the plane of constant N:O ratio.



in the usual way for a three-component system.

This representation was adopted to describe the limits of glass formation in the different metal-sialon systems that were explored in the present work. Thus, the limit of the metal alumino-silicate glass region is plotted on the oxide face of the prism and it is possible to observe how the glass region extends into the M-Si-Al-O-N prism on replacing oxygen by nitrogen. Vitreous regions in both the Mg-Si-O-N and Si-Al-O-N systems are represented on their respective faces of the Jänecke prism.

Investigation of glass formation in sub-systems explored previously at Newcastle (see Jack, 1977b) and by Loehman in his early work (1978) cannot satisfactorily explore the full extent of any particular nitrogen glass system. For example, the MgO-SiO₂-AlN sub-system only examines compositions within the triangle bounded by the Mg₆O₆-Si₃O₆, the Mg₆O₆-Al₄N₄ and the Si₃O₆-Al₄N₄ joins and the same argument applies to the MgO-Al₂O₃-Si₃N₄ sub-system. Without a detailed, systematic exploration at successively increasing fixed N:O ratios it is possible to miss detecting the glass-forming region or at least not obtain the compositions of maximum nitrogen solubility.

IV. Scope of the Present Investigation

The aim of the present work was to determine the limits of glass formation in various M-Si-O-N and M-Si-Al-O-N systems and to study the effect on glass properties replacing oxygen by nitrogen.

A detailed investigation of glass formation was carried out in the magnesium and yttrium systems the results of which are presented in Chapter VI. The formation of nitrogen glasses in a variety of other systems is included in the discussion.

Chapter VII describes and discusses the viscosity, devitrification characteristics, and optical properties of some glasses. Electrical measurements obtained for some selected glasses at Durham University are presented in an Appendix.

An attempt is made to relate the synthesised bulk nitrogen glasses with grain-boundary glasses occurring in densified nitrogen ceramics by studying their respective devitrification behaviours. This mainly involved the use of X-ray methods for detecting and characterizing crystalline species and these are

discussed in Chapter VIII.

During investigation of glass formation in the Mg-Si-Al-O-N system a phase isostructural with β -Si₃N₄ but containing substantial amounts of magnesium was discovered; Chapter IX describes the preparation of the phase by devitrification of glasses with metal:non-metal atom ratios 3M:4X .

V. Experimental Methods

V.1 Materials specifications

The analyses of the nitrides and alumina powders are given in Table V.1. Silicon nitride was most frequently used as a starting nitride although some compositions were made up using aluminium nitride or a mixture of both AlN and Si_3N_4 . Adjustments in compositional calculations were made to take into account the surface oxide i.e. 4 w/o silica on the Si_3N_4 and 6 w/o alumina on the AlN.

Silica was in the form of crushed, fused quartz supplied by Thermal Syndicate Limited.

Both MgO and CaCO_3 powders (BDH Chemicals Limited) and Nd_2O_3 (Ventron Limited) were calcined at 800°C - 900°C to remove volatiles, carbon dioxide and chemically absorbed water respectively. 99.9% purity Y_2O_3 was obtained from Rare Earth Products. All materials were kept in a desiccator prior to use.

V.2 Powder mixing

Weighed powders were usually mixed in a Glen-Creston

Table V.2

Nitride and alumina powder specifications

powder and supplier	specifications		X-ray analysis
	particle size	impurities	
Si ₃ N ₄ Starck-Berlin	0.85 μm	C, max 0.2 w/o Fe, max 0.3 w/o	95% α 5% β
H.S. 130 Si ₃ N ₄ Joseph Lucas	0.9 μm	Ca, Fe, Al, Si 0.8 w/o total	88% α 10% β 2% Si ₂ N ₂ O
high β-Si ₃ N ₄ A.M.E.	50 μm	C -0.2w/o Al-0.5w/o Fe-0.5w/o Ca-0.2w/o O -1.3w/o	30% α 70% β
AlN Starck-Berlin	4 μm	C, max 0.08 w/o Fe, max 0.15 w/o	100% AlN
A15, A16 and A17 reactive Al ₂ O ₃ Alcoa	1 μm	Na ₂ O, max 0.1 w/o SiO ₂ , max 0.05w/o Fe ₂ O ₂ , max 0.03w/o	100% α- Al ₂ O ₃

mill using an alumina ball and mill capable of holding batches from 5-25 grams. Contamination from the mill was negligible. Mixing was carried out dry and times of 5-20 minutes were employed; the larger the batch, the longer the milling time. 5 g mixes were made for investigating glass formation and 20-25 g batches were used when firing bulk samples for property measurements.

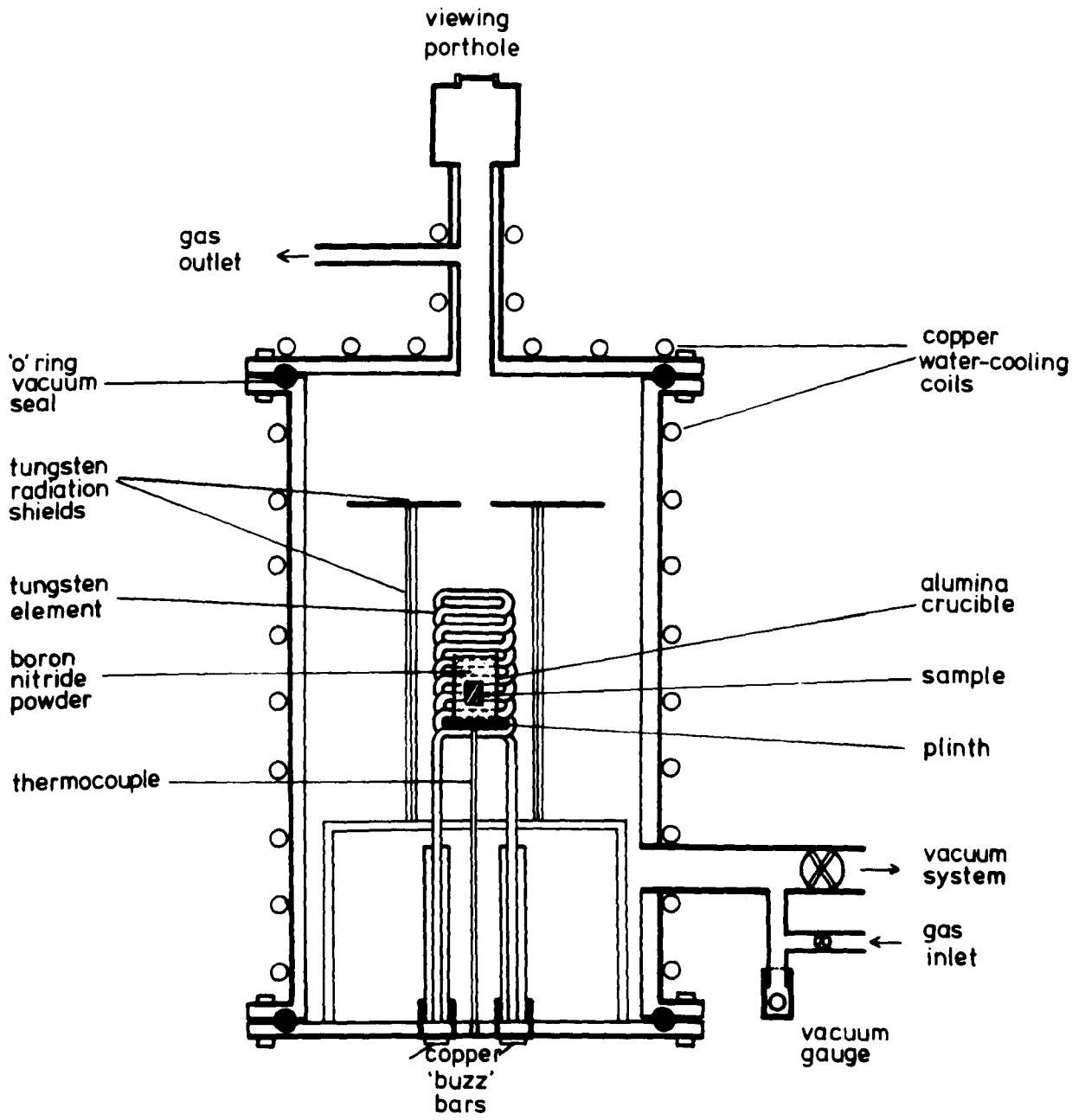
Mixing of large batches was also carried out by placing the powder in 3" diameter polythene jars containing alumina balls and Vibro-milling for about two hours.

V.3 High-temperature fusion methods

(a) Tungsten resistance furnace

Figure V.1 shows the schematic layout of the furnace. The hot-zone was 1-2 cm long and crucibles of not more than 2.5 cm diameter could be placed in the coil, thus restricting the furnace to the firing of small samples of less than 2 g. The power supply was from a low-voltage, high-current transformer and the temperature was measured using an Ir-Ir:40w/oRh thermocouple which had been calibrated against a Pt:6w/oRh-Pt:30w/oRh thermocouple placed temporarily in the hot-zone. Fast cooling rates could be achieved ($>250^{\circ}\text{C}/\text{minute}$) since the furnace had water-cooling

Figure V.1 The tungsten resistance furnace.



and a low thermal mass. Prior to heating, the furnace was evacuated and filled with nitrogen purified from oxygen and moisture by a zirconium getter operating at 920°C.

Samples were uniaxially compacted into pellets in a 1 cm diameter steel die with a pressure of 4000 p.s.i (27.6 MN m⁻²). The surface was removed after pressing to avoid contamination from the die. The weighed pellet (0.5-2.0 g) was introduced into either a 1.5 cm diam. x 2.5 cm high alumina crucible which had been lined with boron nitride powder, or placed in an isostatically pressed boron nitride crucible of similar dimensions. The pellet, after heat-treatment, was cleaned of adherent BN and re-weighed.

(b) Molybdenum resistance furnace

The furnace arrangement is shown in Figure V.2. The element was made from molybdenum strip and had a 4-5 cm hot-zone. The furnace had a fairly slow cooling rate because the distance between the water-cooled chamber and the element was large, and also the large number of reflector cylinders increased the thermal mass. Fast cooling (greater than 250°C per minute) could be obtained by purging the furnace with nitrogen gas at the

Figure V.2 Molybdenum resistance furnace.

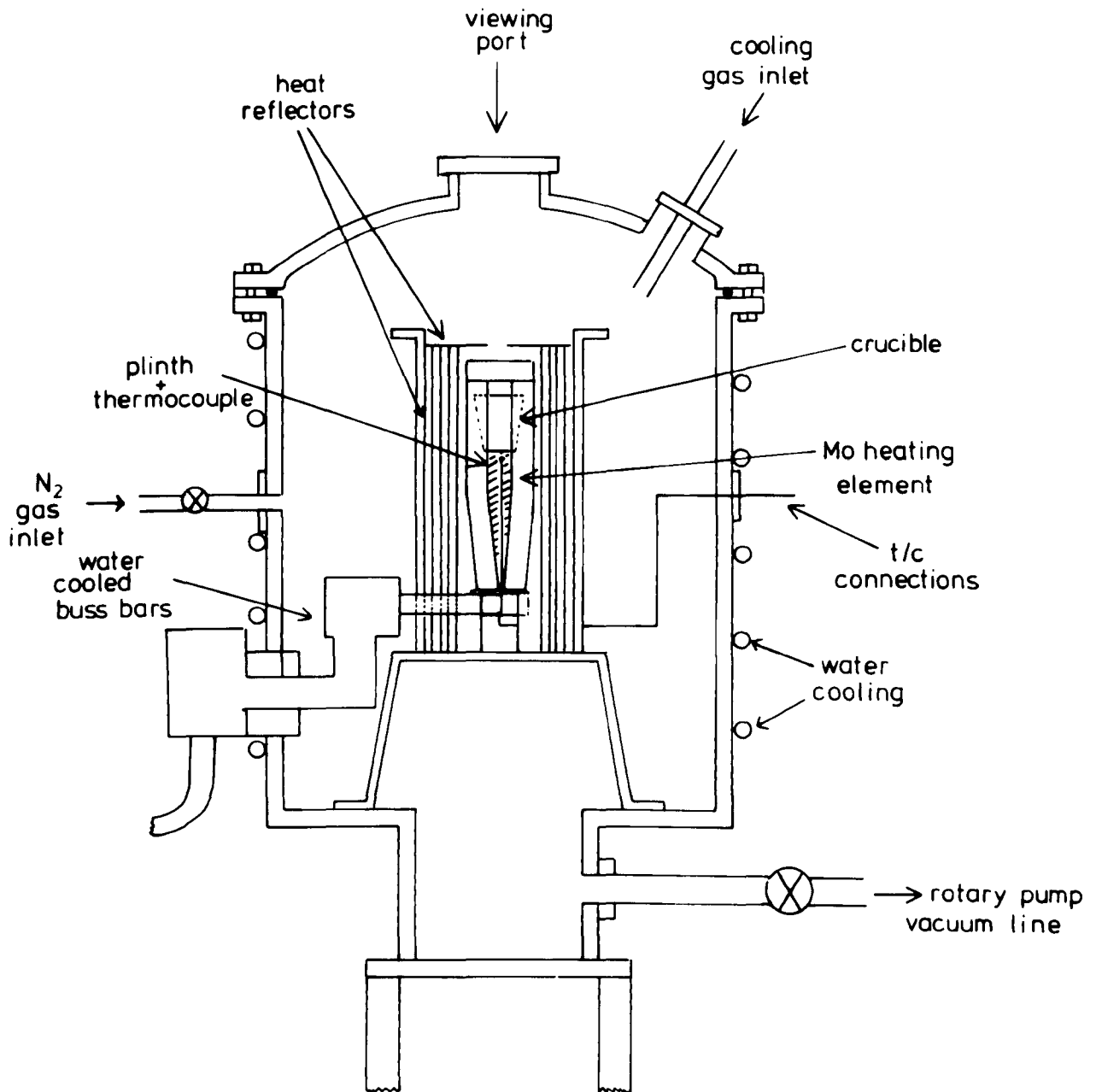
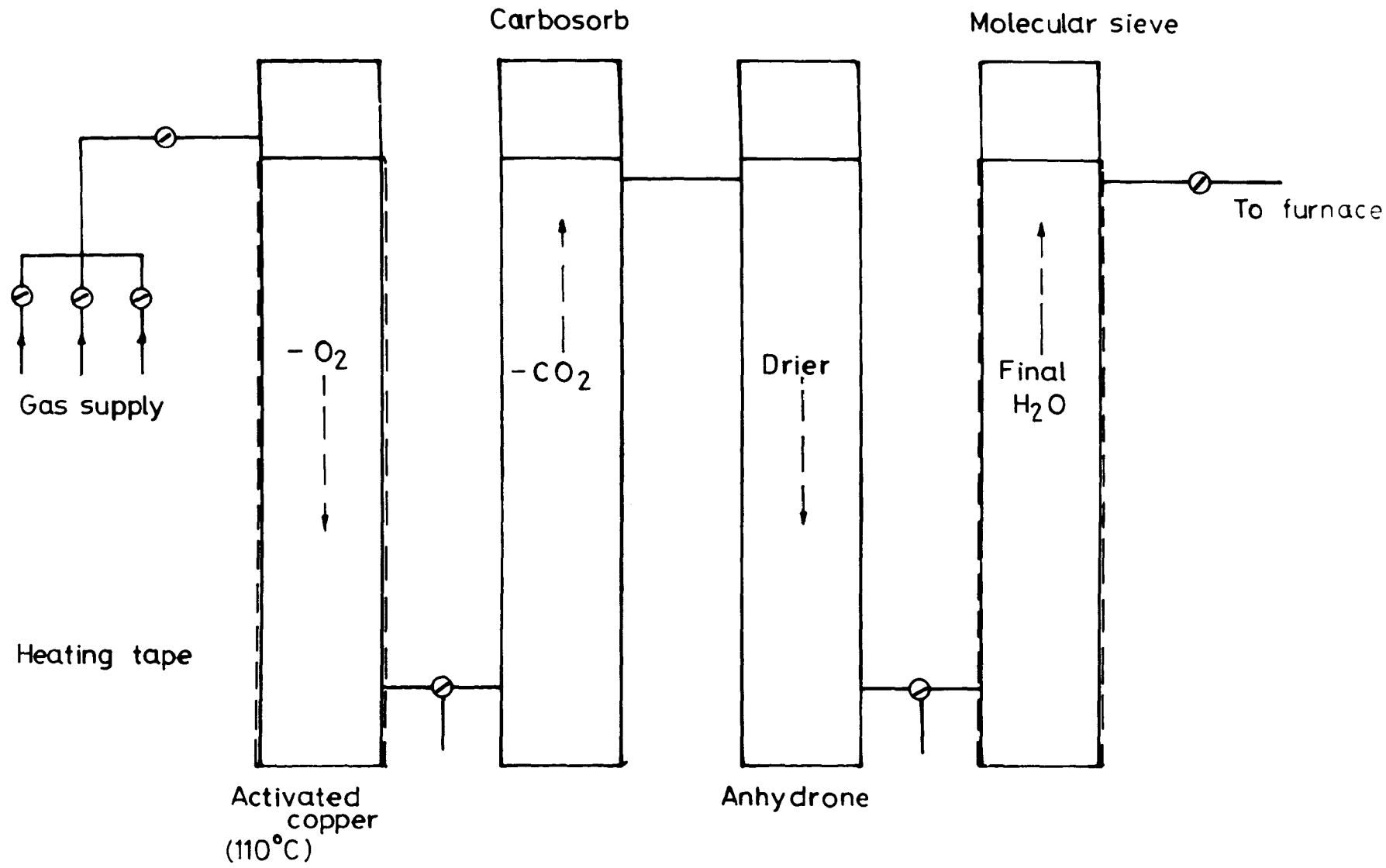


Figure V.3 The gas purification train.



Gas Purification Train

end of a heat-treatment. Temperature measurement, and the power supply were the same as described above. The chamber was evacuated prior to use and then filled with nitrogen that had been passed through a gas purification train (Figure V.3).

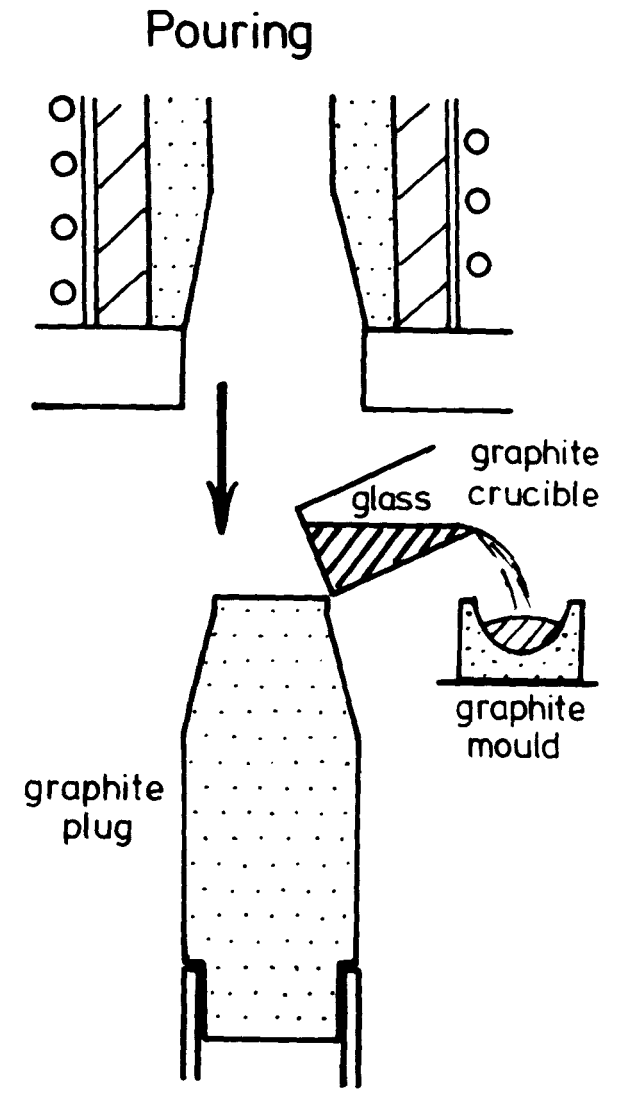
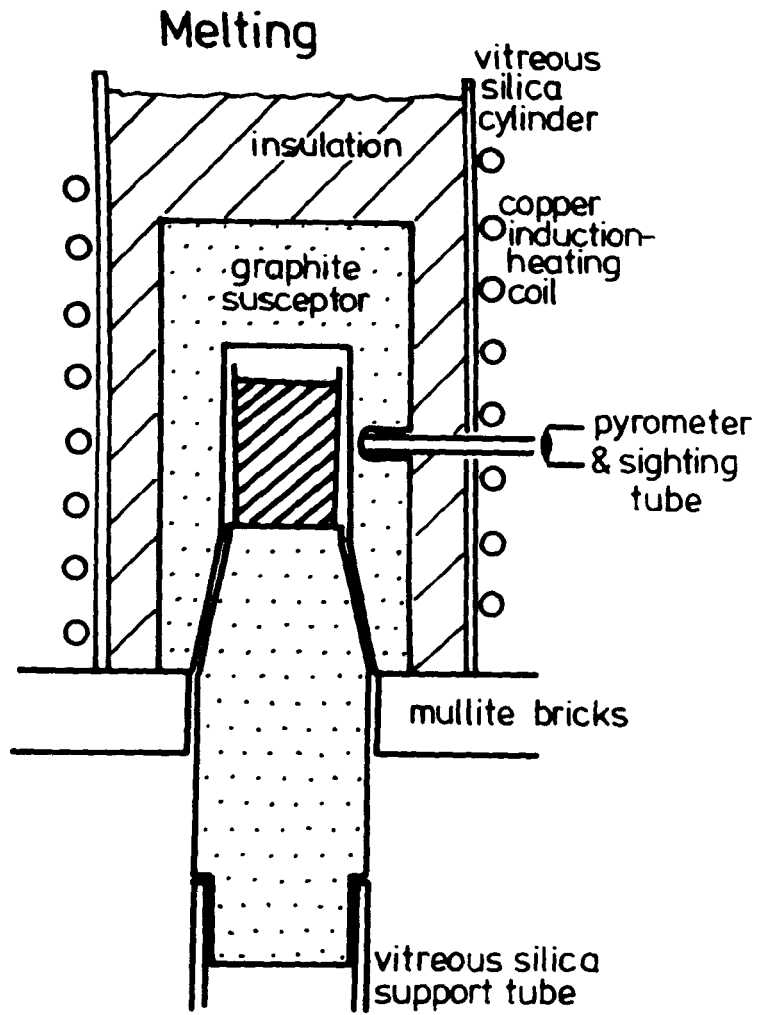
The 10-20 g of pre-mixed powder of each batch was isostatically pressed to 20,000 p.s.i. (138 MN m^{-2}) in a 3 cm diameter rubber sleeve. Pre-weighed pieces were then packed into an isostatically pressed boron nitride crucible of 2.5 cm diameter x 5 cm high.

The bulk glass, after fusing, was cleaned ultrasonically, re-weighed and weight losses were calculated. It was then annealed for 15 minutes in a standard tube muffle furnace after determining the appropriate annealing temperature by differential thermal analysis (DTA).

(c) Inductively-heated graphite furnace

Figure V.4 shows the furnace layout. The graphite susceptor was inductively heated by a Radyne R150E radio-frequency generator with a maximum power of 15 kW. Temperature was measured with a disappearing filament optical pyrometer accurate to $\pm 20^\circ\text{C}$.

Figure V.4 Inductively-heated graphite furnace.



Induction heated glass melting pot

The isostatically pressed sample was fused in an alumina crucible which had a lid to avoid excessive contact with the reducing environment. A temperature of 1700°C could be achieved in 30-40 minutes from cold, or the sample could be introduced when the furnace was at the required temperature.

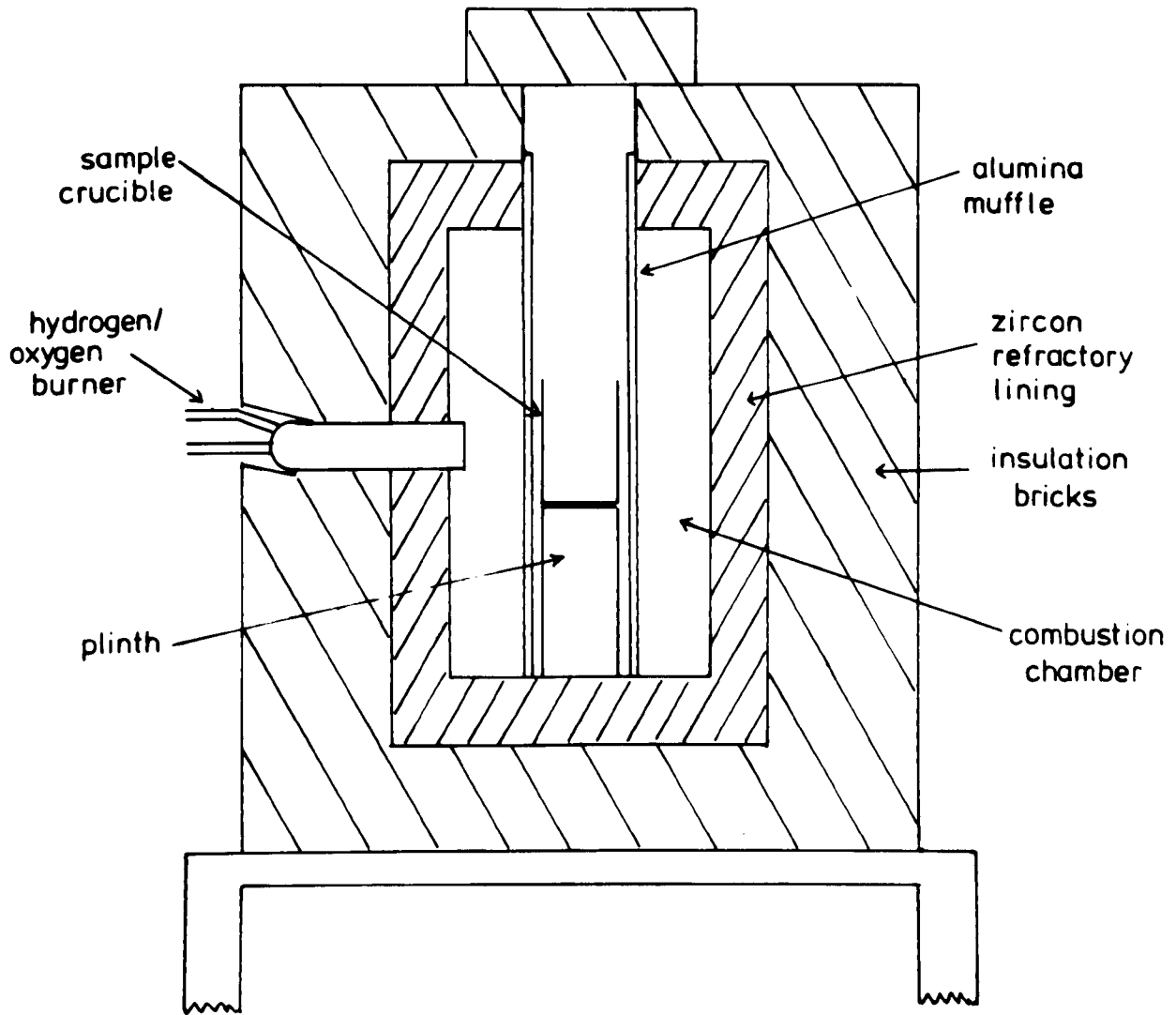
The crucible was removed at the end of the fusion and the contents were either air-cooled in the crucible, or were poured into a large graphite mould (as shown) if quenching was required.

(d) Air-fusion methods

The hydrogen-oxygen gas furnace illustrated in Figure V.5 was used to prepare oxide glasses by fusing pre-mixed powders in alumina crucibles. Heating took three hours from ambient to 1600°C , whereupon the sample was held at temperature for approximately two hours. The crucible was then removed and the melt poured into a pre-heated graphite mould and subsequently transferred to an annealing furnace.

Oxide glasses were also prepared in large platinum crucibles in a standard high-temperature muffle furnace.

Figure V.5 The hydrogen-oxygen gas furnace.



V.4 Heat-treatment

Devitrification experiments were carried out, under a nitrogen atmosphere, in a vertical tube muffle furnace as shown in Figure V.6. Temperatures up to a maximum of 1500°C obtained with a crucilite element were measured with a Pt-Pt:13w/oRh thermocouple with the specimen embedded in boron nitride powder inside an alumina crucible. The apparatus was evacuated, filled with purified nitrogen (see Figure V.3), and the sample was lowered and raised slowly into the furnace hot zone to avoid problems of thermal shock.

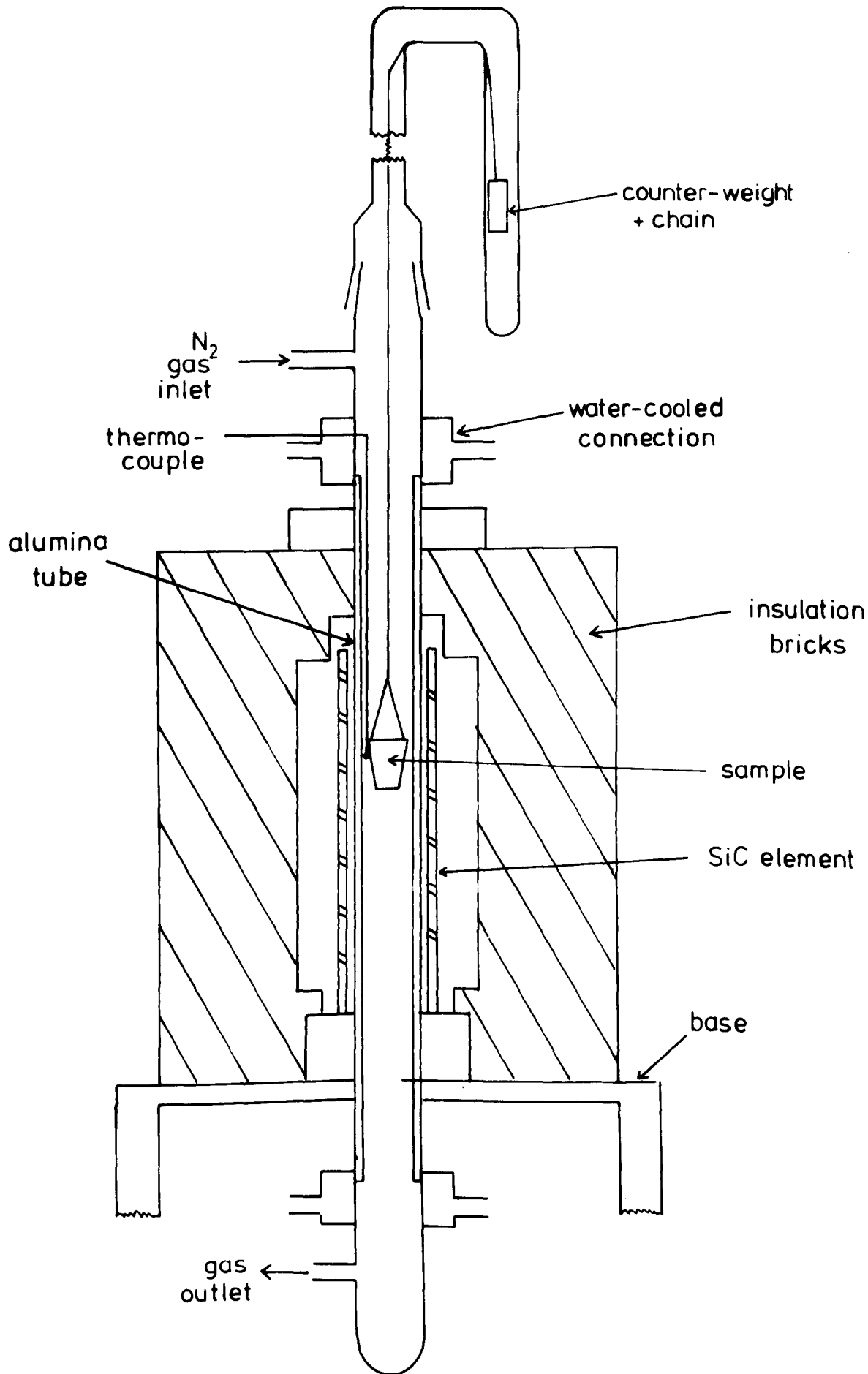
V.5 X-ray methods

X-ray powder methods were used to identify crystalline phases occurring during fusion or after devitrification. Hagg-Guinier focussing cameras were used with $\text{CuK}\alpha_1$ radiation and a potassium chloride internal standard.

V.6 Measurement of glass transition and crystallization temperatures

It is well-established that an abrupt change in properties occurs in a glass at the glass transition temperature, e.g. thermal expansion coefficient, specific volume and specific heat. It is reasonable to

Figure V.6 The silicon carbide vertical tube
muffle-furnace.

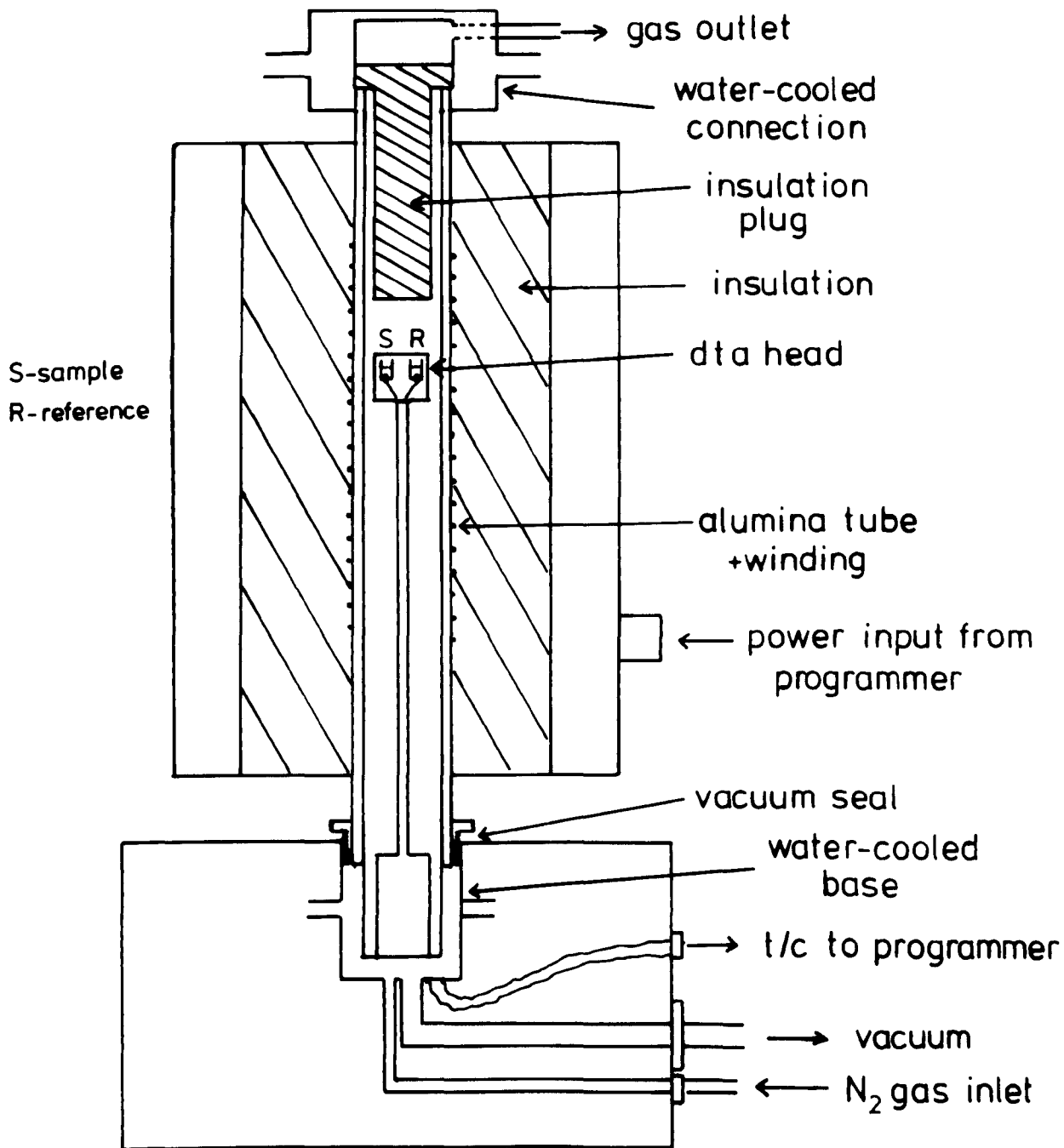


associate the glass transition on cooling with the slowing down of rearrangement in a glass structure. When rearrangement occurs rapidly the glass has the properties of a liquid, and when it is slow the structure is "frozen-in" and the glass behaves like a solid. The rate of structural rearrangement is closely associated with viscous flow and the glass transition temperature occurs at an approximate viscosity of 10^{13} poise.

The glass transition (T_g) can be detected by differential thermal analysis (DTA). Since there is a change in specific heat at T_g , then the value of dH/dT will change and cause an endothermic drift in the ΔT trace. The point on the trace which is the easiest to identify is the minimum point and roughly corresponds to the end of the transition range (Briggs, 1975). It has been shown that this point corresponds to a viscosity of about 10^{11} poise (Yamamoto, 1965).

DTA can also be used for obtaining the crystallization temperature (T_c) in a glass since it usually manifests itself as an exothermic peak. Crystallization can be extremely complicated and the mechanisms are still not fully understood. It is preceded by nucleation which may occur on free surfaces, internal bubbles or heterogeneities in the glass. Impurities may be added to glass to act as nucleating

Figure V.7 The differential thermal analyser
(Stanton-Redcroft 873-4).



agents as, for example, in the production of glass-ceramics. Nucleation occurs just above the transition temperature whereas crystallization is usually a maximum at some much higher temperature (Doremus, 1973).

The measurement of crystallization was obtained from the maximum point on the exothermic peak of the DTA trace.

The equipment used was a Stanton-Redcroft 873-4 differential thermal analyser (see Figure V.7) which has a linear programmable temperature control. A heating and cooling rate of $10^{\circ}\text{C}/\text{minute}$ was used throughout. Alumina crucibles were employed in preference to platinum ones since some reaction of nitrogen glasses occurs with the latter. BDH alumina powder was the reference material, and glasses were crushed and sieved to a particle size $0.10\text{-}0.25\text{ mm}$. Purified nitrogen was passed through the apparatus to avoid oxidation. The glass sample was heated to just above the transition trough and then cooled to $300\text{-}400^{\circ}\text{C}$ below T_g , after which it was again heated to above the crystallization temperature (T_c).

V.7 Viscosity measurement

The viscosity of a glass is one of its most

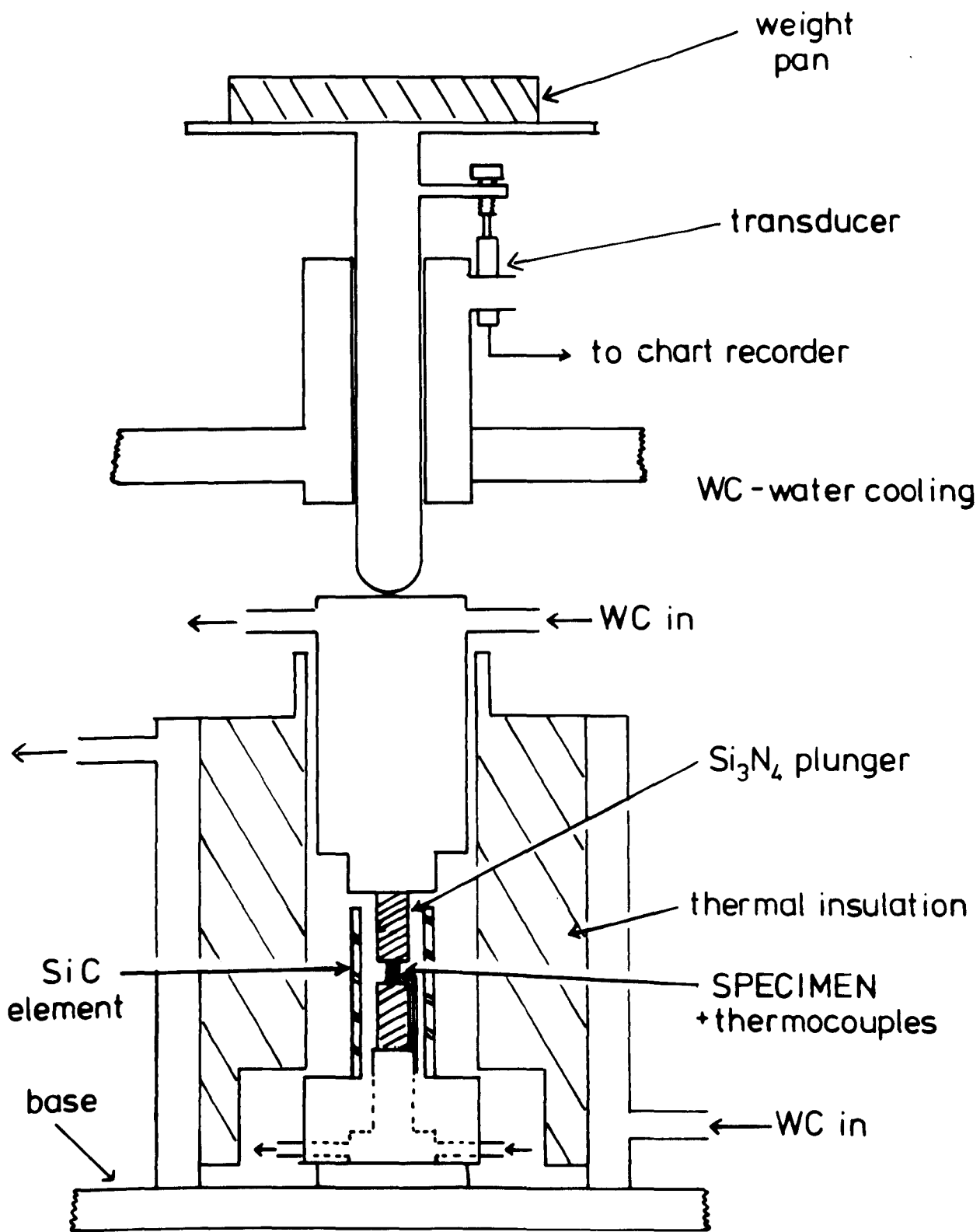
important technological properties and determines the melting conditions, the temperature of working and annealing, the upper temperature of use and its devitrification characteristics.

High viscosities can be measured by two well-established techniques:

- (i) Fibre-elongation which requires flame drawing of the glass and measures the strain rate of a thin fibre under small tensile loads;
- (ii) three-point beam-bending of a simple geometrically-shaped test-piece under an applied load and subsequent measurement of strain-rate (see Hagy, 1963).

In the present work, viscosity of glasses was measured on a modified compressive creep apparatus. A schematic layout is shown in Figure V.8; the cylindrical specimens of glass machined to approximately 5 mm diameter and 4-8 mm in length were placed between the reaction bonded silicon nitride plungers. The furnace was heated by a silicon carbide element operating at high power and employing the minimum thermal insulation so as to allow rapid heating and cooling of the furnace, thereby reducing the time between successive measurements. The required temperature was established and maintained for 30 minutes before testing to obtain

Figure V.8 The modified compressive-creep
measuring apparatus used for
viscosity evaluation.



equilibrium conditions. Loads of 1-10 kg were applied as shown, and the displacement was measured via a transducer coupled with a chart-recorder. Loading ceased once the specimen had deformed by 0.1 mm, and after allowing the furnace to cool, the change in specimen dimensions were noted. The viscosity (η) was calculated using the formula

$$\eta = \frac{m g L t}{3\pi r^2 \Delta L} \quad \text{poise}$$

where m is the applied load (grams), g is the gravitational constant ($981 \text{ dynes cm}^{-2}$), L is the original length (cm), t is the time of loading(s), r is the radius of the specimen (cm) and ΔL the change in length in time t . The unit of viscosity is the poise (grams per centimetre per second).

As with many transport properties, viscosity fits an Arrhenius-type equation

$$\eta = \eta_0 \exp E/KT$$

where E and η_0 are temperature independent coefficients called the apparent activation energy and the pre-exponential constant, respectively. Viscosity

is therefore usually presented as a logarithmic plot versus reciprocal temperature.

Figure V.9 shows there is good agreement between the viscosities of Spectrosil (synthetic vitreous silica) measured by this present method and the original data reported by Hetherington et al. (1964) obtained using a fibre-elongation technique.

V.8 Refractive index measurement

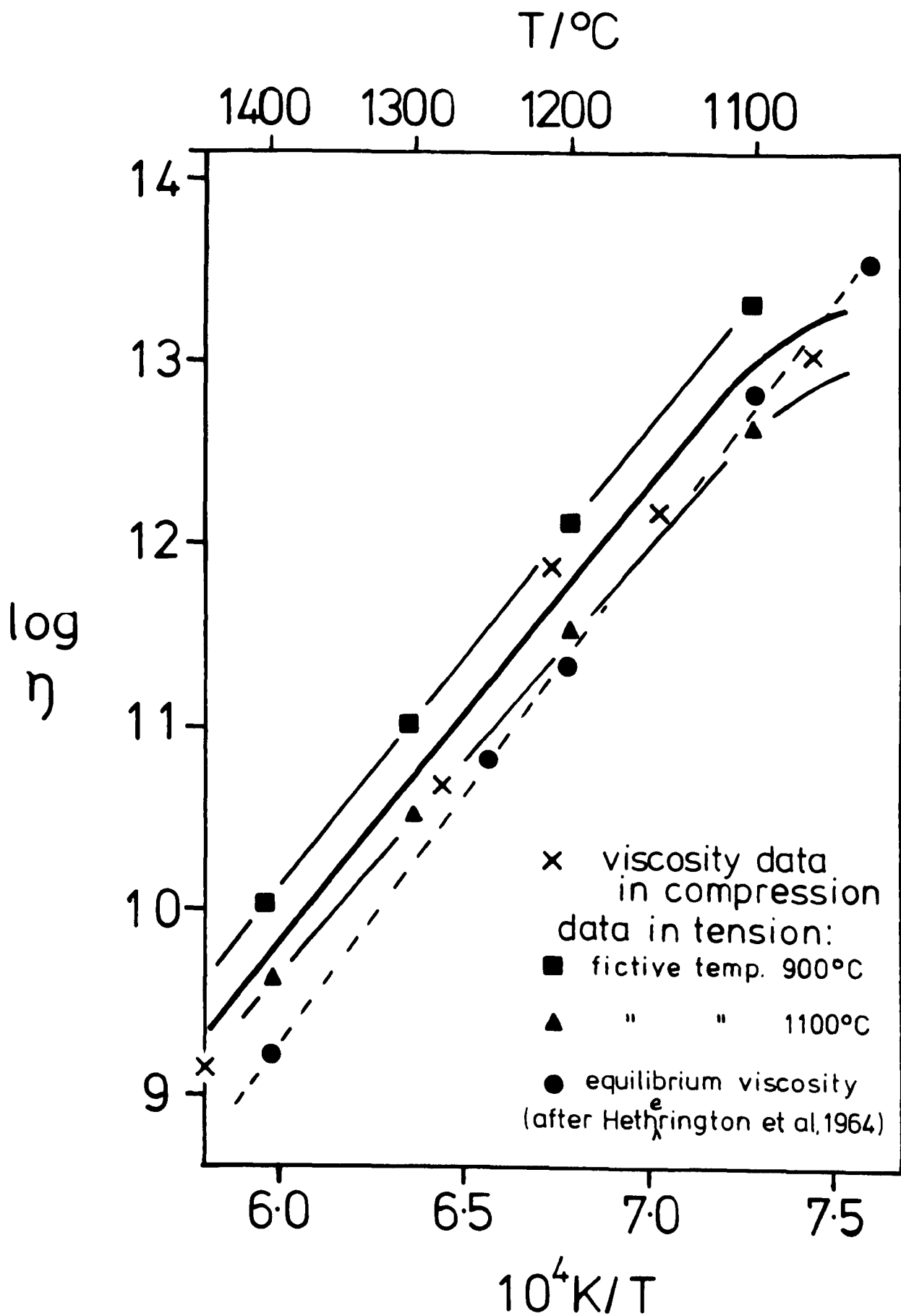
Electromagnetic radiation travels "in vacuo" with constant velocity, $c = 3 \times 10^{10} \text{ ms}^{-1}$. In a material media it travels with a slower velocity (v) where

$$v = c/n$$

and the frequency dependant constant n is the refractive index. Liquids and solids have values of n in the range 1.3 to 2.1. Glasses are optically isotropic and the value of n is important in optics since it is related to the refraction of light.

It can be shown that there is a direct relationship between refractive index (n) and the dielectric constant (ϵ) of a material and for an isotropic medium

Figure V.9 Comparative viscosity data for Spectrosil,
measured in compression (bold line), and
by the fibre-elongation technique
(after Hetherington et al., 1964).



$$n = \epsilon^{1/2}$$

The "immersion technique" was employed for the measurement of refractive index and involves the matching of the refractive index of the crushed material with that of organic liquid mixtures of known n . The refractive index of the liquid can then be measured on a standard refractometer.

An Abbé refractometer was used for values of up to 1.70 and higher values (1.70-1.90) were obtained from a Leitz-Jelley instrument.

V.9 Microscopy

Specimens were mounted in bakelite and ground and polished to $1\mu\text{m}$ finish using silicon carbide paper and diamond impregnated laps. Samples were etched with a dilute solution of hydrofluoric acid.

(a) Optical microscopy

Samples were examined on a Reichart MeF2 microscope and micrographs were taken either on flat-plates or with a 35 mm camera attachment.

(b) Scanning electron-microscopy and electron-probe microanalysis

Examination of specimen surfaces at higher magnification was carried out using a Cambridge Stereoscan 600 scanning electron-microscope. Samples were carbon coated to reduce charging by the electron beam and were earthed to the specimen holder.

Some well-characterized specimens were analysed using a Cameca "Camebax" electron-probe microanalyser at the United Kingdom Atomic Energy Authority Establishment, Harwell. The "Camebax", equipped with two wavelength-dispersive spectrometers, is sufficiently sensitive to give semi-quantitative X-ray analysis for oxygen and nitrogen in addition to energy-dispersive analysis of three or more heavy elements. Standardization using internal standards, correction for background and comparison of energy-dispersive spectrum with standard element spectra are carried out automatically. The ZAF corrections were performed on the heavy elements assuming the rest of the sample to be oxygen.

VI. Nitrogen Glass Formation

VI.1 Introduction

Exploration of glass formation was by study of compositions on planes with constant N:O ratio within the Jänecke prism for the M-Si-Al-O-N systems and by examination of the appropriate faces of the prism in the case of the M-Si-O-N or Si-Al-O-N glasses (see Chapter III.8). Mixes were prepared from the powders as described in Chapter V and the compositions investigated are shown as solid circles on the behaviour diagrams which follow. Fusion was carried out in the tungsten resistance furnace at 1600° or 1700°C for one hour.

Si-Al-O-N compositions were fused in either the tungsten resistance furnace at 1700°C when slow-cooling was required, or in the inductively-heated graphite furnace if higher temperatures or quenching were necessary. Various firing temperatures in the range 1700°-1850°C were employed in the latter case.

VI.2 The Mg-Si-Al-O-N system

The glass region on the 14 e/o nitrogen plane

after firing at 1600°C is quite small and nitrogen solubility is fairly limited (see Figure VI.1(a)). One of the residual crystalline products on the periphery of the glass region was $\alpha\text{-Si}_3\text{N}_4$ implying that reaction had been incomplete. It was observed that the glass region also followed the liquidus valley since peripheral compositions had not entirely melted at this temperature.

Increasing the firing temperature to 1700°C extends the glass region dramatically and the peripheral crystalline phases did not contain any unreacted starting material. Similarly, the glass region on the 17 e/o nitrogen plane also increases in area by about five times on raising the firing temperature from 1600° to 1700°C (see Figure VI.1(b)). In both cases the peripheral compositions, which contained some crystalline phases, had all been substantially liquid at the higher temperature.

It is clear that firing temperature is important in the incorporation of nitrogen in the glasses. However, raising the temperature from 1600° to 1700°C increased the weight-losses from 2-3 w/o up to 4-6 w/o and at temperatures in excess of 1750°C weight-losses were as high as 10 w/o. The nature of the volatiles was not ascertained since the use of a "cold-finger" revealed only an amorphous product either

Figure VI.1 The Mg-Si-Al-O-N glass-forming region
at 1600^o and 1700^oC on:
(a) the 14 e/o nitrogen plane
(b) the 17 e/o nitrogen plane

(a)

Mg-Si-Al-O-N
system
vertical plane

14e/oN

Glass formation
at:

--- 1600°C

— 1700°C

Major crystalline
phases:

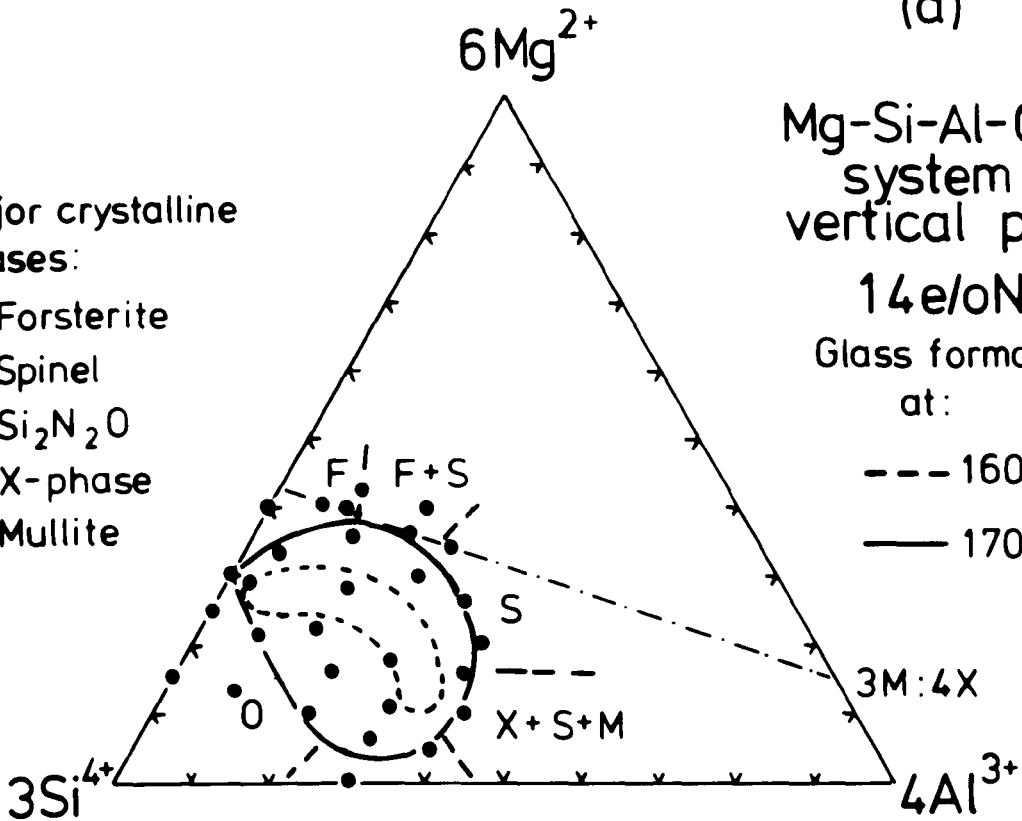
F - Forsterite

S - Spinel

O - $\text{Si}_2\text{N}_2\text{O}$

X - X-phase

M - Mullite



(b)

Mg-Si-Al-O-N
system
vertical plane

17e/oN

Glass formation
at:

--- 1600°C

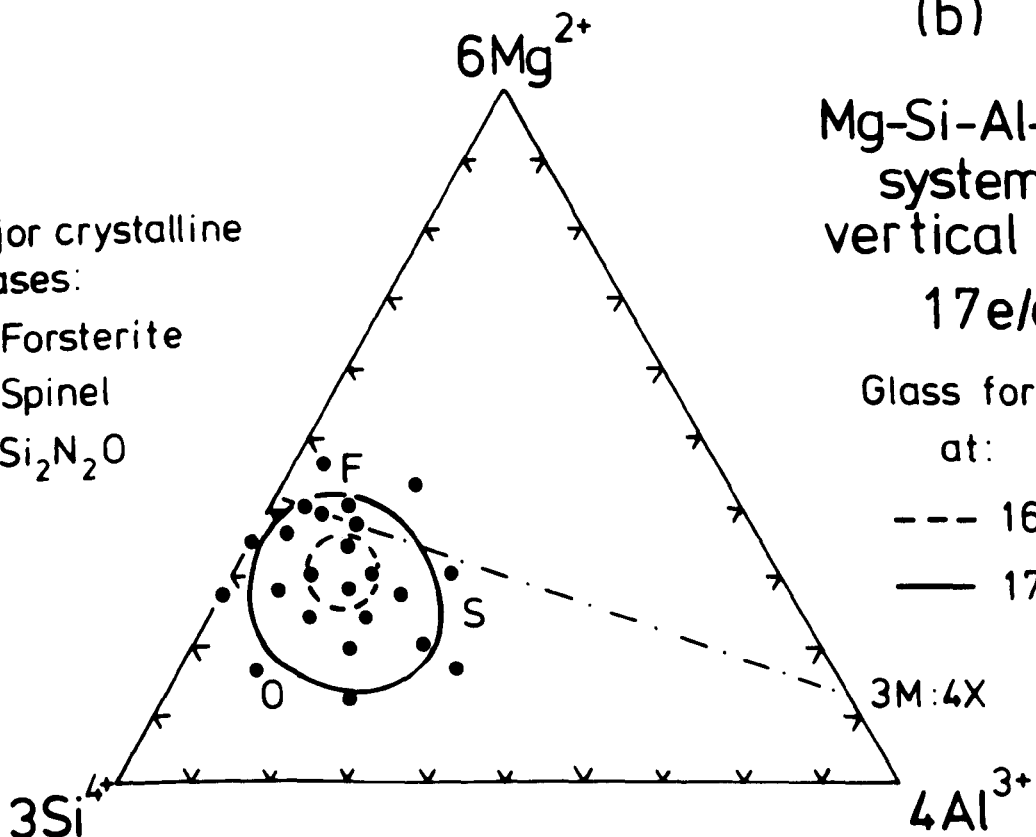
— 1700°C

Major crystalline
phases:

F - Forsterite

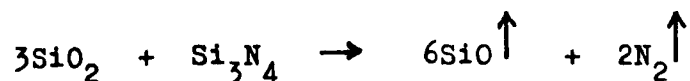
S - Spinel

O - $\text{Si}_2\text{N}_2\text{O}$

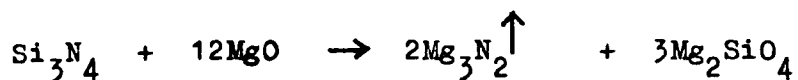


yellow-white or sometimes light-brown in colour.

Other work at Newcastle and elsewhere suggests that they must be silicon monoxide (SiO) and nitrogen produced by the reaction:

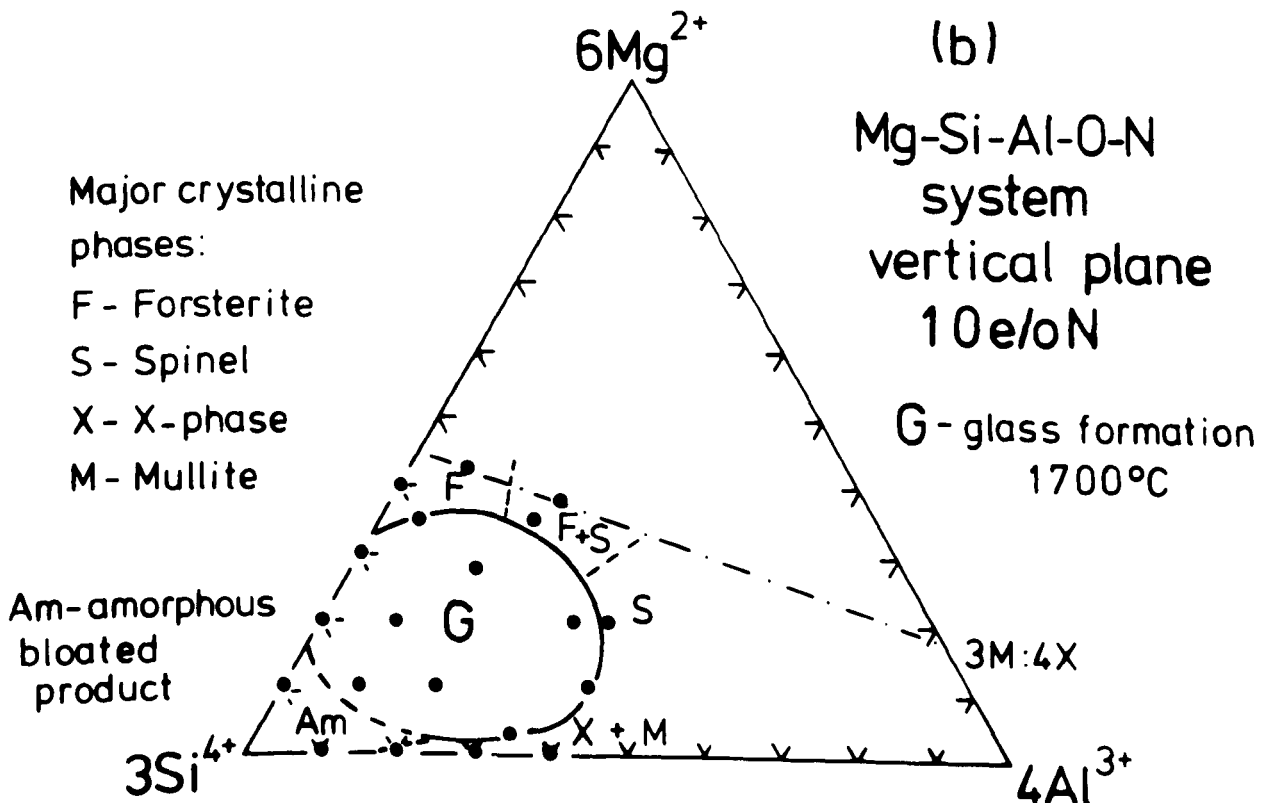
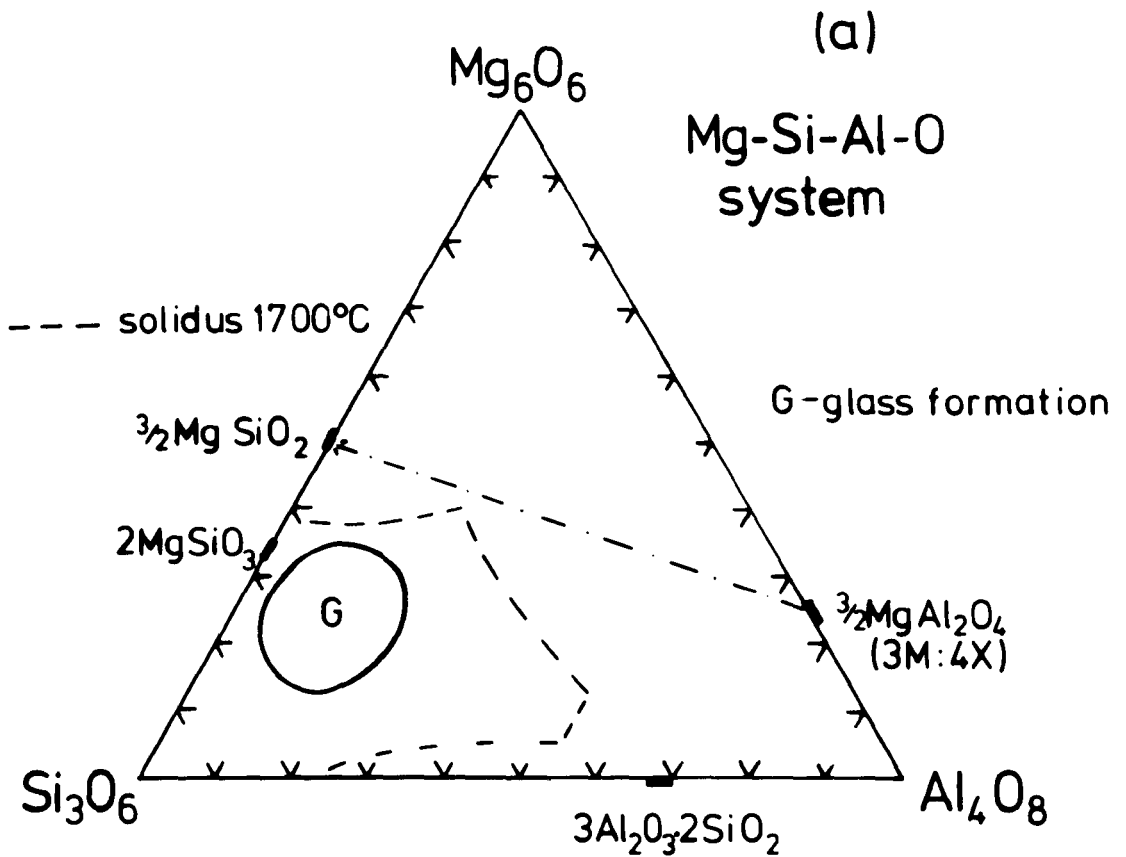


Volatile Mg_3N_2 may also be lost (Kelen & Mulfinger, 1968) according to the reaction proposed by Perera (1976),



Both reactions involve the loss of nitrogen. Since weight losses were high above 1750°C and melting and reaction incomplete below 1650°C , then a firing temperature of 1700°C was employed for all subsequent investigations.

The oxide glass region in the Mg-Si-Al-O system reported by McMillan (1964) is illustrated in Figure VI.2(a), and comparison with Figure VI.2(b) shows that 10 e/o (4 a/o) of nitrogen substitution increases the area of glass formation significantly and even extends it to the silicon-magnesium join on the behaviour diagram. With 10 e/o N, homogeneous glasses near and on the Si-Al-O-N basal plane were not obtained under slow cooling conditions ($250^\circ\text{C}/\text{minute}$). A frothy,



amorphous product was obtained with 90 e/o silicon but weight losses were high and the stability of such glasses is questionable (see later).

The glass-forming regions at 1700°C on the 14 e/o and 17 e/o nitrogen planes have been discussed previously and as shown in Figure VI.1(a) & (b) the size of vitreous region contracts above 10 e/o N addition. The 22 e/o nitrogen plane (see Figure VI.3(a)) shows the area of glass formation to be very small and it passes through the 3M:4X (metal:non-metal) plane. A phase designated as β'' -magnesium sialon was found in peripheral compositions either on or below the 3:4 plane and its nature and the composition are discussed in Chapter IX.

The glass-forming regions for 0, 10 and 22 e/o N are shown superimposed on each other in Figure VI.3(b). The immediate observation is that the glass region in this system initially expands and then contracts in size resulting in it moving away from the silicon corner of the diagram towards magnesium.

The glass composition with 22 e/o N

	Mg	Si	Al	O	N
e/o	36	57	7	78	22
a/o	22.3	17.6	2.9	49.0	9.2

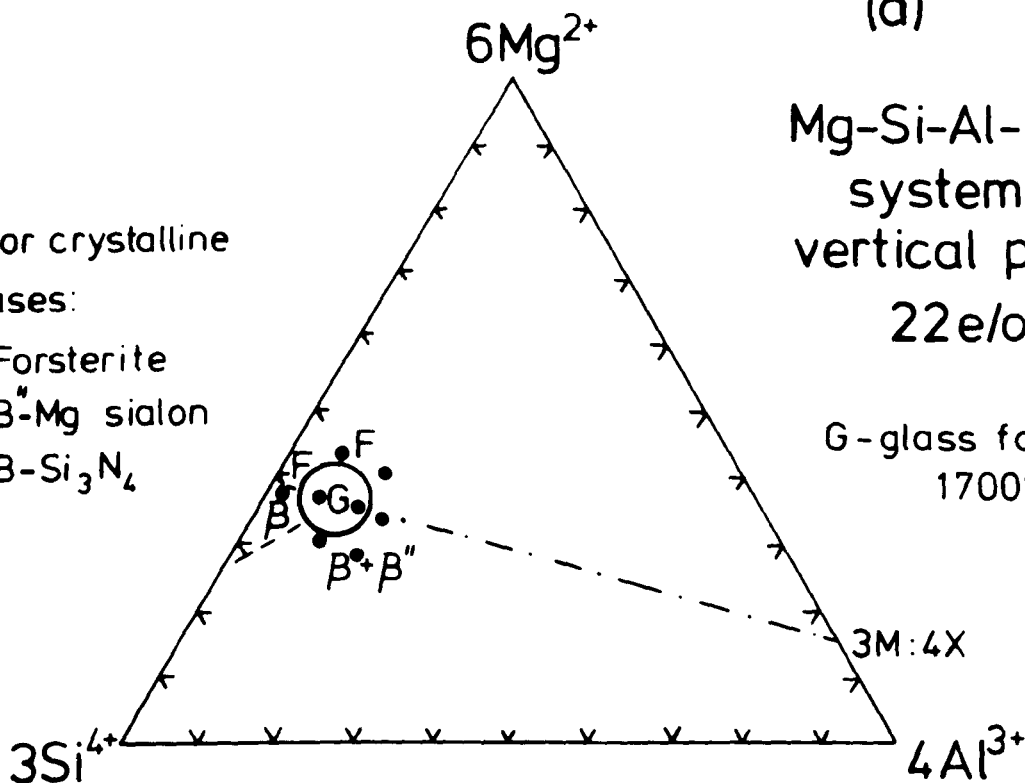
(a)

Mg-Si-Al-O-N
system
vertical plane
22e/oN

G-glass formation
1700°C

Major crystalline
phases:

F-Forsterite
 β "- β "-Mg sialon
 β - β - Si_3N_4

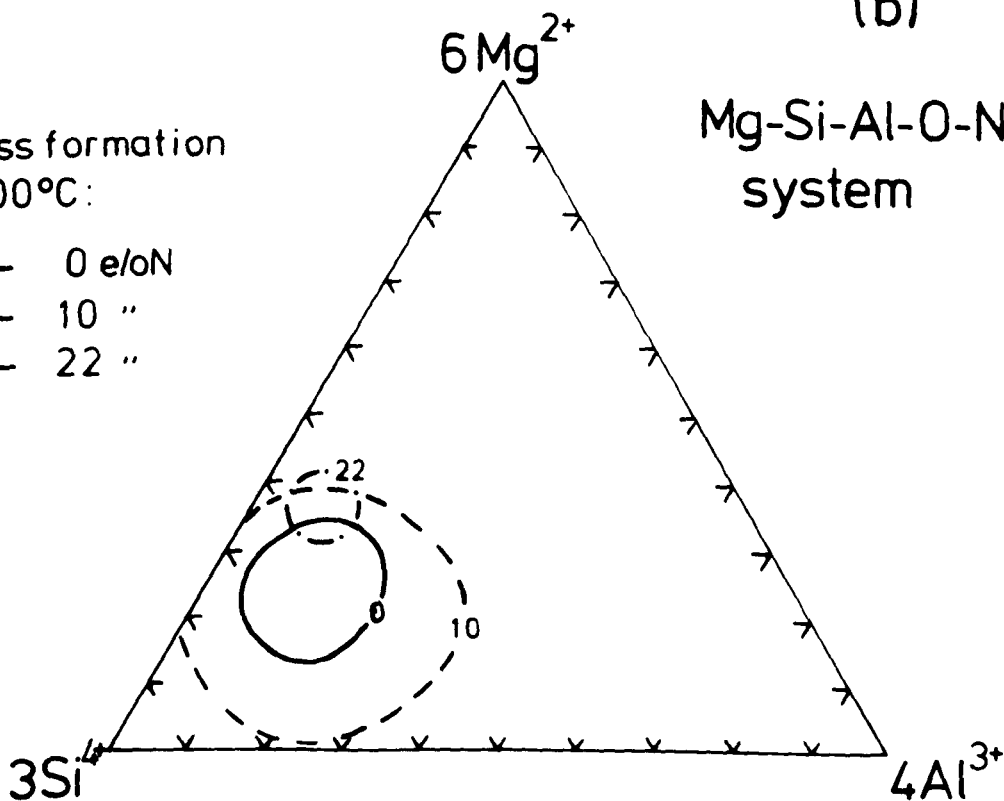


(b)

Mg-Si-Al-O-N
system

Glass formation
1700°C:

- 0 e/oN
- - - 10 "
- · - · 22 "



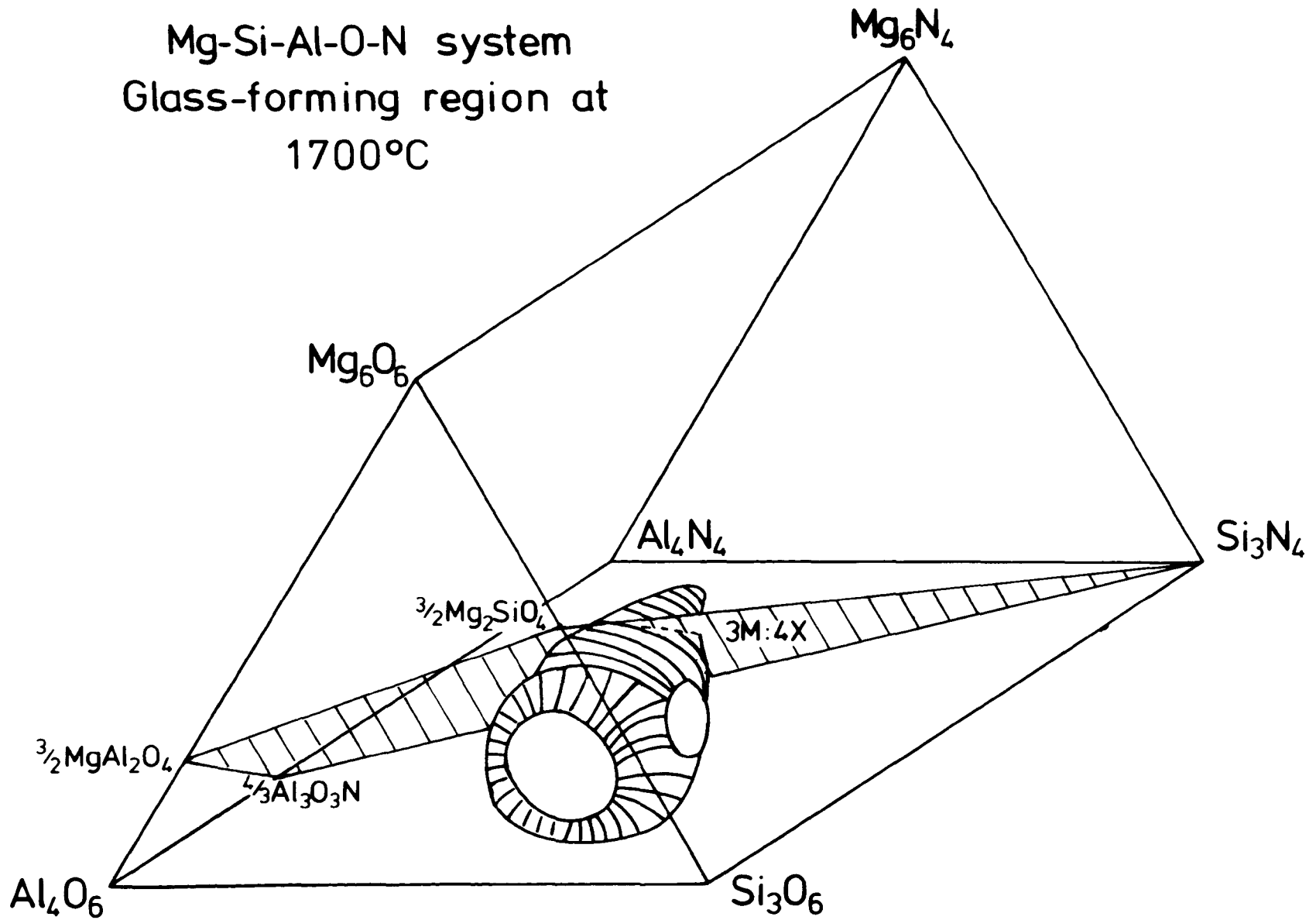
contains more magnesium than silicon plus aluminium and so the 1:1 ratio of modifier:network-former discussed in Chapter II is exceeded. It is probable that some magnesium enters the network in order to maintain the glass structure. McMillan (1964) proposed that this might occur because the field strength of the magnesium ion is quite high and closer to that of an "intermediate oxide" cation. Nitrogen also facilitates the change in the role of magnesium because although it is usually octahedrally coordinated by oxygen, it is always tetrahedrally coordinated in nitrides and so, presumably, also in nitrogen glasses.

The limit of glass formation in the Mg-Si-Al-O-N system is 25 e/o N (10.3 a/o) and corresponds to a composition $Mg_{22.9}Si_{16.7}Al_{3.7}O_{46.4}N_{10.3}$ which is a replacement of one in 5.5 oxygens by nitrogen. A three-dimensional representation of the glass-forming region is illustrated in Figure VI.4, and shows how the glass region passes through the 3M:4X plane.

Lochman (1979) has carried out preliminary investigations of glass formation in this system and he predicted a fairly wide glass region, although only a limited number of compositions were examined and no systematic approach was adopted.

Figure VI.4 The Mg-Si-Al-O-N glass-forming region
represented in three dimensions.

Mg-Si-Al-O-N system
Glass-forming region at
1700°C



VI.3 The Mg-Si-O-N system

Figure VI.5 shows the homogeneous glass-forming region on the Mg-Si-O-N face of the Jänecke prism at 1700°C. Vitrification did not give a homogeneous glass below 1650°C, but a phase-separated, unconsolidated amorphous product was obtained. The glass region is nearer the enstatite/forsterite composition than reported by Perera (1976). Weight losses within the glass region were about 2 w/o and electron-probe microanalysis indicated the composition of the starting mix and the resultant glass were extremely close:

	Mg	Si	O	N
starting composition	18.6	21.7	55.6	4.1
average EPMA results	18.8	21.5	55.7	4.0

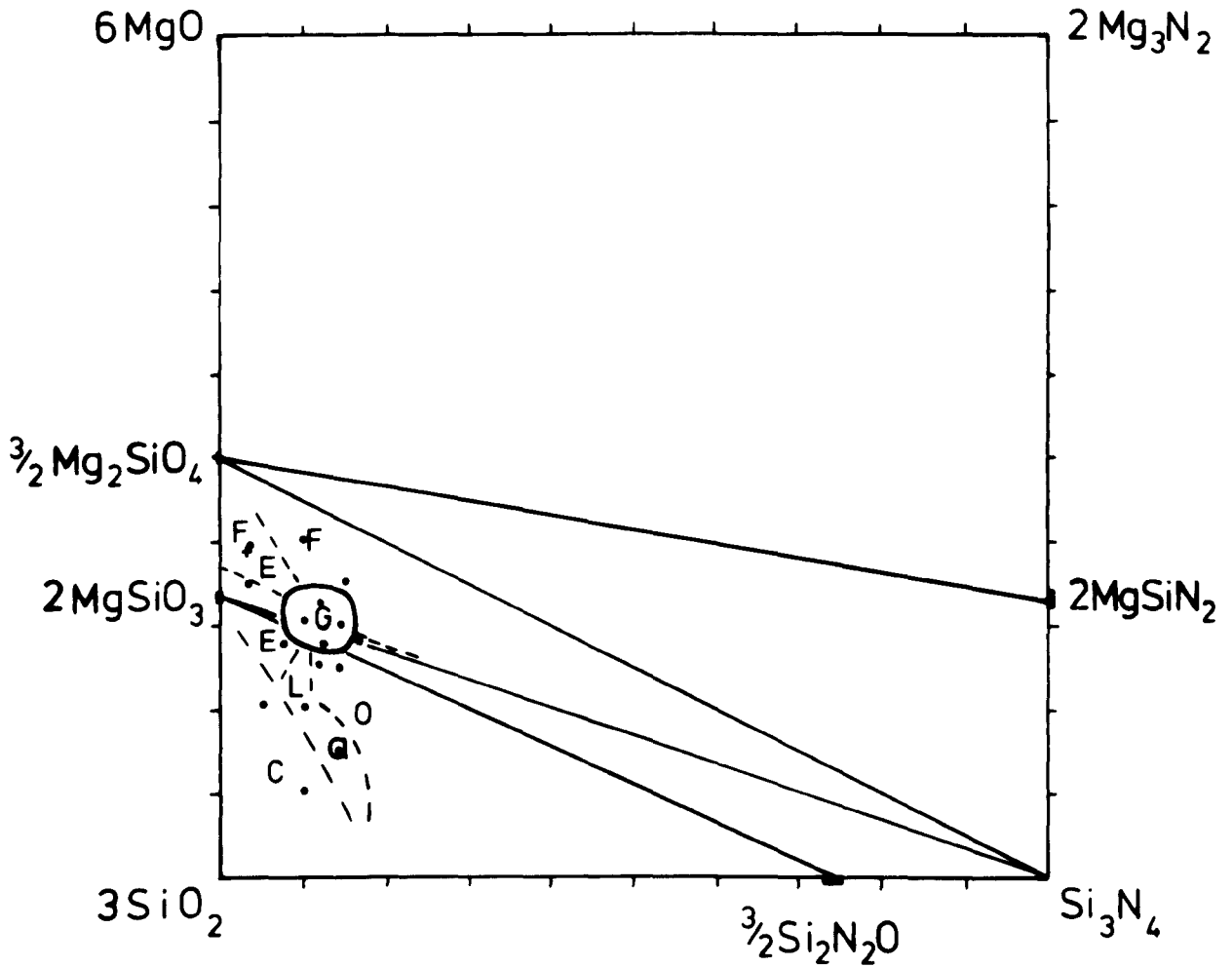
Small weight losses are consistent with the loss of SiO and N₂ as discussed previously.

The glass region shown in Figure VI.5 must therefore be correct and is appreciably different in composition to that reported by Perera (1976) and shown in Figure III.3. The discrepancy might be attributed to the high weight losses (10 w/o) that Perera encountered during his work. If the compositions had lost silicon as silicon monoxide, then the glasses would have been more magnesium-rich

Figure VI.5 The Mg-Si-O-N glass-forming region at 1700°C.

Mg-Si-O-N system

1700°C



G - Glass forming region

L - region of 2 liquids → amorphous product

Major crystalline phases:

C - Cristobalite E - Enstatite

F - Forsterite O - silicon oxynitride

a - amorphous product + Si₂N₂O
(2-phase)

than indicated and closer in composition to the vitreous region shown in the present work. Loehman (1979) also reports a Mg-Si-O-N glass region close to the eutectic composition in good agreement with the present findings.

VI.4 The Y-Si-Al-O-N system

An optimum firing temperature of 1700°C was used when investigating the Y-Si-Al-O-N system. The oxide glass region (expressed in equivalents) is reproduced from Makishima (1978).

The area of glass formation increases with increasing nitrogen concentration up to approximately 10 e/o N. Comparison of Figure VI.6(a) (0 e/o N) and Figure VI.6(b) (10 e/o N) indicates the nature of the expansion, whereas on further nitrogen incorporation the area of glass formation contracts as shown in Figure VI.7(a) (16 e/o N) and Figure VI.7(b) (20 e/o N) and is reduced dramatically at 22 e/o N addition (see Figure VI.8(a)). Maximum nitrogen incorporation is between 25 and 28 e/o N (11-12.5 a/o) and corresponds to a composition $Y_{16}Si_{13}Al_{11}O_{48}N_{12}$, that is, one in five oxygen atoms are replaced by nitrogen.

Figure VI.6 The Y-Si-Al-O-N glass-forming regions on:

(a) the 0 e/o nitrogen plane

(after Makishima, 1978)

(b) the 10 e/o nitrogen plane (1700°C).

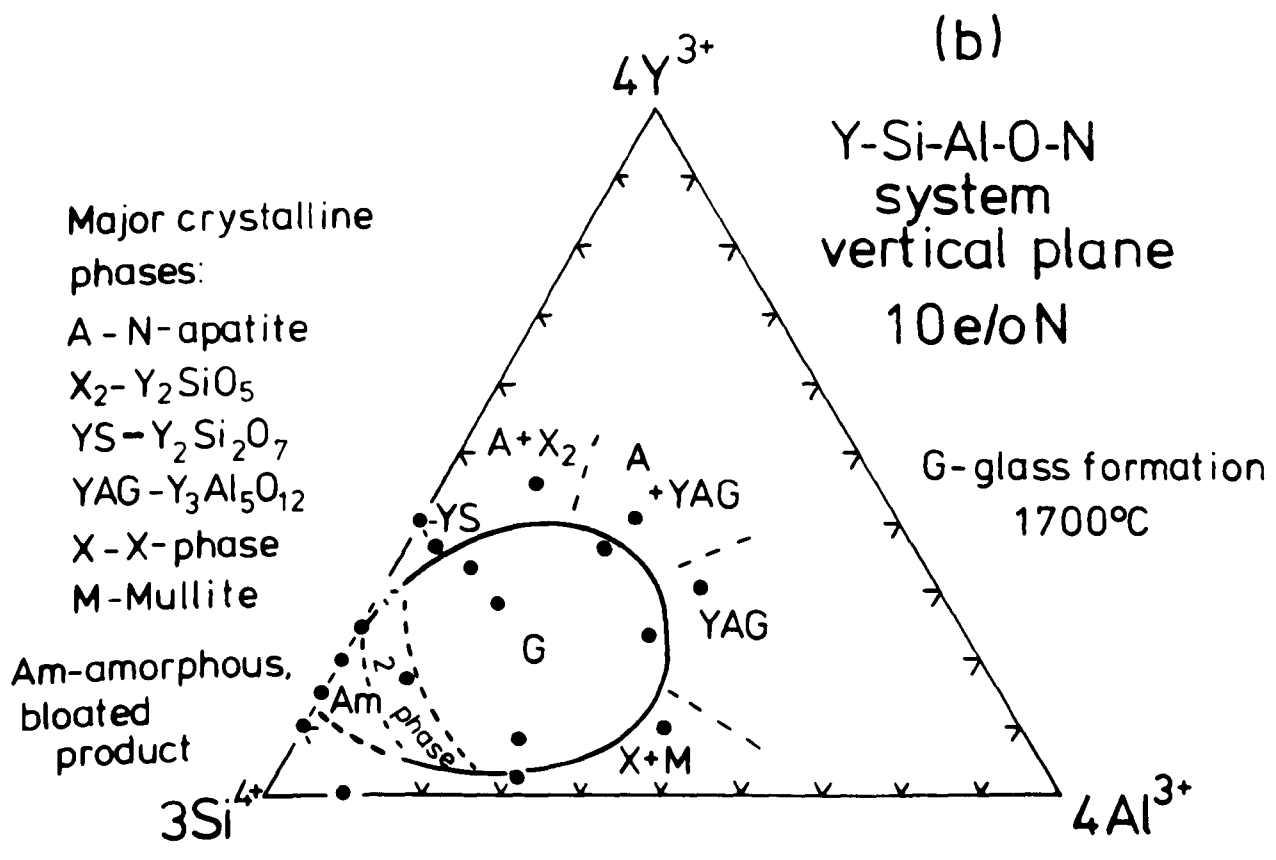
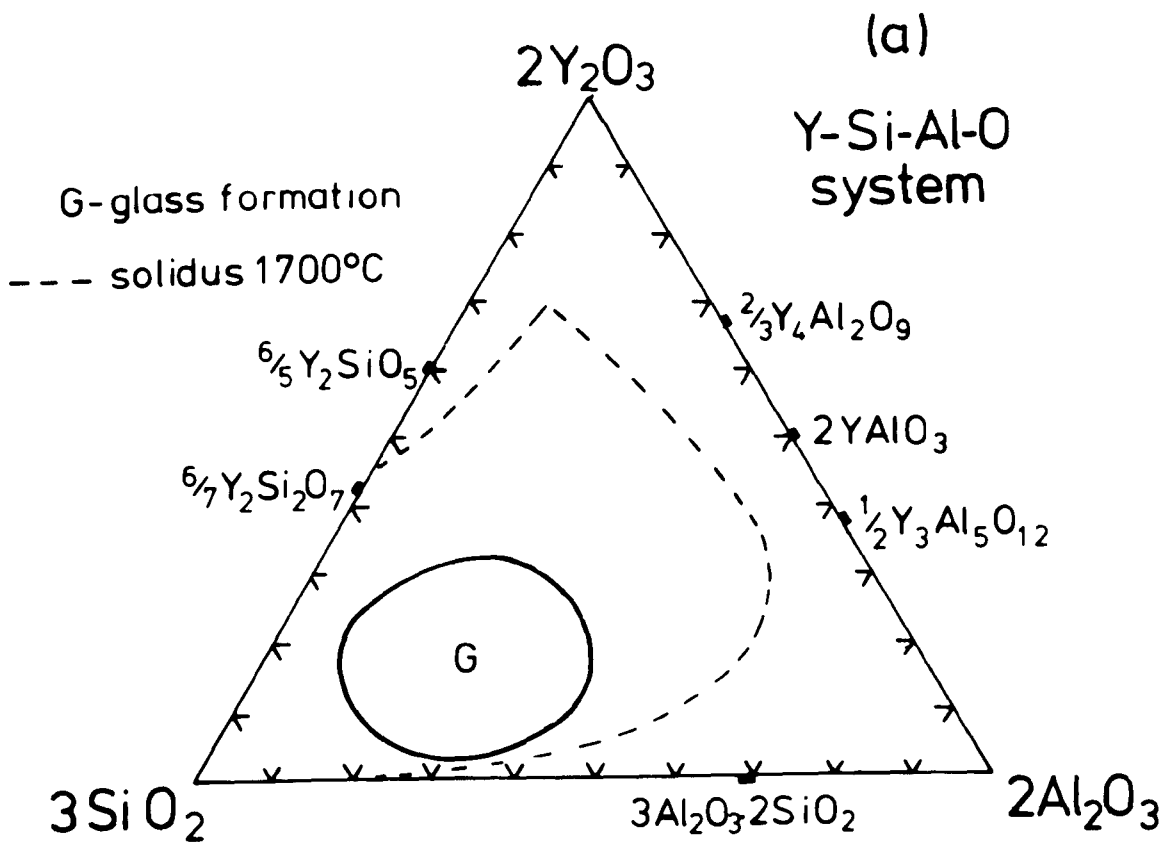


Figure VI.7 The Y-Si-Al-O-N glass-forming regions
at 1700°C on:
(a) the 16 e/o nitrogen plane
(b) the 20 e/o nitrogen plane.

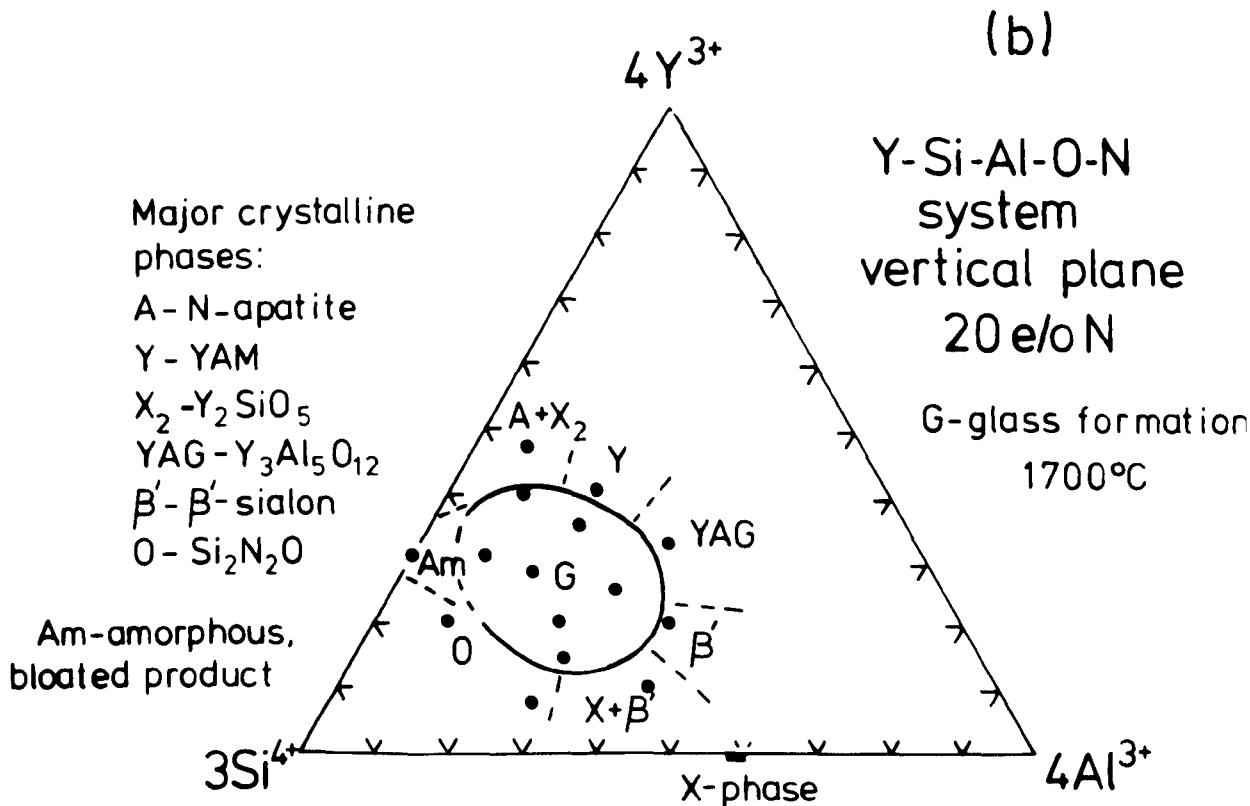
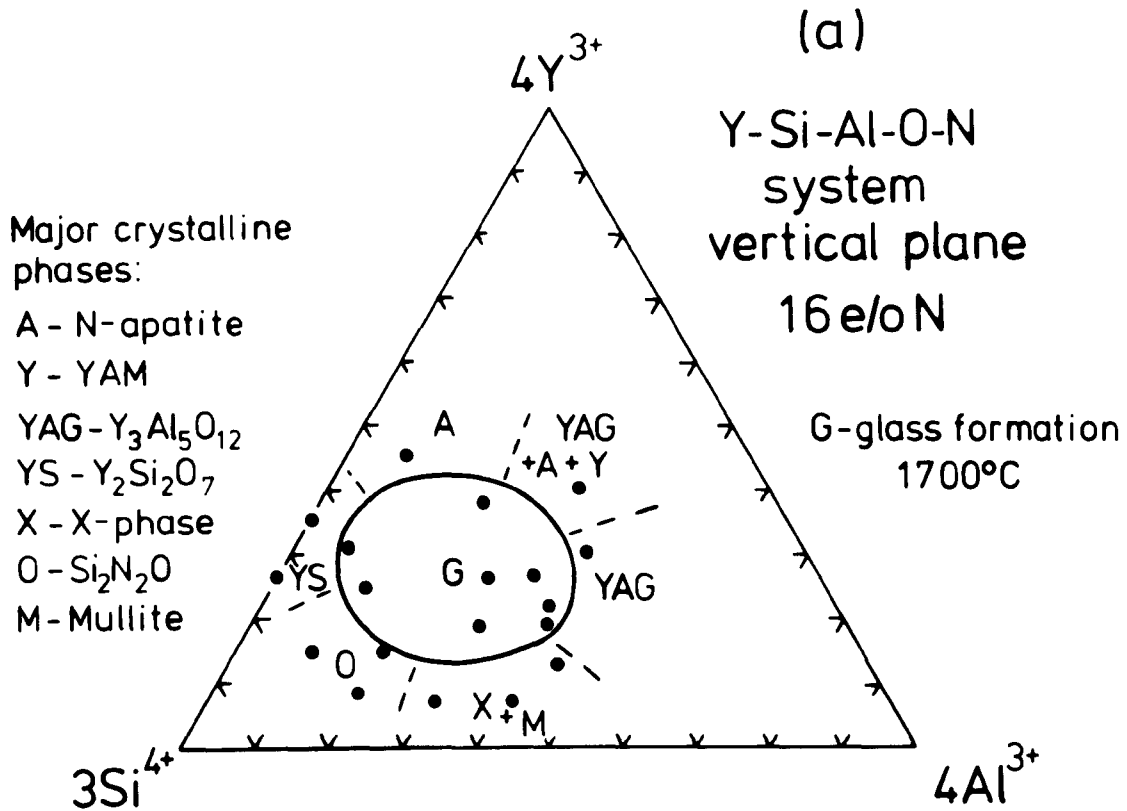
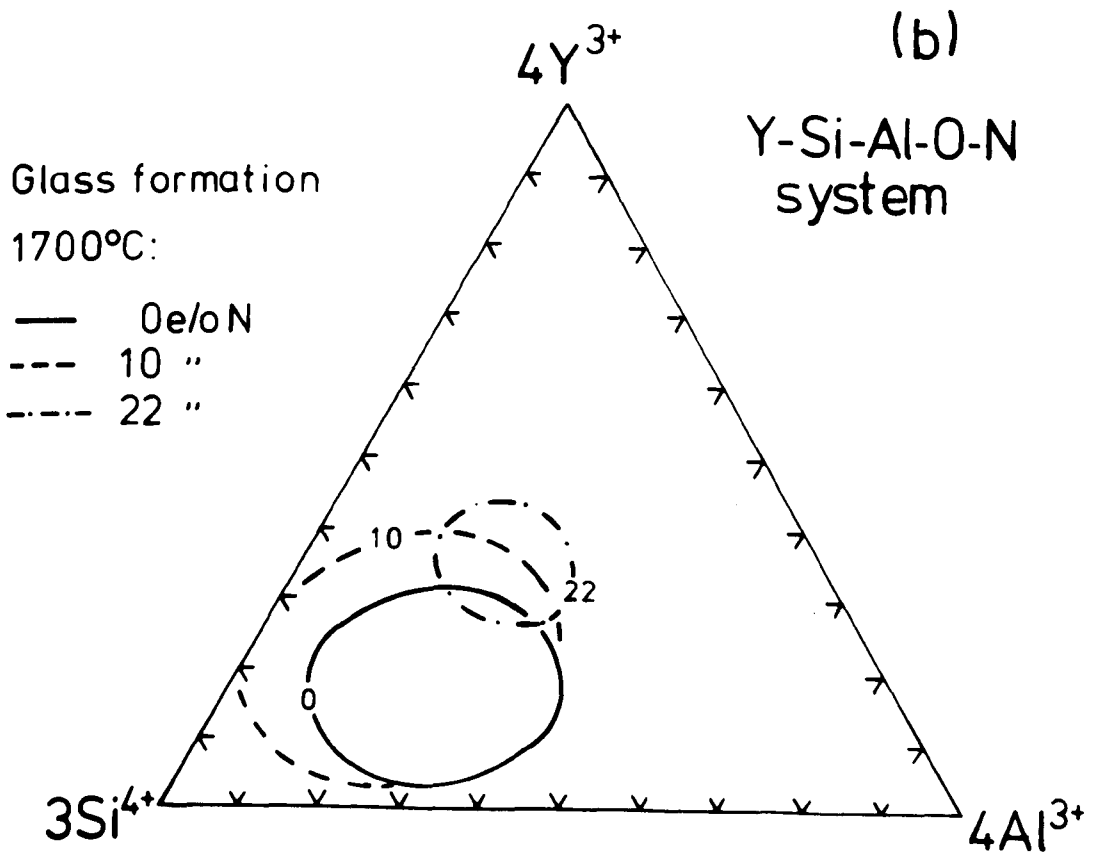
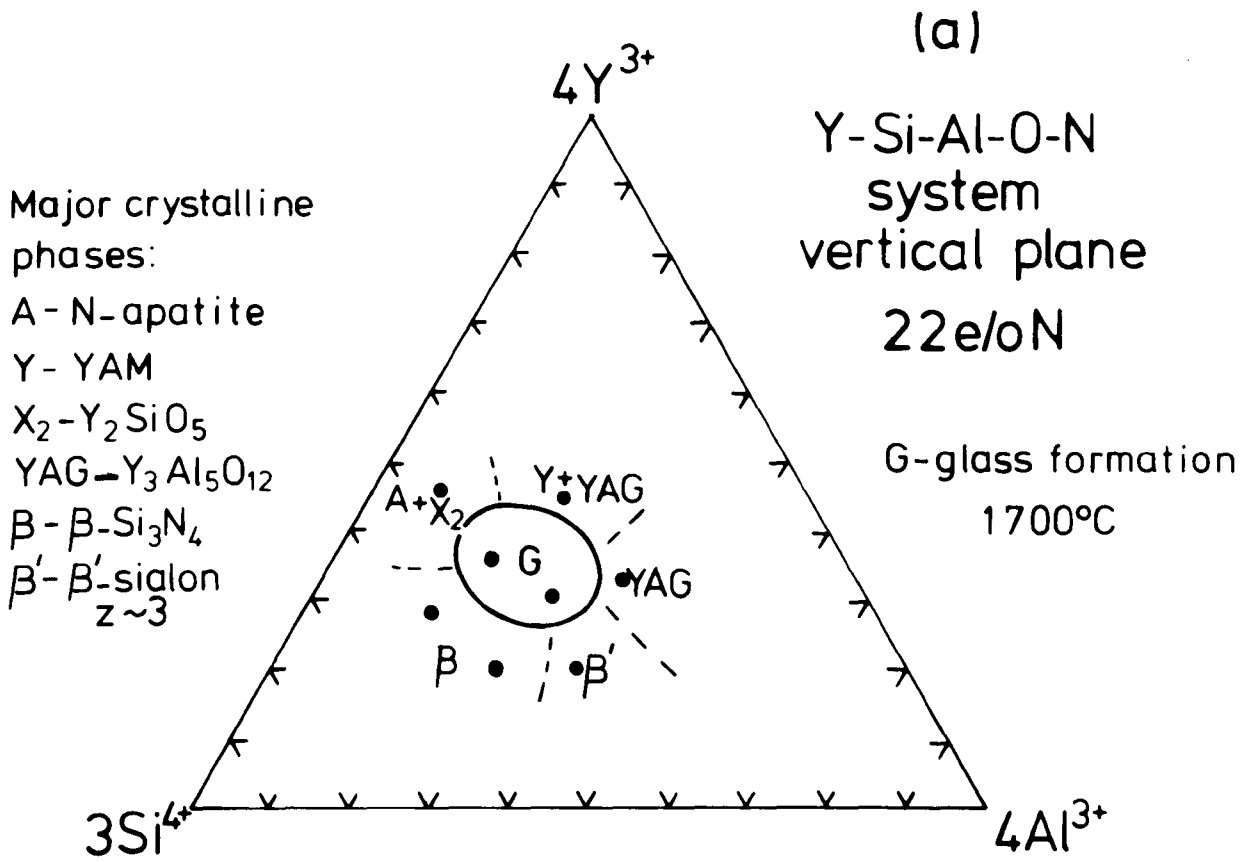


Figure VI.8 The Y-Si-Al-O-N glass-forming regions
at 1700°C on:
(a) the 22 e/o nitrogen plane
(b) the 0, 10 and 22 e/o nitrogen planes.



Amorphous products in the Y-Si-O-N system were obtained on the 10 and 20 e/o nitrogen planes but with different Y:Si ratios (see Figures VI.6(b) and VI.7(b)), but no glasses were formed on the 16 e/o nitrogen plane (Figure VI.7(a)).

The Y-Si-O-N glasses observed were phase-separated and invariably bloated, being full of large bubbles. The use of alumina crucibles coated with boron nitride powder for firing Y-Si-O-N compositions containing 20 e/o N gave bloating followed by consolidation, whereas if isostatically pressed boron nitride crucibles were employed no consolidation and only bloating was observed. Since the top of the alumina crucibles was not entirely coated with boron nitride powder, the rising fusion mixture probably reacted with some alumina to reduce its viscosity and melting point and so release gas bubbles resulting in homogeneous glass formation.

High weight losses were observed in all Y-Si-O-N compositions. The mixes with 20 e/o N often gave losses higher than 10 w/o and a yellow/brown amorphous deposit, assumed to be SiO and formed as previously discussed, was found in the furnace. Even in the presence of aluminium, weight losses (2-5 w/o) were high on this nitrogen plane whereas other Y-Si-Al-O-N

compositions showed much lower weight losses, approximately 0.5-2 w/o. No explanation can be given for these observations.

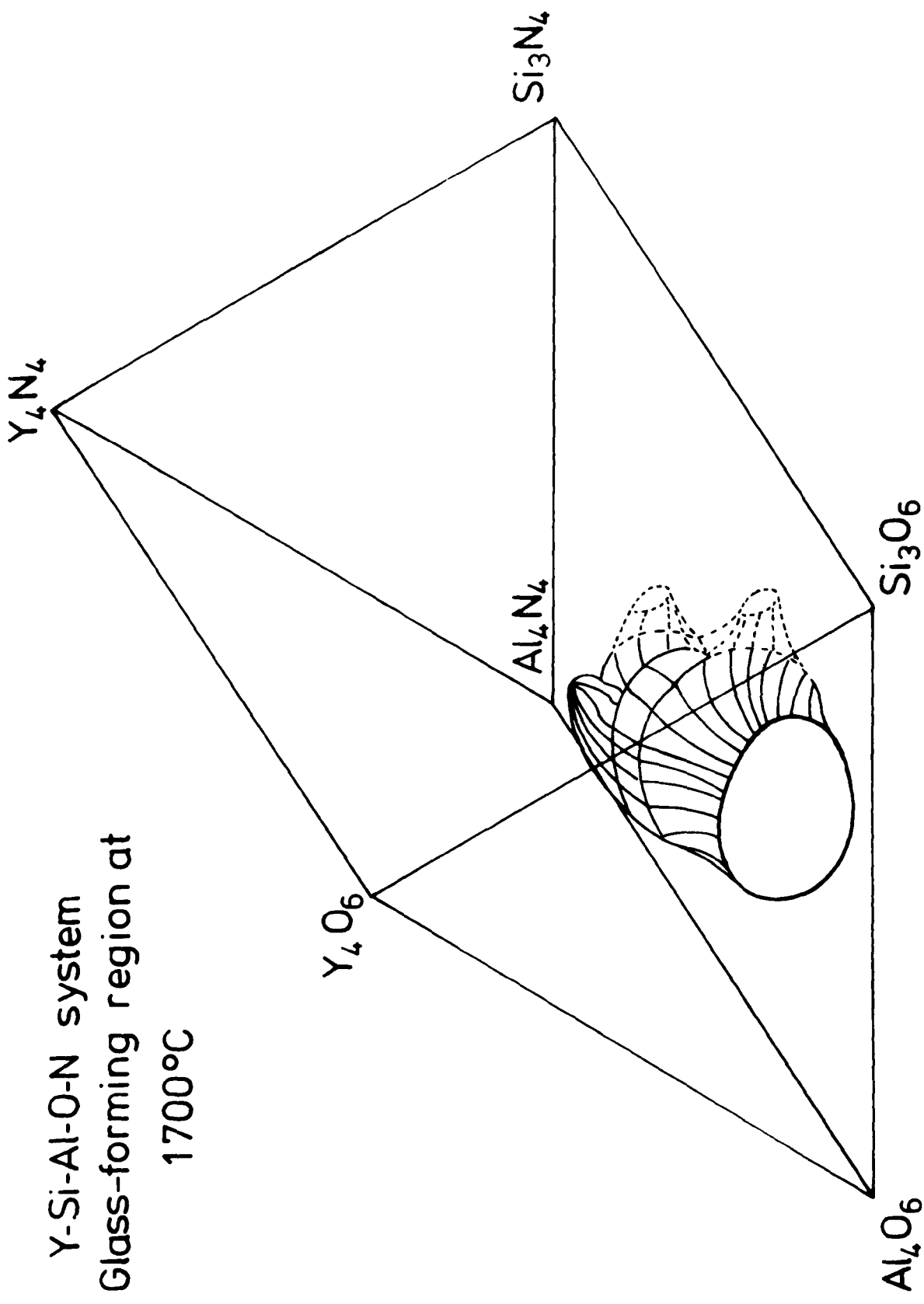
A three dimensional representation of the complete Y-Si-Al-O-N glass region is shown in Figure VI.9 and a superimposed picture of glass formation on the 0, 10 and 22 e/o nitrogen planes in Figure VI.8(b) illustrates how the glass region changes on addition of nitrogen. It is apparent that nitrogen incorporation produces similar effects in both the magnesium and yttrium sialon glass systems. The expansion at 10 e/o N is not as great with yttrium as with magnesium, but the maximum nitrogen solubility is higher.

Compositions on the 22 e/o nitrogen plane (Figure VI.8(a)) with high silicon contents showed peripheral crystalline phases of either β -Si₃N₄ or β' -sialon, depending on the aluminium content, in conjunction with substantial amounts of glass. It is clear that α -Si₃N₄ (in the starting batch) transforms during firing to precipitate β or β' from the liquid and so provides further evidence that the α - β (or β') transformation is a solution-precipitation reaction requiring the presence of a liquid.

Loehman (1978, 1979) describes a fairly large glass-forming region in the Y₂O₃ - SiO₂ - AlN sub-

Figure VI.9 The Y-Si-Al-O-N glass-forming region represented
in three dimensions.

Y-Si-Al-O-N system
Glass-forming region at
1700°C



system, but he was unable to form stable Y-Si-O-N glasses. As discussed in Chapter III it is clear that the complete investigation of any M-Si-Al-O-N system cannot be carried out effectively by the study of more restricted sub-systems. It is probably fortuitous that Loehman was able to produce glasses with up to 7.5 a/o N in his investigation.

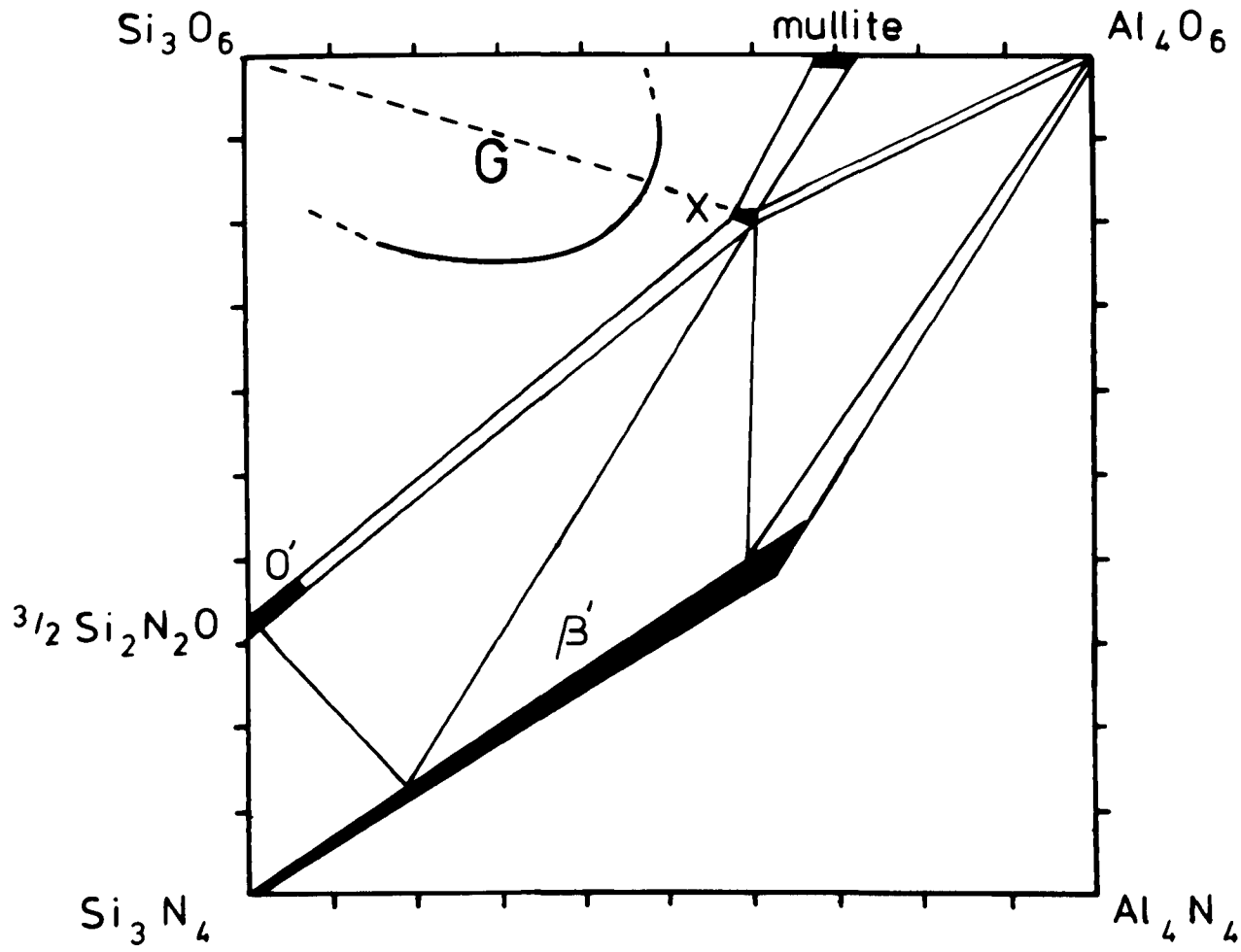
VI.5 The Si-Al-O-N system

The liquid region in the Si-Al-O-N system is quite extensive at 1700°C (see Figure III.2) and glasses have been obtained from compositions within these composition limits (Roebuck, 1978). In the present work such glasses are shown to be more than usually unstable because it was necessary to quench the liquid at cooling rates greater than 500°C/minute to obtain a completely vitreous product. However, it is proposed that under such conditions glass formation occurs within the area shown in Figure VI.10. The liquid close to the X-phase composition was very fluid (qualitative observation) and, as expected, the viscosity of the liquid at any given temperature increased as the composition approached the Si₃O₆ corner. However, weight losses also increased and were attributed to SiO volatilisation caused by contact with the reducing environment of the

Figure VI.10 The Si-Al-O-N system: glass formation
at 1700^o-1850^oC under fast-cooling
conditions (> 500^oC/minute).

Si-Al-O-N system

G-glass formation (quenching)



inductively-heated graphite furnace.

The above compositions examined under slower cooling conditions in the same furnace gave different proportions of the following: X-phase, mullite, $\text{Si}_2\text{N}_2\text{O}$ and cristobalite plus some glassy phase. Compositions fired in the tungsten resistance furnace at 1700°C did not vitrify although some had been liquid at temperature. An exception was a high silicon, low nitrogen mix ($\text{Si}_{30}\text{Al}_{4.5}\text{O}_{61}\text{N}_{4.5}$) which gave an amorphous, but bloated product, with about 7 w/o loss, and probably contained very little nitrogen.

It is clear that bulk, homogeneous glasses in the Si-Al-O-N system are not very stable and do not form by conventional fusion and relatively slow cooling methods.

VI.6 Other glass-forming systems

Glass formation occurs in a variety of other M-Si-Al-O-N systems where oxide vitreous regions are already known to exist (Hampshire, 1979). In particular calcium sialon glasses are of interest since they occur as a second phase during the production of α' -sialons (Hampshire et al., 1978). Also, calcium is often a major impurity in the

grain-boundary glasses of sintered nitrogen ceramics. Figures VI.11(a) and (b) show glass formation on the 20 e/o and 25 e/o nitrogen planes (see Hampshire, 1979). The maximum nitrogen incorporation is about 26 e/o N (11 a/o) corresponding to a composition $\text{Ca}_{18}\text{Si}_{18}\text{Al}_6\text{O}_{47}\text{N}_{11}$, and is of the same order as reported for both yttrium and magnesium sialon glasses.

The Ca-Si-O-N glass region is shown in Figure VI.12 (see Hampshire, 1979) and is very similar in size and composition to that of the Mg-Si-O-N system. It is suggested that a similar expansion of the glass-forming region occurs in the Ca-Si-Al-O-N system as was discussed previously for both the magnesium and yttrium systems.

Lang et al. (1979) obtained glassy phases at 1350°C in the lanthanide-sialon system with the general composition 50-60 m/o SiO_2 , 10-15 m/o Ln_2O_3 and 30-40 m/o AlN. Glasses have been prepared (Spacie, 1980) in the Nd-Si-Al-O-N system with a cation ratio of 28 e/o Nd : 56 e/o Si : 16 e/o Al and up to 25 e/o nitrogen incorporation. It is suggested that glass formation in the neodymium system is similar to that of the yttrium system since both are trivalent and close to each other in the Periodic System.

Figure VI.11 The Ca-Si-Al-O-N glass-forming regions

on:

(a) the 20 e/o nitrogen plane

(1600° and 1700°C)

(b) the 25 e/o nitrogen plane

(1700°C)

(after Hampshire, 1979).

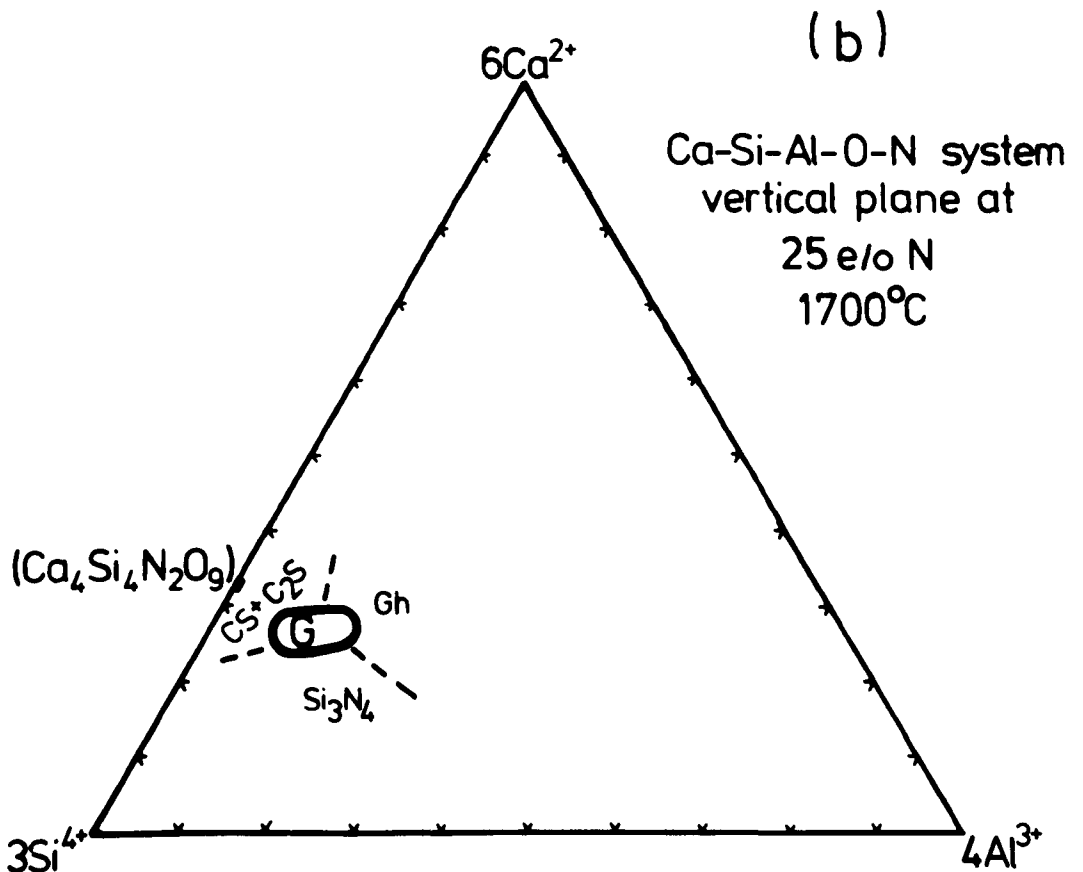
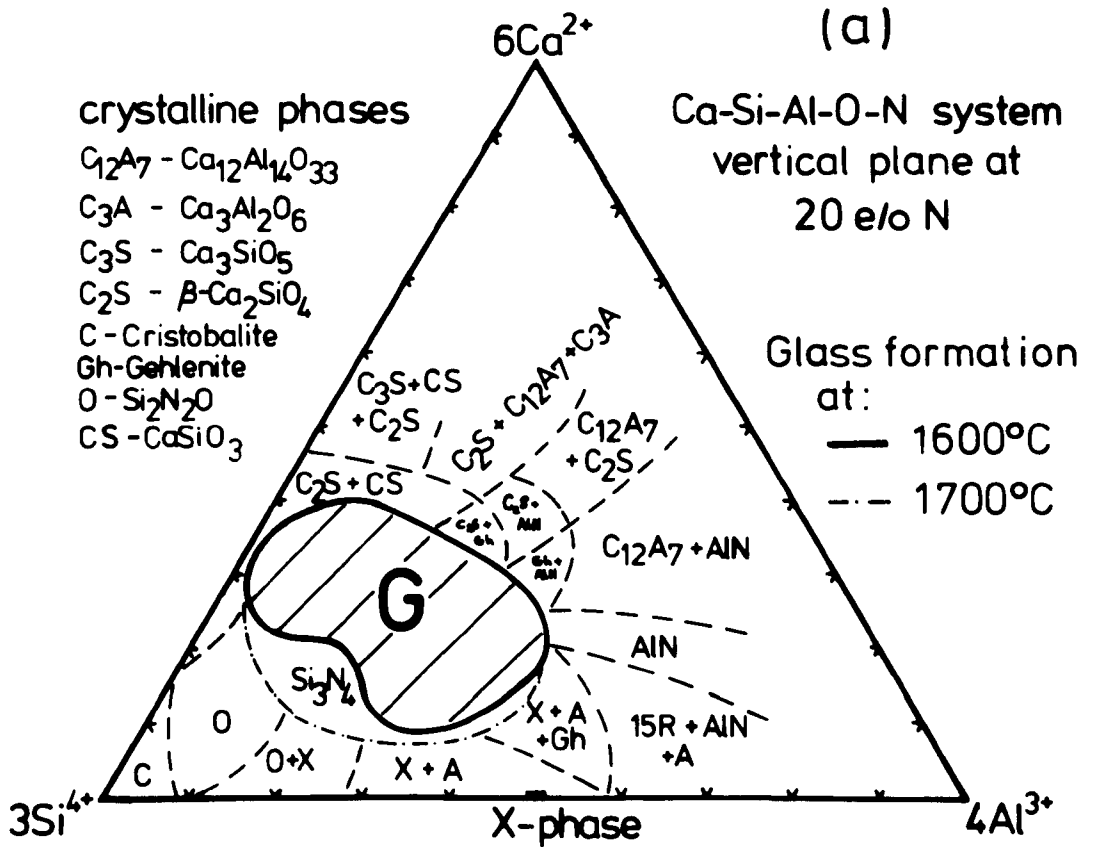
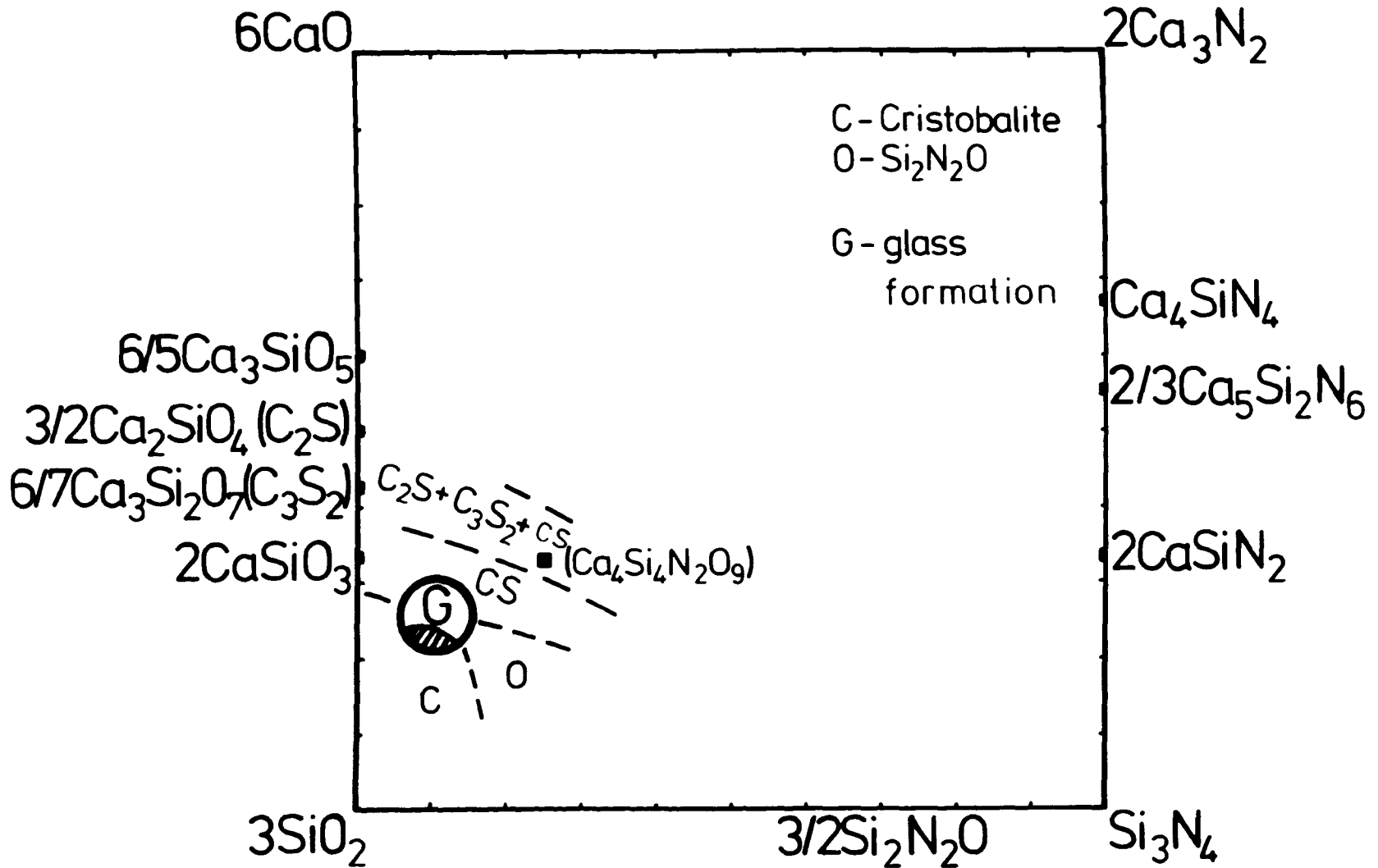


Figure VI.12 The Ca-Si-O-N glass-forming region
at 1700°C (after Hampshire, 1979).

Ca-Si-O-N system 1700 °C



VI.7 Conclusions

The amount of nitrogen that can be incorporated in M-Si-Al-O-N glasses is in the range 10.3-12.5 a/o which corresponds to a replacement of oxygen by nitrogen of about one atom in five. The cation composition of the highest nitrogen-containing glasses is variable and depends on the particular system. The glass regions generally increase in area on addition of about 10 e/o N (~ 4 a/o) and on further substitution the area diminishes in size until no further substitution of nitrogen for oxygen can be made in the glass structure. It is suggested that glass formation in the majority of M-Si-Al-O-N systems will follow the same pattern and that the maximum solubility will be of the same order.

Mg-Si-O-N and Ca-Si-O-N glasses can be produced reasonably easily. However, although there is extensive liquid formation in the Y-Si-O-N system, homogeneous Y-Si-O-N glasses occur only when some impurity is present to lower the viscosity and melting point.

Quenching is necessary to obtain homogeneous Si-Al-O-N glasses although some vitreous phase often forms in conjunction with crystalline material when slower cooling is employed.

VII. Properties of Nitrogen Glasses

VII.1 Introduction

Property measurements were carried out on glasses in the magnesium, yttrium, calcium and neodymium sialon systems. A cation composition of 28 e/o M : 56 e/o Si : 16 e/o Al was employed to enable comparisons to be made both within the particular M-Si-Al-O-N system and between individual systems when replacing oxygen by nitrogen. This cation composition will be subsequently referred to as the "standard cation composition". One central Mg-Si-O-N glass composition was also examined.

Properties investigated were:

- (a) viscosity and glass transition temperature (T_g)
- (b) crystallization temperature (T_c)
- (c) optical properties, i.e. transmission in the UV and IR spectral regions and refractive index.

Electrical properties were studied on selected magnesium and calcium glasses at Durham University and are discussed in an Appendix.

VII.2 Viscosity

The change in glass transition temperature (T_g) for the four sialon glass systems are presented in Figures VII.1(a)&(b) and VII.2(a)&(b), and indicate an almost linear increase of T_g with nitrogen content. The yttrium glass series shows a slight apparent deviation from linearity but this is probably due to uncertainties in the compositions of the glasses. Figure VII.3 shows that the value of T_g is increased in two ways: (i) by substituting nitrogen for oxygen, and (ii) by changing the modifying cation.

The relationship between T_g and viscosity was discussed in Chapter V. Viscosity data for varying amounts of nitrogen incorporation in the four M-Si-Al-O-N glass systems are presented in Figures VII.4-7 inclusive. It is clear that there is a marked increase in viscosity with nitrogen content, which supports the observations of Elmer & Nordberg (1967) and Harding & Ryder (1970) that chemically dissolved nitrogen increases viscosity or softening point in glasses.

Comparative plots of viscosity at constant N:O ratios of 10 and 18 e/o N but with different modifying cations are presented in Figures VII.8 and 9, respectively. It is evident the highest values of

Figure VII.1 Variation of glass transition temperature
(T_g) with nitrogen concentration:
(a) the Ca-Si-Al-O-N system
(b) the Mg-Si-Al-O-N system.

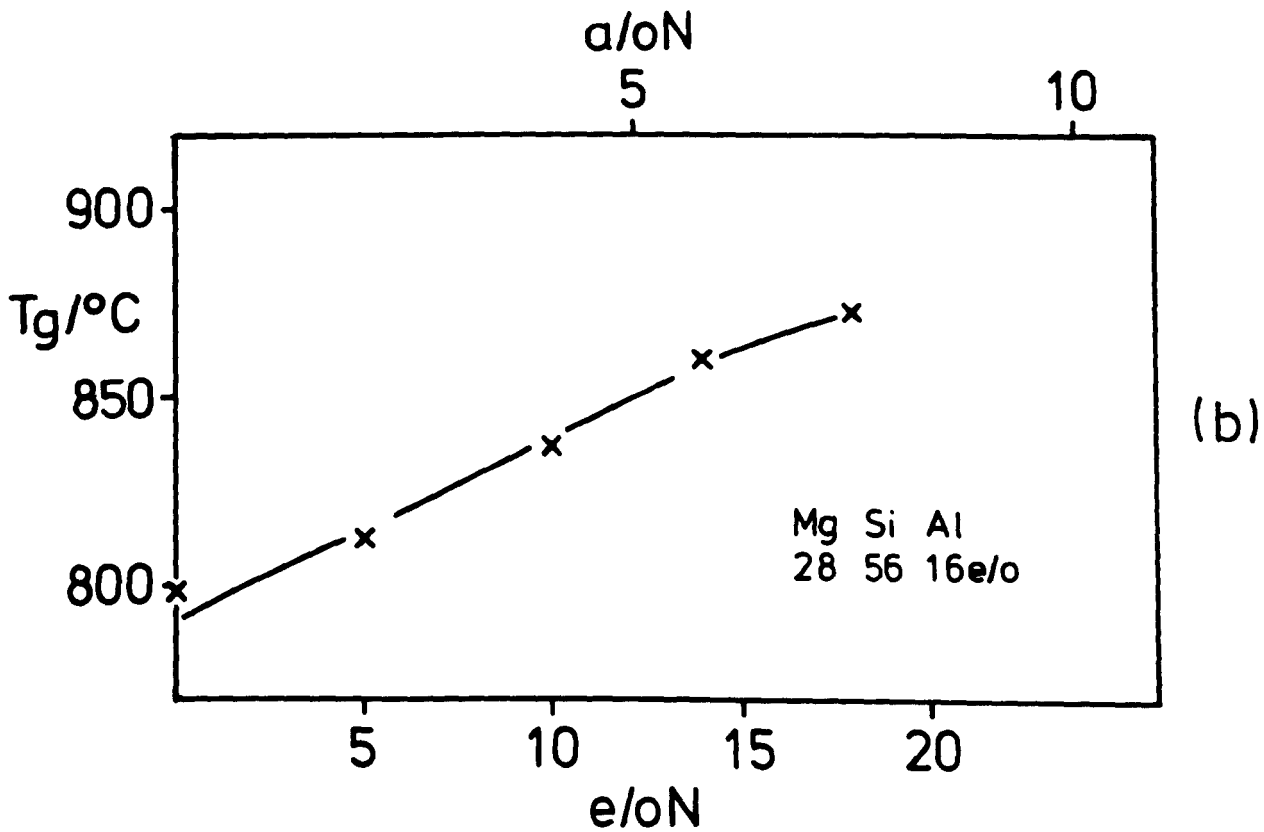
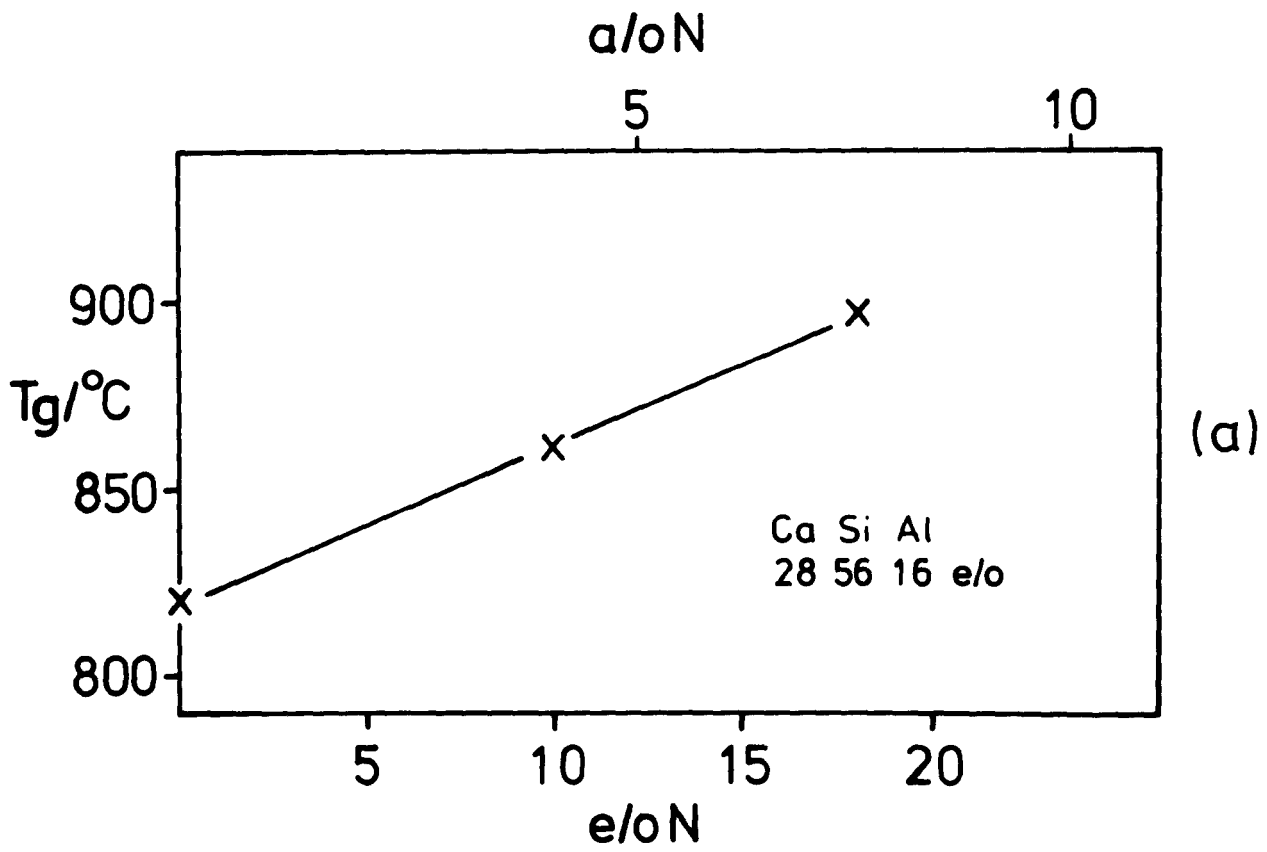


Figure VII.2 Variation of glass transition temperature (T_g) with nitrogen concentration:

- (a) the Y-Si-Al-O-N system
- (b) the Nd-Si-Al-O-N system.

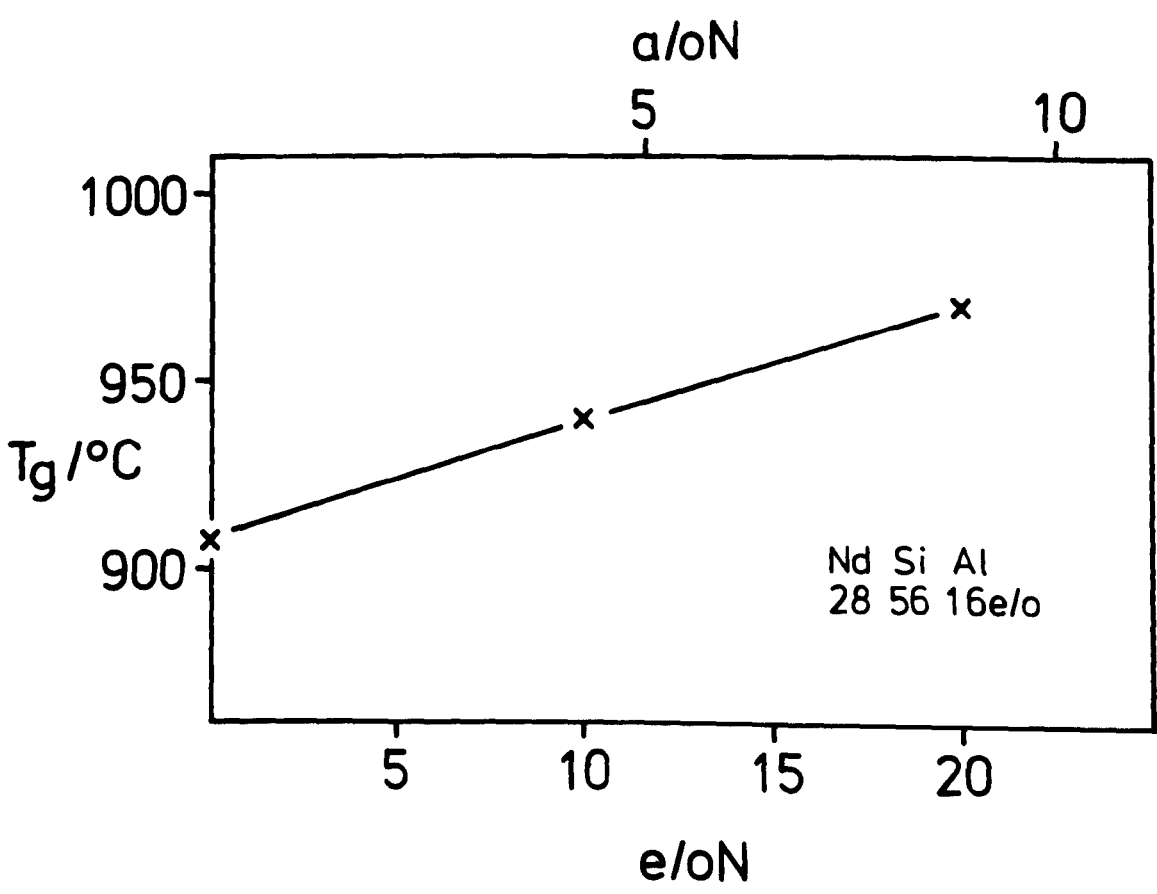
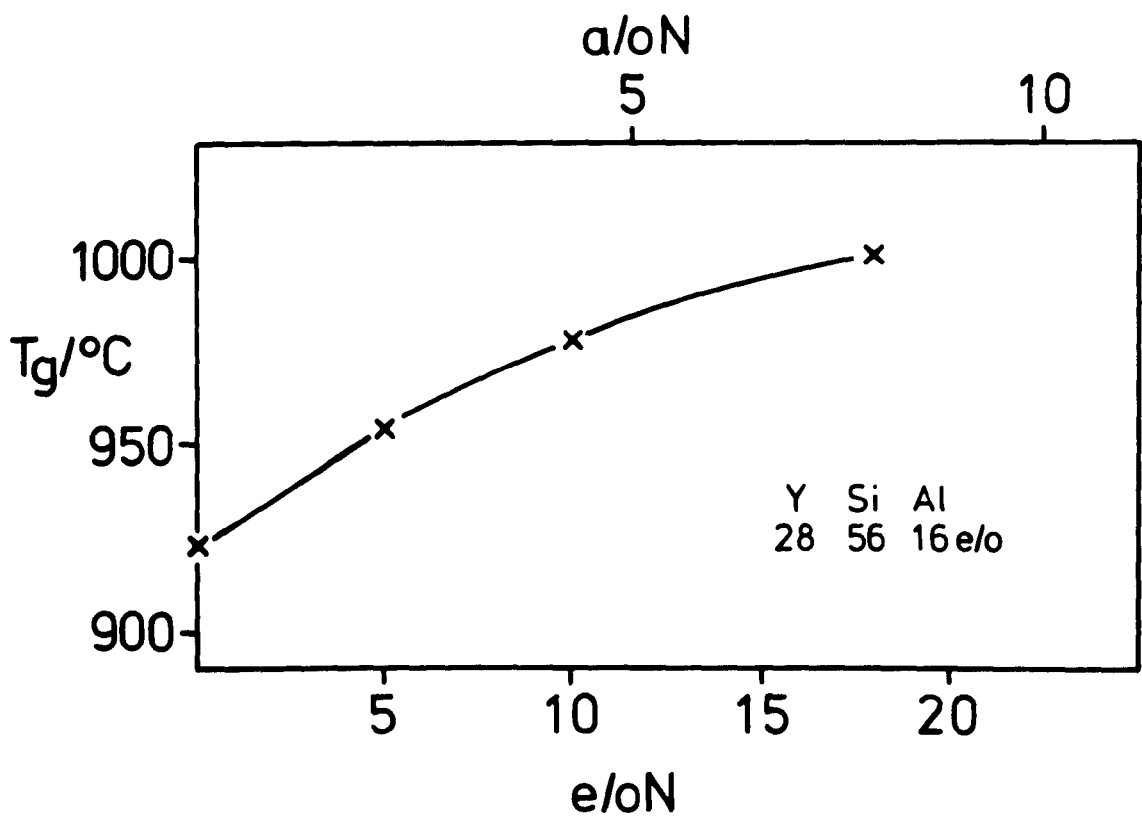


Figure VII.3 Comparison of T_g against nitrogen concentration for Y, Nd, Ca and Mg sialon glasses (28M : 56Si : 16 Al).

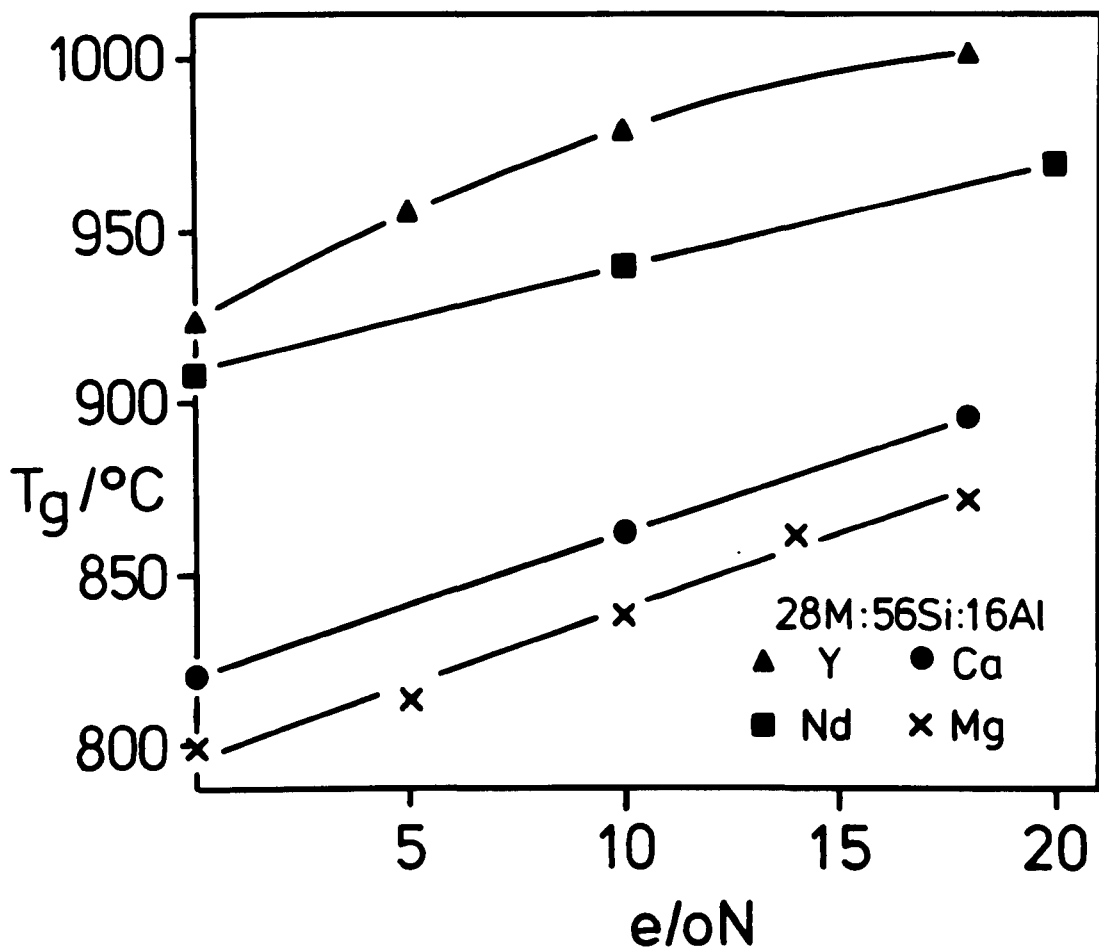


Figure VII.4 Variation of viscosity with temperature for Mg-Si-Al-O-N glasses of different nitrogen concentrations.

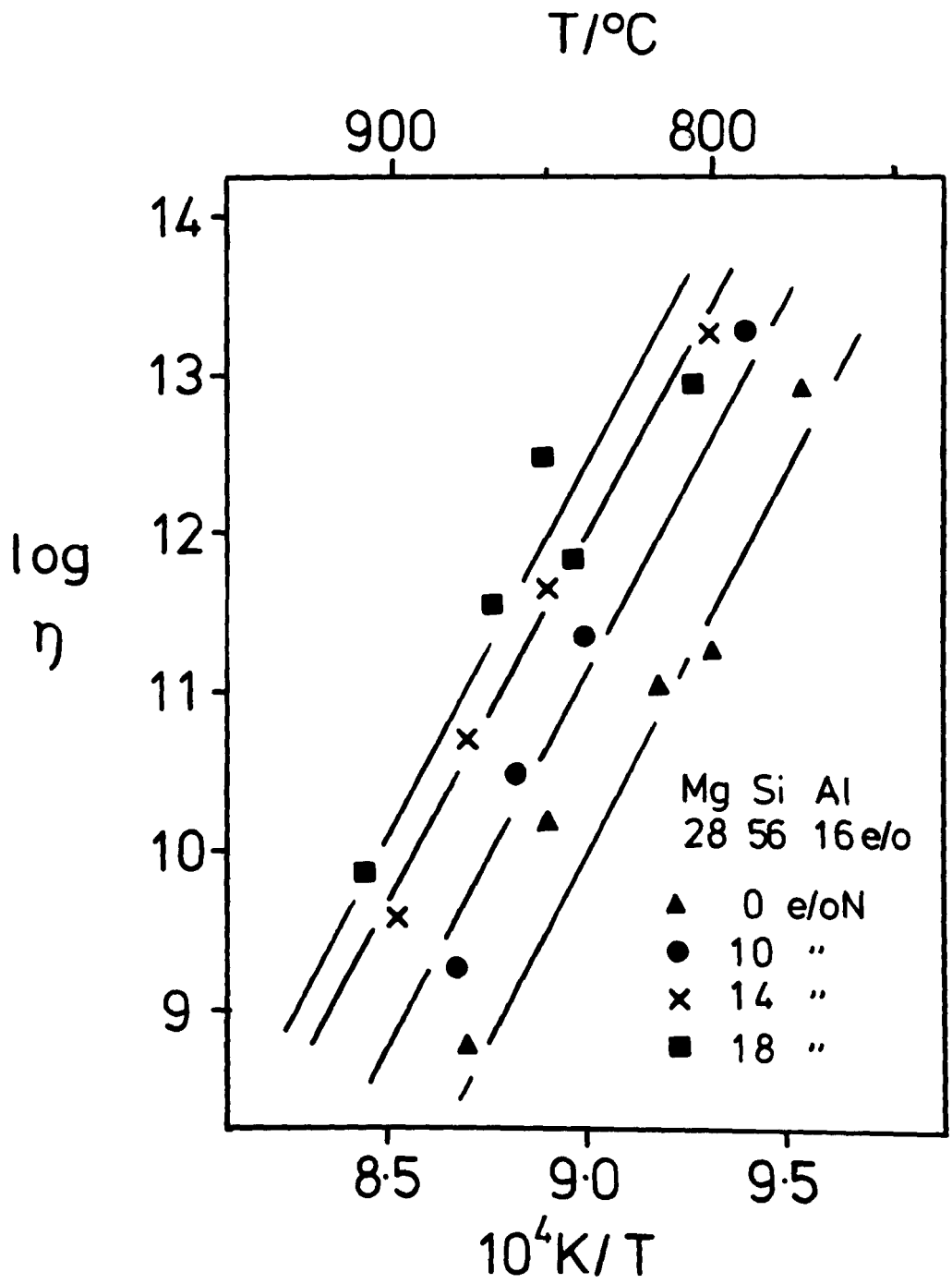


Figure VII.5 Variation of viscosity with
temperature for Y-Si-Al-O-N glasses
of different nitrogen concentrations.

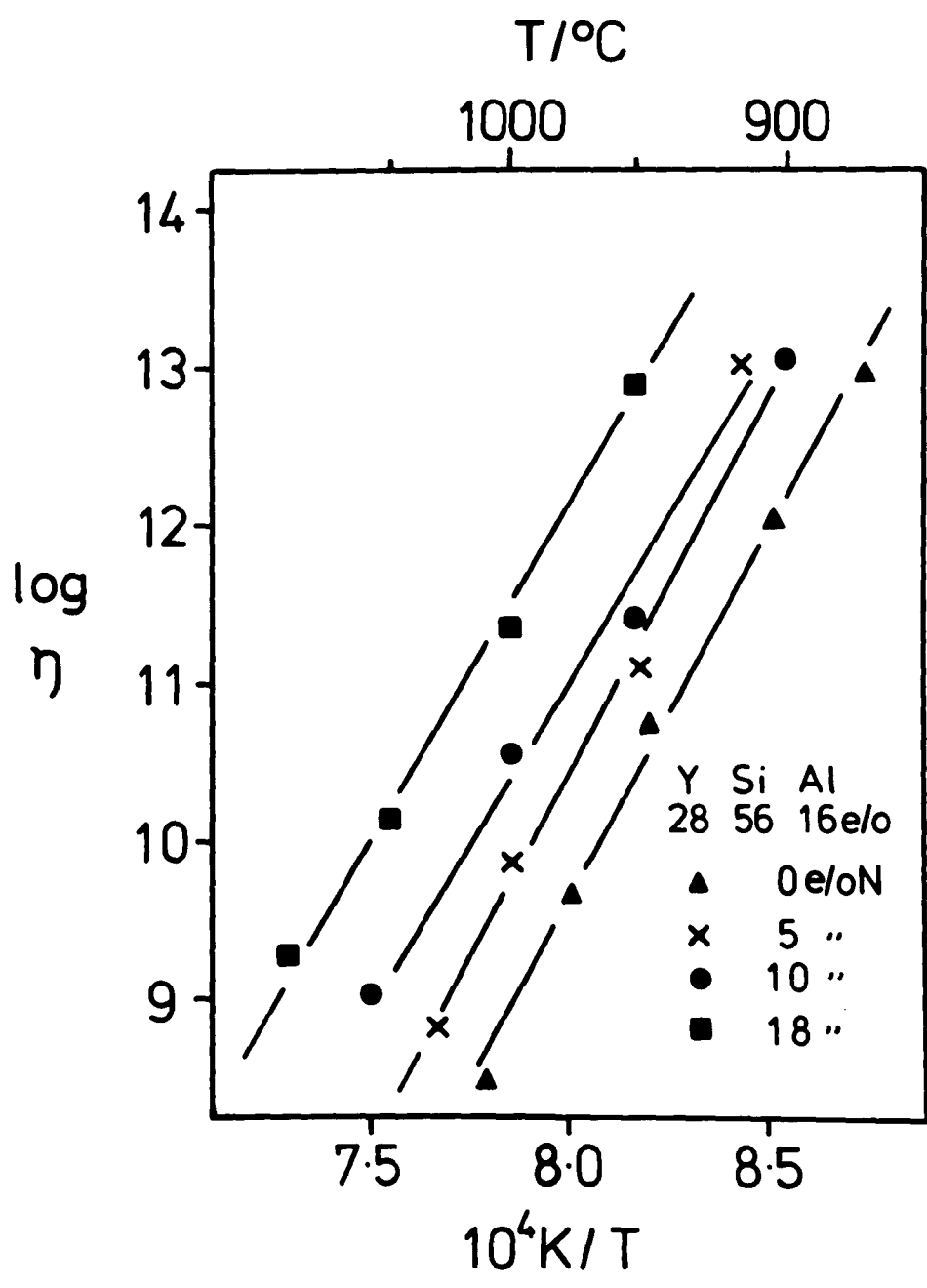


Figure VII.6 Variation of viscosity with
temperature for Ca-Si-Al-O-N glasses
of different nitrogen concentrations.

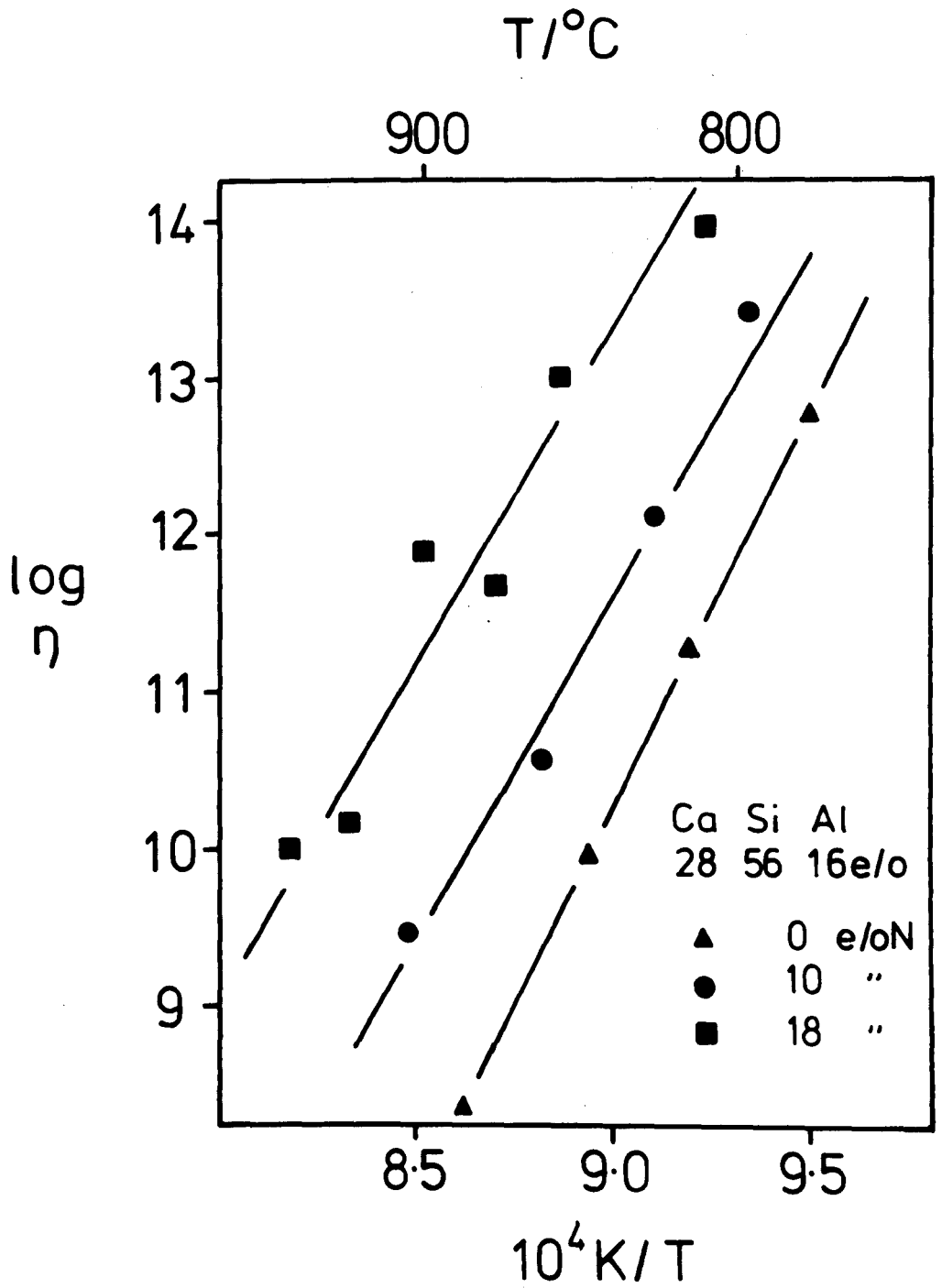


Figure VII.7 Variation of viscosity with temperature for Nd-Si-Al-O-N glasses of different nitrogen concentrations (after Spacie, 1980).

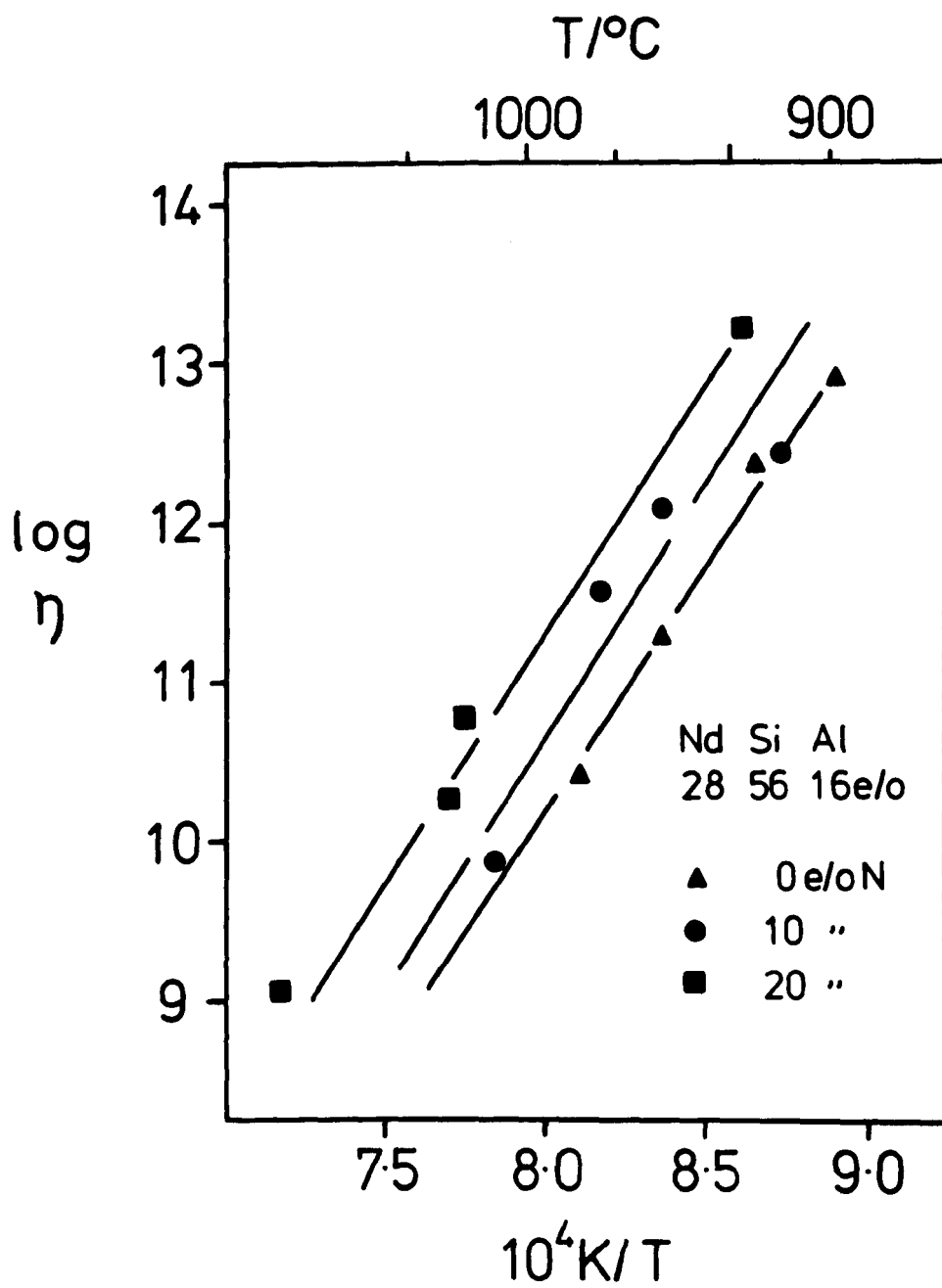


Figure VII.8 Variation of viscosity with temperature for Y, Nd, Ca and Mg silon glasses (28M:56Si:16Al) with 10 e/o nitrogen concentration.

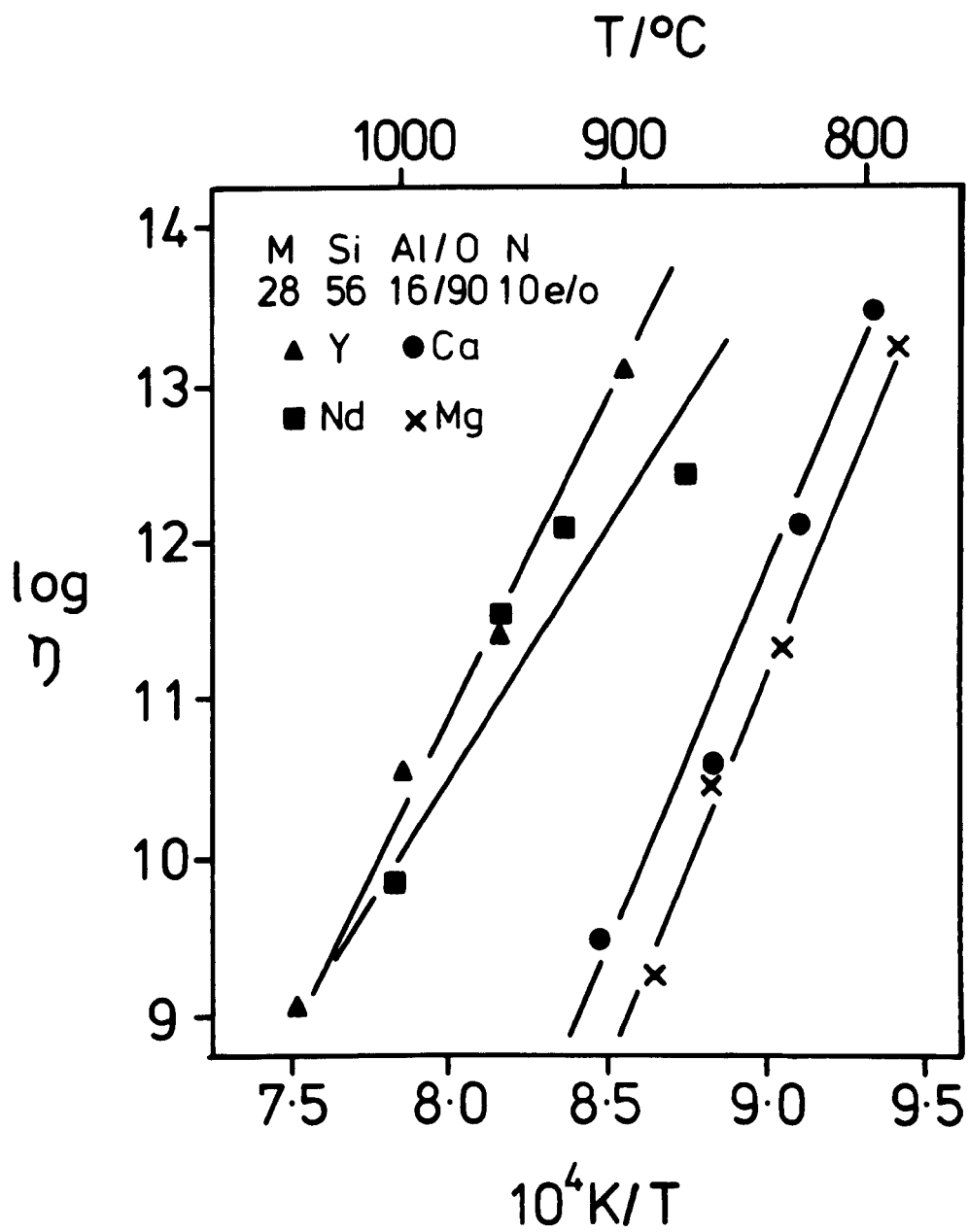
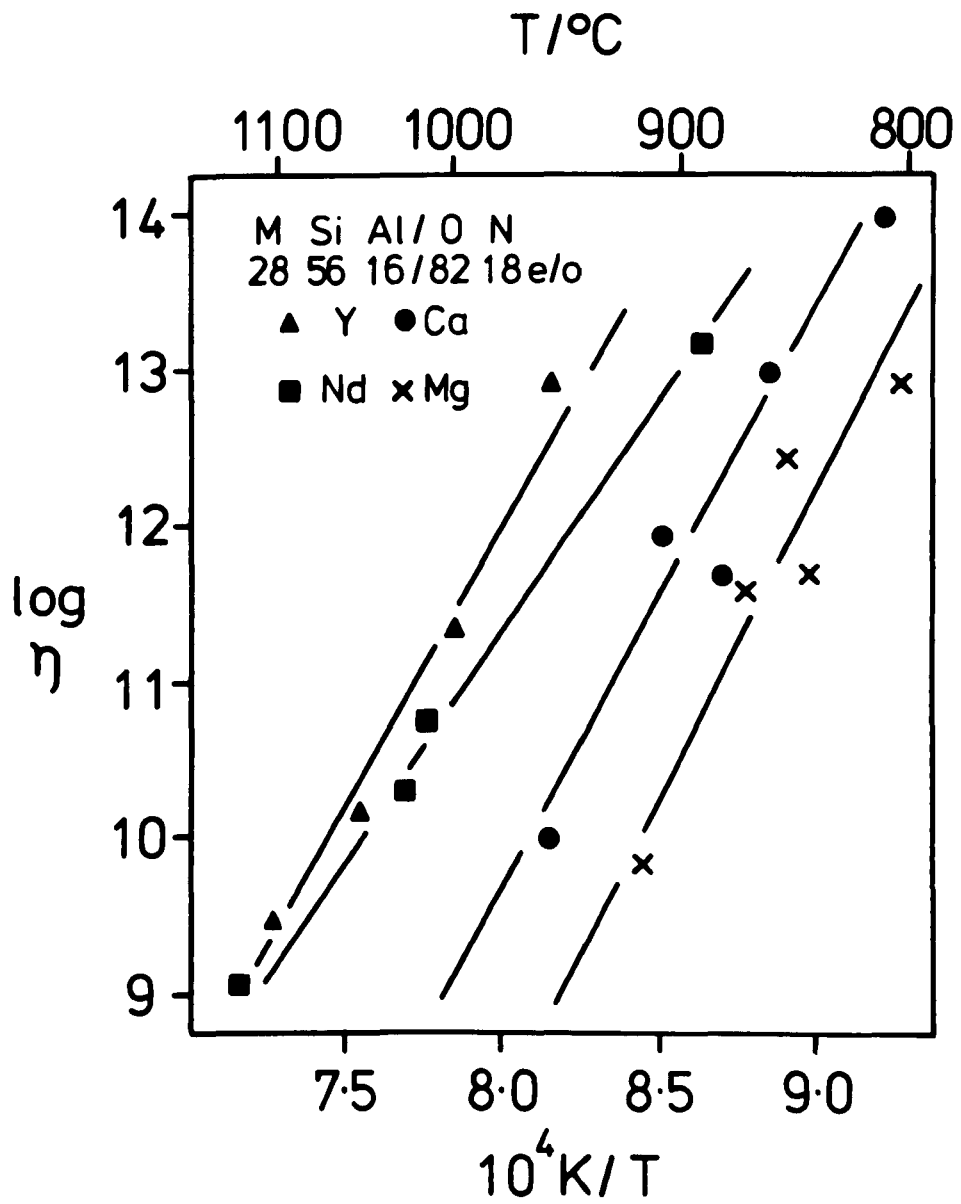


Figure VII.9 Variation of viscosity with
temperature for Y, Nd, Ca and Mg
sialon glasses (28M:56Si:16Al)
with 18 e/o nitrogen concentration.



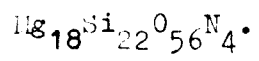
viscosity are obtained in the yttrium sialon glasses and the lowest for the magnesium glasses. The viscosity curves for both the neodymium and calcium glasses are between these extremes.

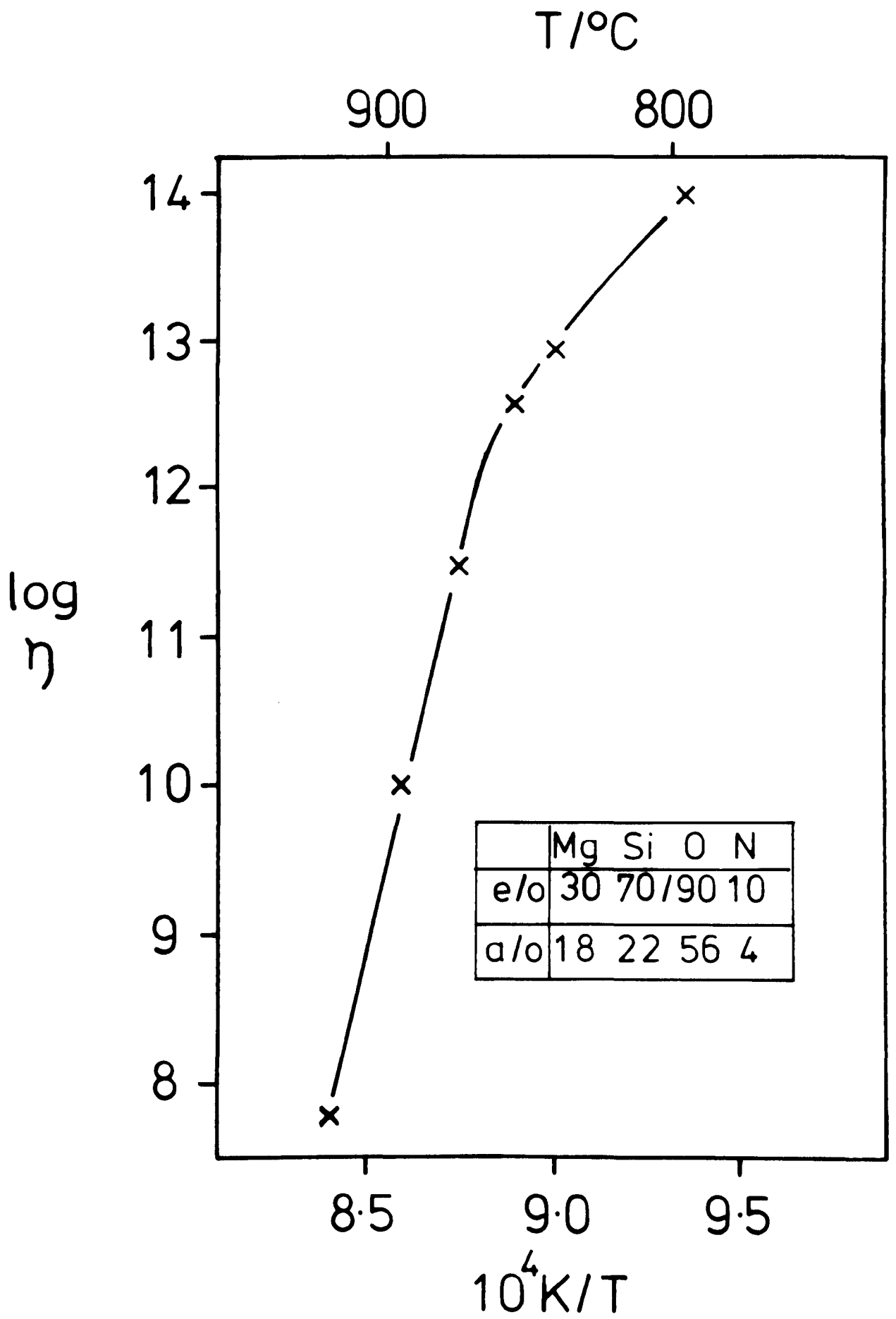
A Mg-Si-O-N glass of composition $Mg_{18}Si_{22}O_{56}N_4$ (i.e. with 10 e/o N) has a glass transition temperature of $870^{\circ}C$; the viscosity data for the same glass are presented in Figure VII.10. The viscosity behaviour of this glass is similar to that of the highest nitrogen (18 e/o N) magnesium sialon glass which has an atomic composition $Mg_{17.4}Si_{17.4}Al_{6.7}O_{51.0}N_{7.5}$ (see Figure VII.4).

Loehman (1978) reports increases in glass transition temperature with increasing nitrogen content for some Y-Si-Al-O-N glasses. His results were obtained from glasses of varying cation ratios which would themselves give different values of T_g since the latter is very sensitive to the silicon content. Two directly comparable compositions, however, without nitrogen and with 1.5 a/o nitrogen, indicated the same trend as reported in the present work.

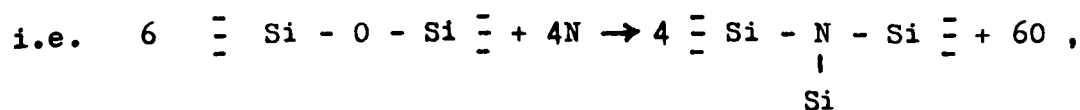
The lowering of viscosity of a glass on raising its temperature is a result of breaking primary bonds, thus enabling a greater mobility of the structural

Figure VII.10 Variation of viscosity with temperature for a Mg-Si-O-N glass of composition,





units in the material. The covalent bonding of oxygen to silicon in a silicate involves the overlap of the lone-pair 2p electrons of oxygen with the 3d orbitals of silicon (Revesz, 1970). Nitrogen has three half-filled 2p orbitals available thus providing an extra bond which could overlap with the 3d orbitals of silicon. Mulfinger (1966) proposed that the substitution of oxygen by nitrogen,

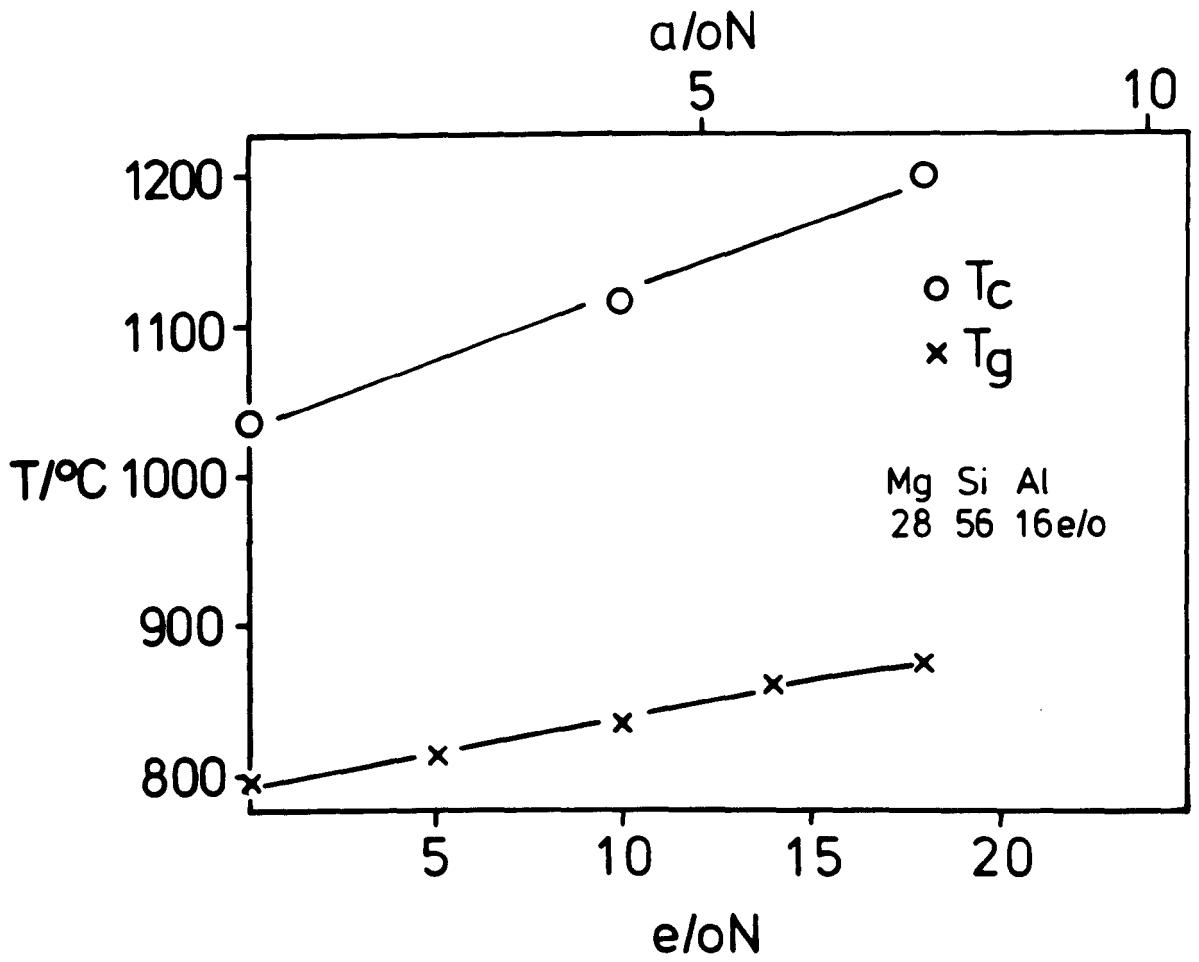


leads to higher coordination of the non-metal atoms in the glass network and hence to more crosslinking. Nitrogen can also become coordinated in this way with aluminium or other cations and the greater crosslinking produces a more rigid network. The viscosity data substantiate such a proposal since nitrogen incorporation increases the glass transition temperature and viscosity in all systems.

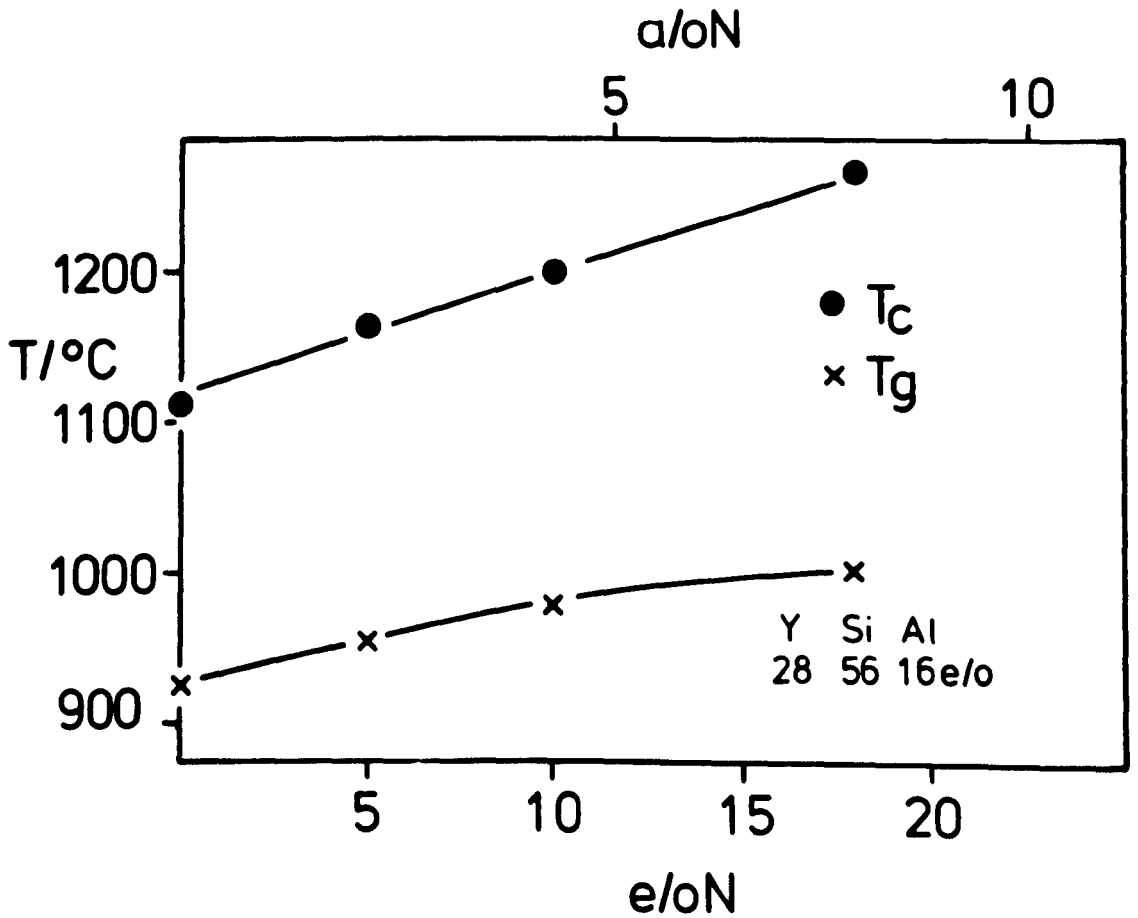
VII.3 Crystallization temperature

The results shown in Figures VII.11 and 12 were obtained from the maximum point on the crystallization peak of the DTA trace. The values of T_g and T_c for

Figure VII.11 Variation of crystallization
and glass transition temperature
with nitrogen concentration in
(a) the Mg-Si-Al-O-N system
(b) the Y-Si-Al-O-N system.

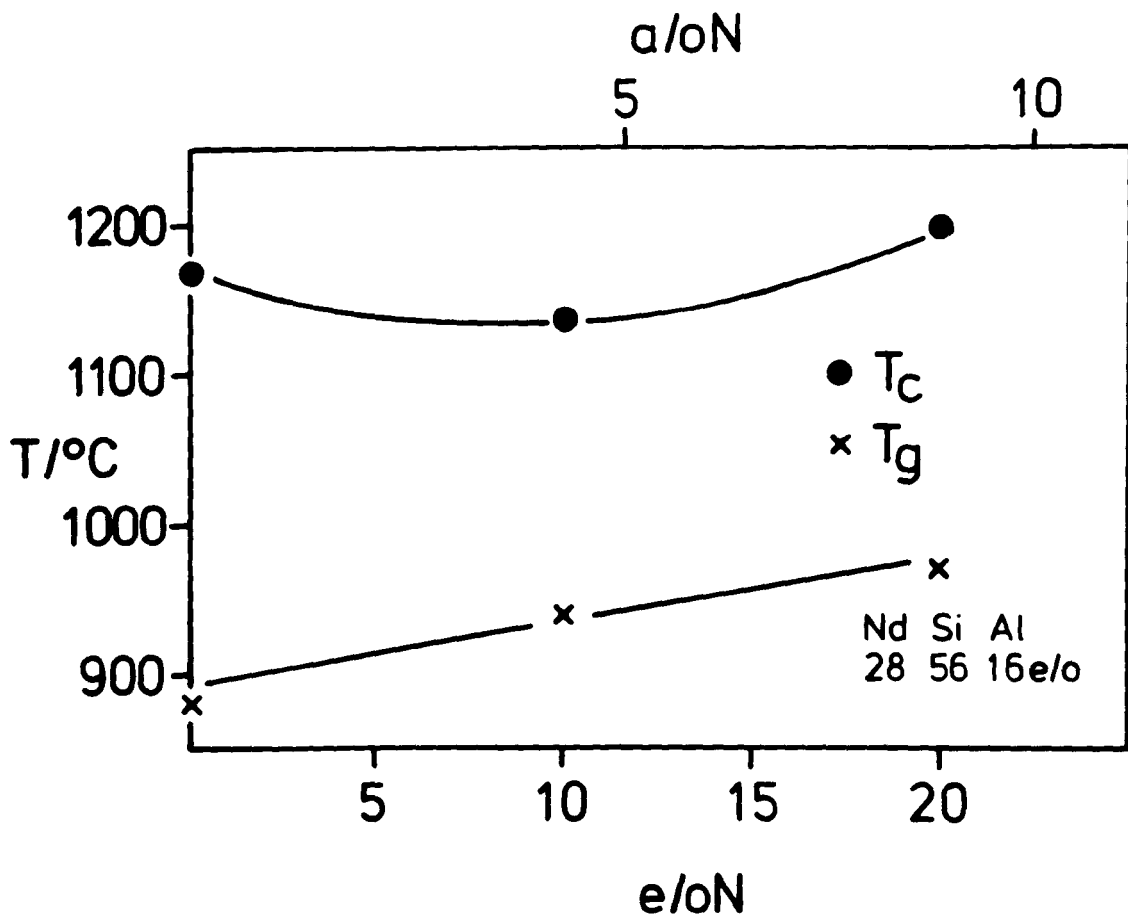


(a)

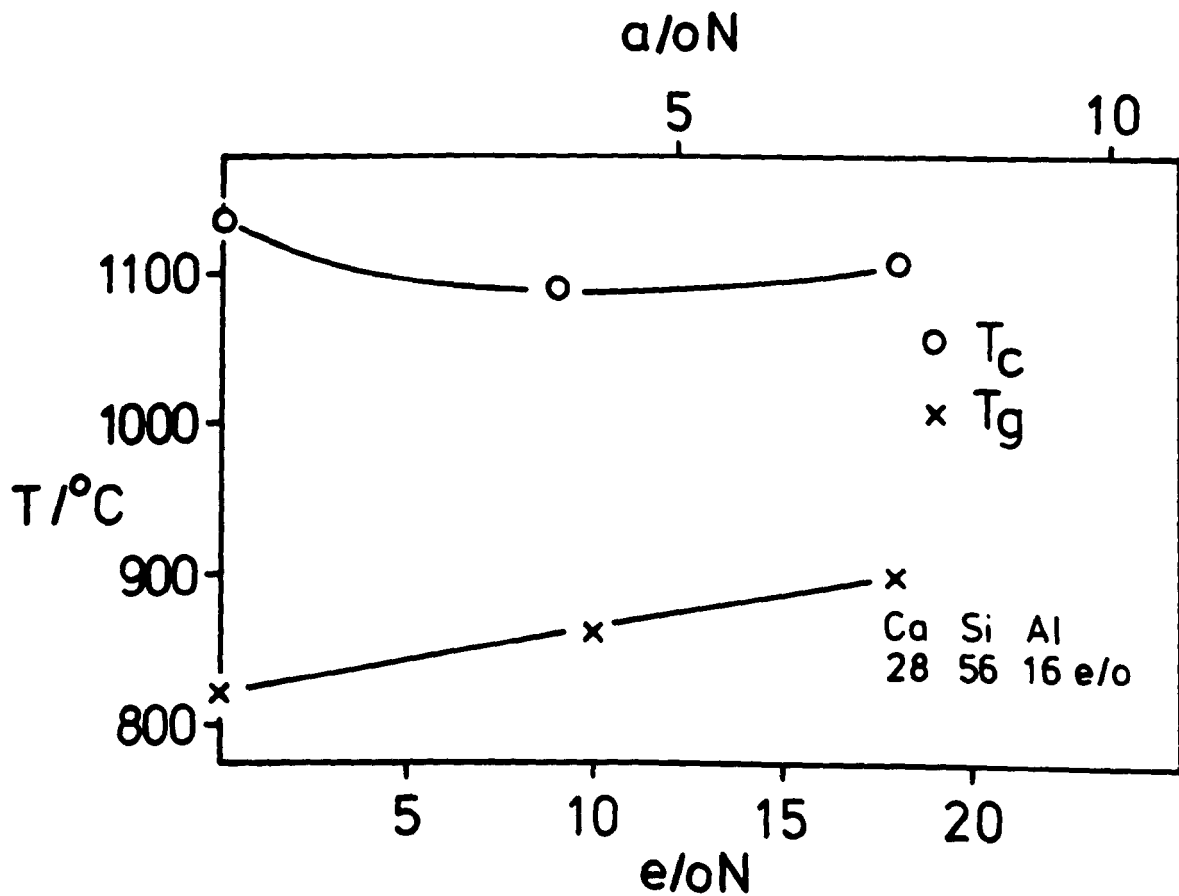


(b)

Figure VII.12 Variation of crystallization
and glass transition temperature
with nitrogen concentration in
(a) the Nd-Si-Al-O-N system
(b) the Ca-Si-Al-O-N system.



(a)



(b)

both the magnesium and yttrium sialon glasses are shown in Figures VII.11(a) and (b). Curves obtained for the neodymium and calcium sialon glasses are presented in Figures VII.12(a) and (b), and Figure VII.13 shows comparative data for all four systems. An interesting observation is that the magnesium and yttrium curves are parallel and there is an increase in T_c with nitrogen content whilst those of the neodymium and calcium glasses are more or less parallel and indicate only a small variation in T_c with nitrogen concentration.

There is a broadening in the crystallization peaks on nitrogen incorporation in the case of both the magnesium and yttrium glasses, whereas the peak shape remains the same for the neodymium and calcium glasses. Figure VII.14 shows this effect for two Y-Si-Al-O-N glasses (5 e/o N and 18 e/o N) and Table VII.1 provides a more detailed analysis of the peaks, giving the temperature of the start of crystallization and the peak maximum (T_c). The temperatures of the start of crystallization for each of the glass systems change only slightly with nitrogen concentration, and for each glass series, these temperatures are probably the same, within experimental error, particularly considering the accuracy of the DTA technique. The peak maxima (T_c) shown for glasses of

Figure VII.13 Comparison of crystallization temperature (T_c) with nitrogen concentration for the Y, Nd, Ca and Mg sialon glasses.

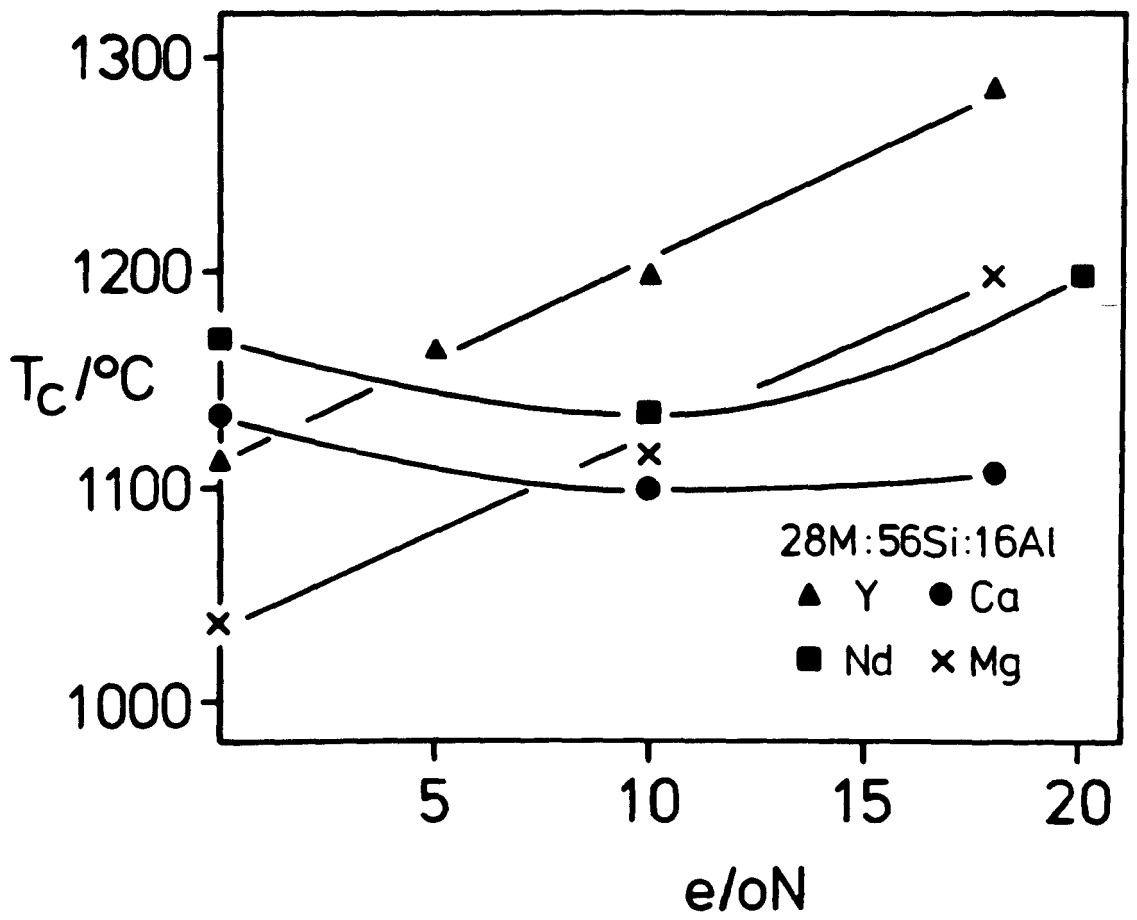


Figure VII.14 DTA traces showing the glass transition (T_g)
and crystallization (T_c) temperatures for
Y-Si-Al-O-N glasses containing
(i) 5 e/o N (ii) 18 e/o N.

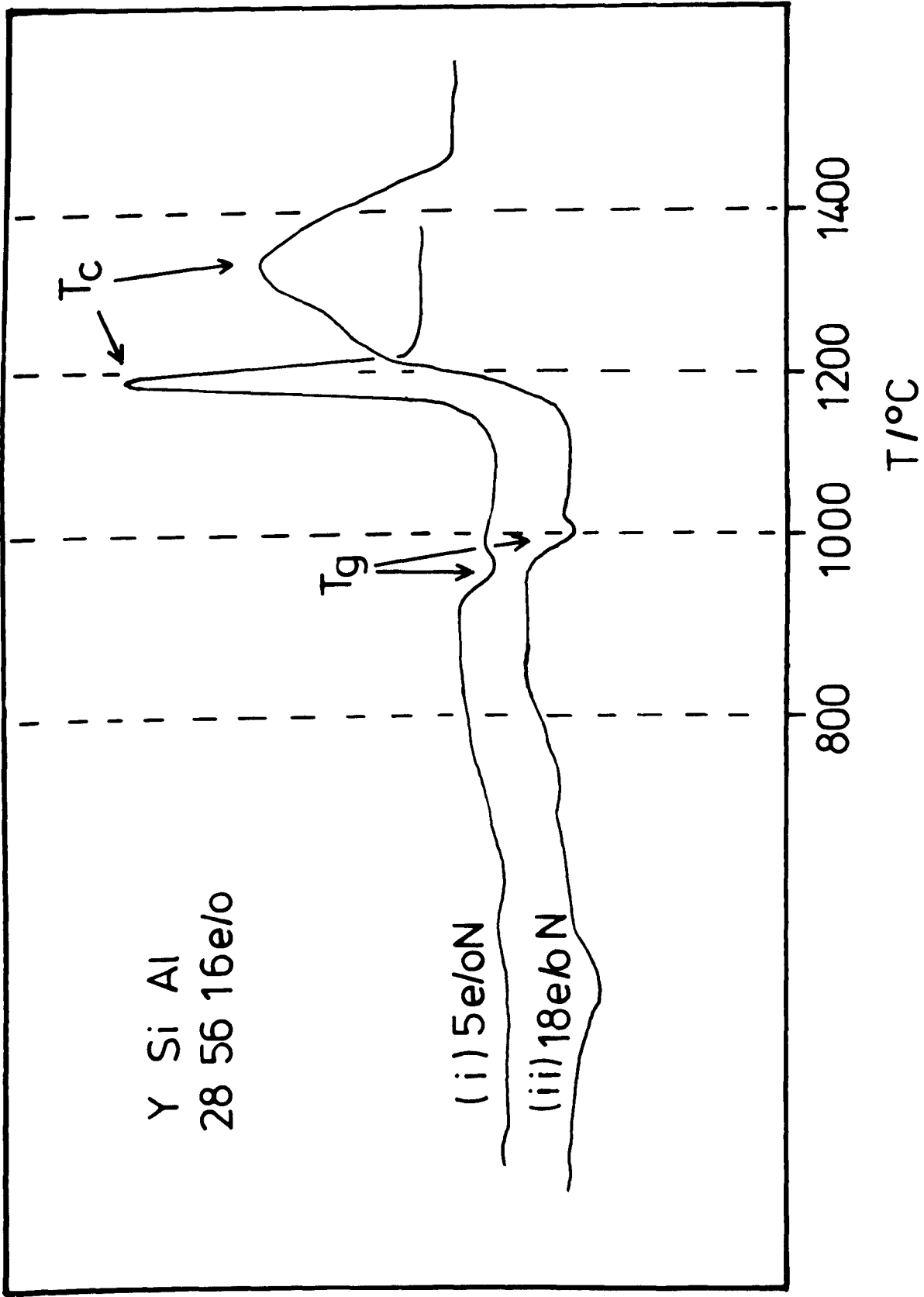


Table VII.1

Analysis of the crystallization peaks (28M : 56Si : 16Al)

M	e/o N	start of peak (°C)	peak maximum (°C)
Y	0	1035	1110
	5	1110	1115
	10	1110	1184
	18	1110	1285
Mg	0	975	1035
	10	1030	1115
	18	1030	1200
Ca	0	1030	1120
	10	975	1090
	18	1030	1105
Nd	0	1020	1170
	5	1070	1184
	10	1040	1135
	20	1070	1200

all four systems in Figure VII.13 indicate that the values of T_c for the magnesium and yttrium glasses increase appreciably with nitrogen concentration, whereas there are only small changes in T_c with nitrogen incorporation in the case of the neodymium and calcium glasses. Without a more detailed study of crystal growth kinetics using hot stage microscopy to determine crystal growth rates (see Briggs & Carruthers, 1976), it is not possible to suggest a plausible explanation for the above observations.

The crystallization temperature (T_c) should increase when there is a corresponding increase in viscosity because devitrification is related to structural mobility which is governed by viscosity. However, some of the present observations on neodymium and calcium glasses are not in accordance with this generalization. As discussed in Chapter II, crystallization is always preceded by nucleation and it is suggested that impurities introduced during fabrication of the glasses, in particular from the silicon and aluminium nitrides, might act as nucleation sites and aid the devitrification process and override the effect of any increase in viscosity. Chyung et al. (1978) discuss "self-nucleation" in oxynitride glass-ceramics, and note that it is unnecessary to add nucleating agents to facilitate the devitrification

process.

Devitrification is extremely complicated in most glass systems (Doremus, 1973) and is still not fully understood. It depends not only on viscosity, but also on glass-stability, nucleation behaviour and the phase-relationships of the final crystalline products. It cannot, therefore, be concluded that nitrogen substituting for oxygen in glasses always increases the crystallization temperature.

VII.4 Optical properties

VII.4.1 Introduction

All glasses prepared were grey or bluish-grey, the coloration generally increasing with the amount of nitride added and varying slightly according to whether AlN or Si_3N_4 was used as a starting material; the former impaired optical transparency more than the latter. These observations imply that impurities or micro-heterogeneities cause the poor transparency rather than structural nitrogen. Figure VII.15 is a photograph of two nitrogen glasses, shaped and polished both as discs and small blocks, showing that they are reasonably transparent in thin section. The discs were used for measuring infra-red and ultra-violet transmission spectra while both the

Figure VII.15 Photograph of shaped and polished nitrogen glasses both of the "standard cation composition" (28M:56Si:16Al) and containing 18 e/o N:

- (i) a Ca-Si-Al-O-N glass
- (ii) a Mg-Si-Al-O-N glass.

stare.—*v.i.* to emit a hard, fierce, dazzling light: to be obtrusively noticeable: to stare fiercely.—*adj.* **glar'ing**, bright and dazzling: flagrant.—*adv.* **glar'ingly**.—*n.* **glar'ingness**.
 [M.E. *glāren*, to shine; akin to **glass**, O.E. *glær*, amber, L. Ger. *glaren*, to glow.]

glass, glās, *n.* a hard, brittle substance, usually transparent, generally made by fusing together a **silica** (as sand) with an alkali (q.v.) and another base (q.v.): an article made of or with glass, esp. a drinking-vessel, a mirror, a weather glass, a telescope, &c.: the quantity of liquid a glass holds: (*pl.*) spectacles.—*adj.* made of glass.—*v.t.* to case in glass: to furnish with glass: to polish highly.—*ns.* **glass'-blow'ing**, one process of making glass-ware: **glass'-blow'er**; **glass'-cloth**, a cloth for drying glasses: a material woven from

i. Ca-Si-Al-O-N

18 e/oN

ii. Mg-Si-Al-O-N

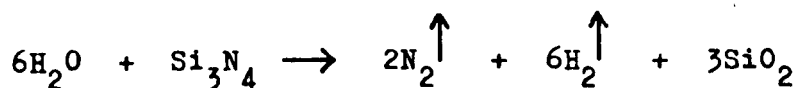
18 e/oN

blocks and the discs were used for electrical measurements.

VII.4.2 Infra-red and ultra-violet transmission

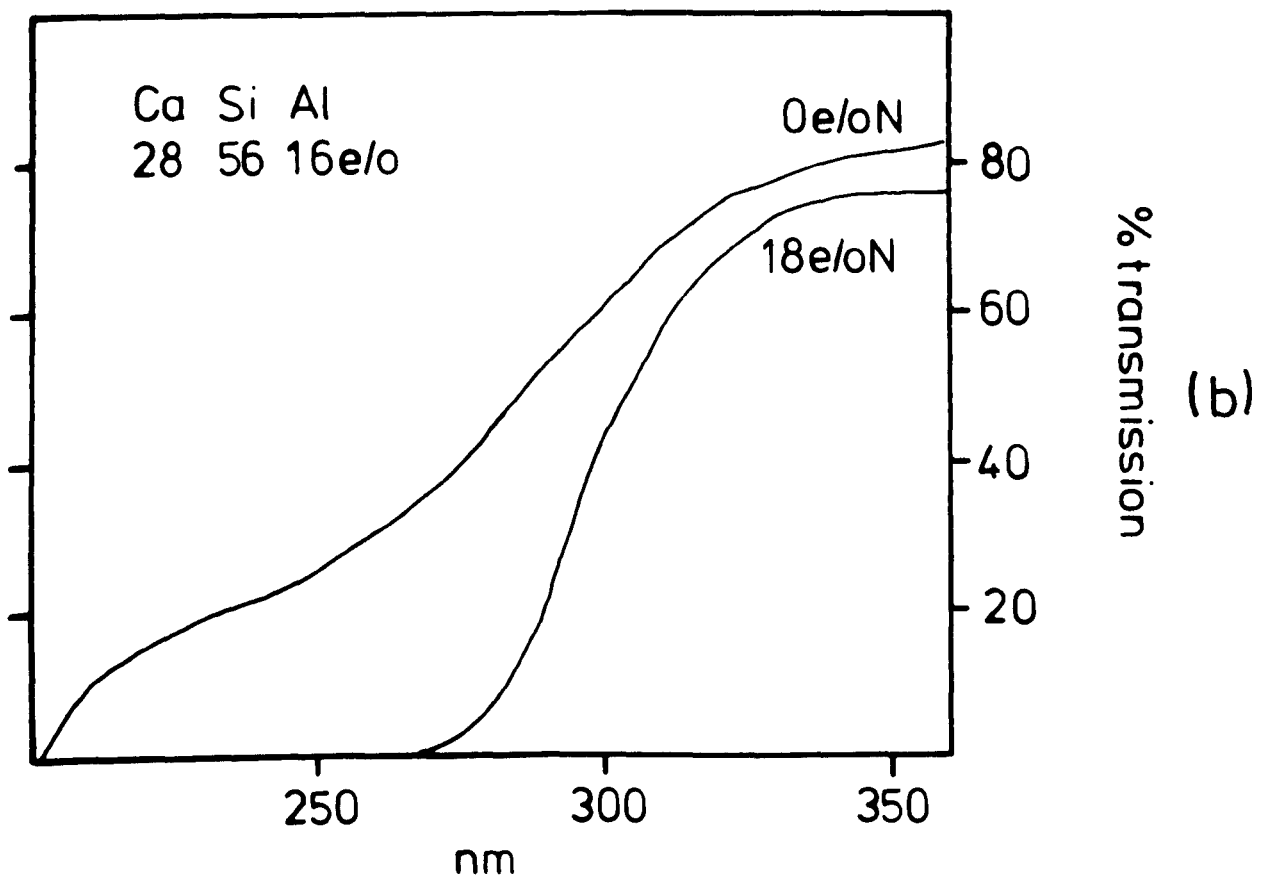
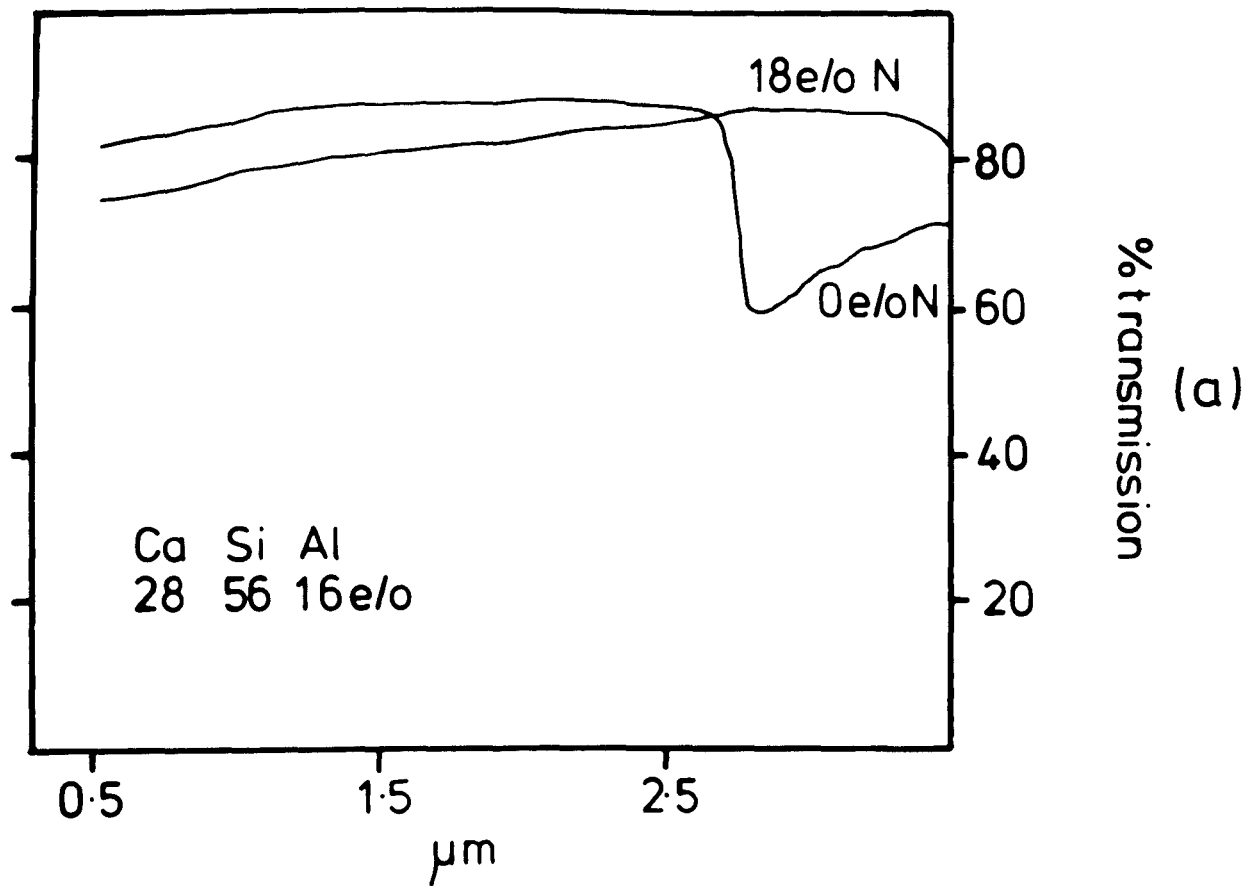
UV and IR transmission spectra were obtained on a Beckman DK2A ratio recording spectrophotometer for 0 e/o and 18 e/o nitrogen glasses in the four systems studied. Typical spectra are shown in Figure VII.16 for glasses of the calcium sialon system.

It is clear that near IR transmission was improved to some extent by the presence of nitrogen, and in particular there is an absence of the band at about 2.7 μm which corresponds to the Si-OH stretching frequency. These observations are attributed to the lowering of the concentration of "water" in the glass by reaction with Si_3N_4 during firing (Harding & Ryder, 1970:



It is suggested that this reaction occurs during the firing of all glasses in the presence of hydrolysible nitrides. Elmer & Nordberg (1965) also noted a diminution or removal of the "water" absorption band

Figure VII.16 Transmission spectra of a calcium
sialon glass (18 e/o) compared with
those of the corresponding oxide
glass (28Ca:56Si:16Al)
(a) the infra-red absorption spectra
(b) the ultra-violet absorption spectra.



on nitriding glasses with ammonia.

The UV spectra of the same glasses show that the incorporation of nitrogen via nitrides impairs the UV transmission and brings the cut-off at ~ 250 nm to even longer wavelengths. The effect is attributed partly to impurities in the glass but also must be a result of nitrogen incorporation as claimed by Swarts (1968).

Loehman (1979) blamed poor transmission in yttrium and magnesium sialon glasses upon impurities of boron and molybdenum picked up from crucibles, as well as on impure starting materials.

VII.4.3 Refractive index

The results presented in Table VII.2 and Figure VII.17 demonstrate that there is a significant increase in refractive index (n) for all glasses with replacement of oxygen by nitrogen. Although the cation content, and in particular the replacement of silicon by yttrium or neodymium, would affect the values of n , the cation ratio is maintained constant in these glasses to within ± 0.25 a/o, so that the increases in refractive index are solely due to nitrogen and so should be related to the nature of the nitrogen bonding

Figure VII.17 Comparison of refractive index (n) with nitrogen concentration for Nd, Y, Ca and Mg sialon glasses (28M:56Si:16Al).

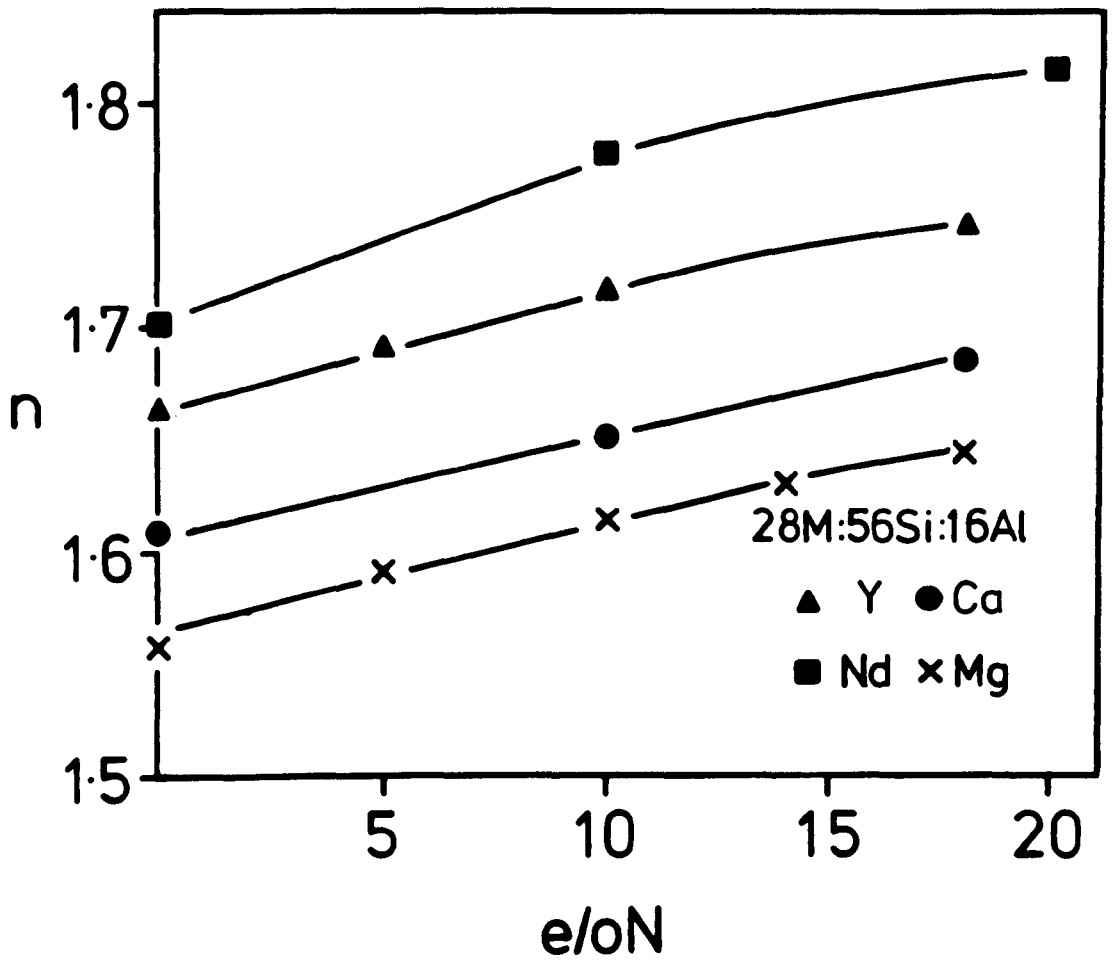


Table VII.2

Variation of refractive index (n) with nitrogen concentration for glasses of cation composition,

28M : 56Si : 16Al

M	e/o N	refractive index n
Nd	0	1.702
	10	1.771
	20	1.815
Y	0	1.662
	5	1.690
	10	1.717
	18	1.745
Ca	0	1.609
	10	1.652
	18	1.686
Mg	0	1.567
	5	1.592
	10	1.618
	14	1.632
	18	1.645

in the glass structure.

Loehman (1979) reported refractive indices of approximately 1.7 for yttrium sialon glasses, and a value as high as 1.76 (Jack, 1977a) has been obtained although no direct comparative measurements with corresponding oxide glasses have been carried out prior to the present work. The values now reported (see Table VII.2) for the high yttrium sialon glasses are much higher than any value of n reported by Makishima (1978) for their oxide equivalents, and show that nitrogen glasses might have interesting optical properties if their transparency can be improved by increasing their purity.

VII.6 Conclusions

Nitrogen replacement of oxygen in glasses increases their viscosity and it is clear that nitrogen is chemically bonded in the glass structure. The presence of nitrogen causes changes in the optical transmission of the glasses and this, together with the increment in refractive index, provides conclusive evidence of nitrogen bonding. These changes in glass properties should be explored in more detail because of their possible technological exploitation.

The present measurements of viscosity of nitrogen glasses provide a better understanding of the behaviour of nitrogen ceramics at high temperatures because the grain-boundary glasses in such materials have compositions within the glass-forming regions of the systems discussed in Chapter VI. The highest viscosity nitrogen glasses are in the Y-Si-Al-O-N system and it is no coincidence that the best high temperature properties of β' -sialon are obtained by using yttria as a densifying additive.

Improved high-temperature strength can be achieved by producing a higher softening temperature grain-boundary glass or by devitrification to form more refractory crystalline phases. It is not possible to obtain more refractory vitreous phases than silica which itself begins to soften above about 1150°C . Thus, the only practicable approach to property improvement of nitrogen ceramics at elevated temperatures must be by post-preparative heat-treatment to form crystalline phases or to incorporate, by chemical reaction, the vitreous or crystalline grain-boundary phases into the structure and finally obtaining a single phase material.

VIII. Devitrification

VIII.1 Devitrification of nitrogen glasses

VIII.1.1 Introduction

Devitrification of selected glasses on the 14 e/o nitrogen plane of the Mg-Si-Al-O-N system and on the 16 e/o nitrogen plane of the Y-Si-Al-O-N system was studied.

Other glasses of the "standard cation composition" (see Chapter VII.1) were devitrified at their appropriate crystallization temperature as determined by DTA (see Chapter VII.3).

All devitrification experiments were carried out under a purified nitrogen atmosphere and crystalline phases were identified by X-ray diffraction.

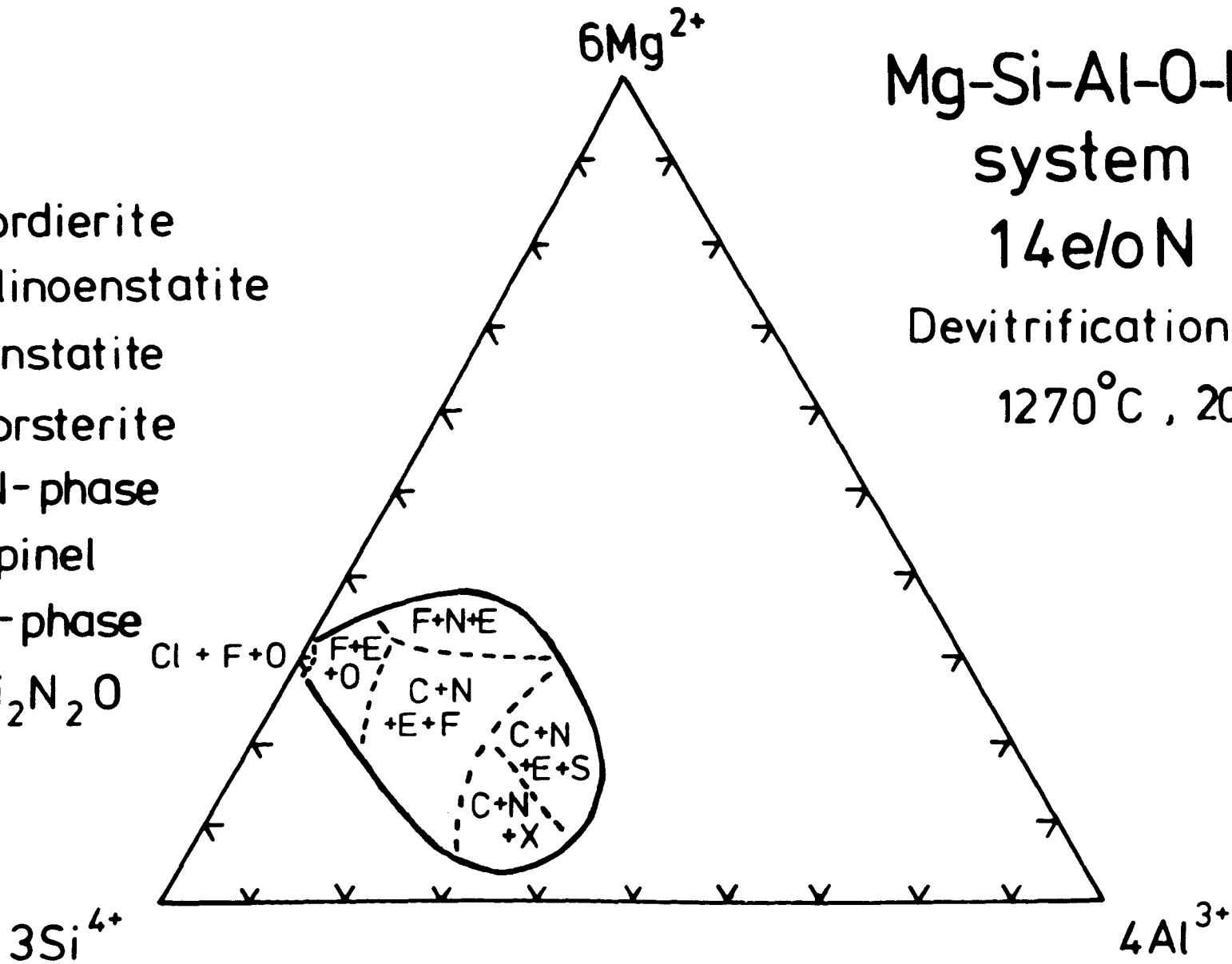
VIII.1.2 Mg-Si-Al-O-N glasses

Devitrification of glasses on the 14 e/o nitrogen plane at 1270°C for 20 hours gave the crystalline phases shown by Figure VIII.1. The predominant nitrogen-containing phase observed was the so-called "N-phase" (Mg_2SiAlO_4N) (see later).

Mg-Si-Al-O-N
system

Devitrification phases
1270°C , 20 hours

- C - cordierite
- Cl - clinoenstatite
- E - enstatite
- F - forsterite
- N - N-phase
- S - spinel
- X - X-phase
- O - $\text{Si}_2\text{N}_2\text{O}$



Other oxynitride phases identified were $\text{Si}_2\text{N}_2\text{O}$, X-phase and spinel (Perera, 1976). Cristobalite was frequently present in varying proportions.

Devitrified samples containing only small amounts of aluminium near the Mg-Si-O-N face showed only enstatite (MgSiO_3), forsterite (Mg_2SiO_4) and $\text{Si}_2\text{N}_2\text{O}$. It is assumed that the small amount of aluminium present in the original glass must have been incorporated in the $\text{Si}_2\text{N}_2\text{O}$ phase on crystallization, as discussed in Chapter III (see Jack, 1973).

Mg-Si-O-N glasses did not completely devitrify at this temperature, but at 1350°C the crystalline products were Mg_2SiO_4 , MgSiO_3 and $\text{Si}_2\text{N}_2\text{O}$ as expected from the behaviour diagram. The proportion of Mg_2SiO_4 increased with increasing nitrogen content for the same Mg:Si ratio, and correspondingly the amount of MgSiO_3 was reduced. This is not unexpected because more silicon is required to form $\text{Si}_2\text{N}_2\text{O}$ and adjustments in the proportion of Mg_2SiO_4 and MgSiO_3 are then necessary to maintain a material balance.

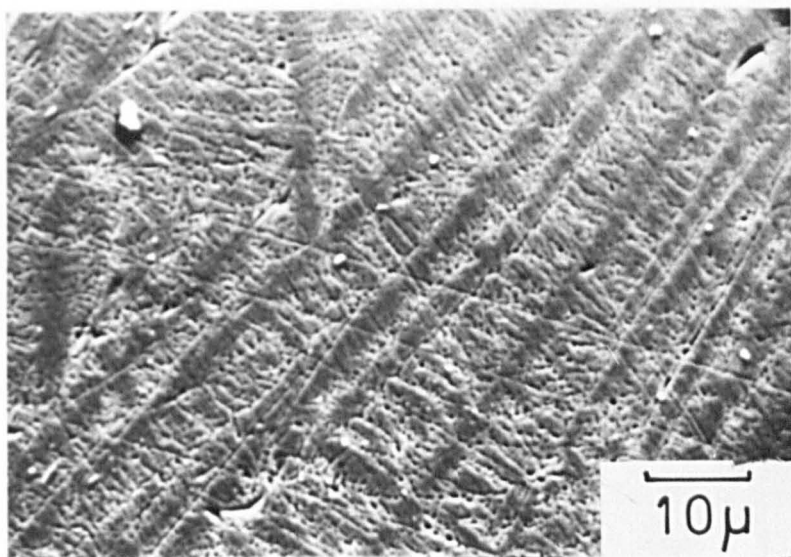
Glasses of the "standard cation composition" (28 e/o Mg : 56 e/o Si : 16 e/o Al) were heat-treated for 20 hours at their appropriate crystallization temperatures. The nitrogen glasses gave different

proportions of forsterite, enstatite and N-phase with only traces of cordierite. The highest nitrogen-containing glass (18 e/o N) produced more N-phase and forsterite and less enstatite than the 10 e/o nitrogen glass. The devitrification product of the oxide glass contained no N-phase and only cordierite, forsterite and enstatite.

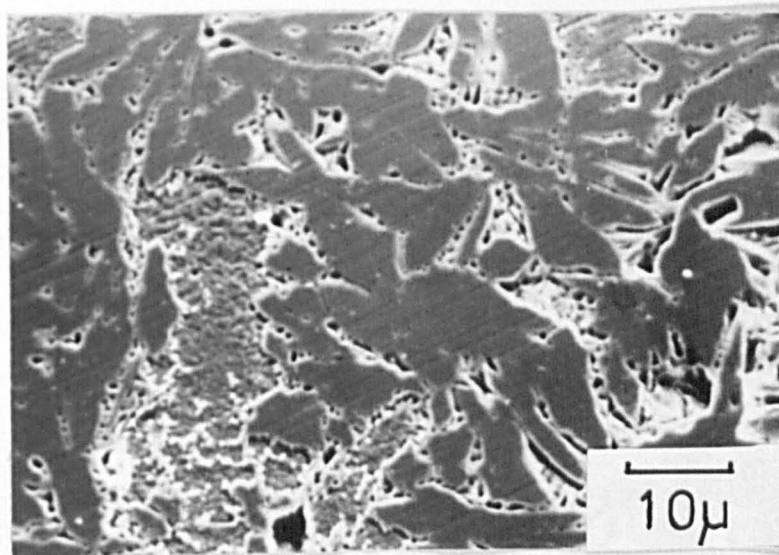
N-phase can best be described as "nitrogen-petalite" (Perera, 1976) because its X-ray diffraction pattern is similar to that of natural petalite ($\text{LiAlSi}_4\text{O}_{10}$). Its assumed composition, $\text{Mg}_2\text{SiAlO}_4\text{N}$, corresponds well with the phase assemblage obtained after complete devitrification of the nitrogen glasses described above. A magnesium-petalite has been observed as a metastable devitrification product in cordierite glasses (Schreyer & Schairer, 1961; Holmquist, 1963; Barry et al., 1978) with a reported composition near $\text{MgAl}_2\text{Si}_3\text{O}_{10}$ which is quite different to that of N-phase and it is concluded that the two are quite separate and distinct phases although they are probably isostructural.

Scanning electron micrographs of the devitrified glasses show how the morphology changes as the phase assemblage alters and is particularly noticeable when comparing Figure VIII.2(a) with Figure VIII.2(b).

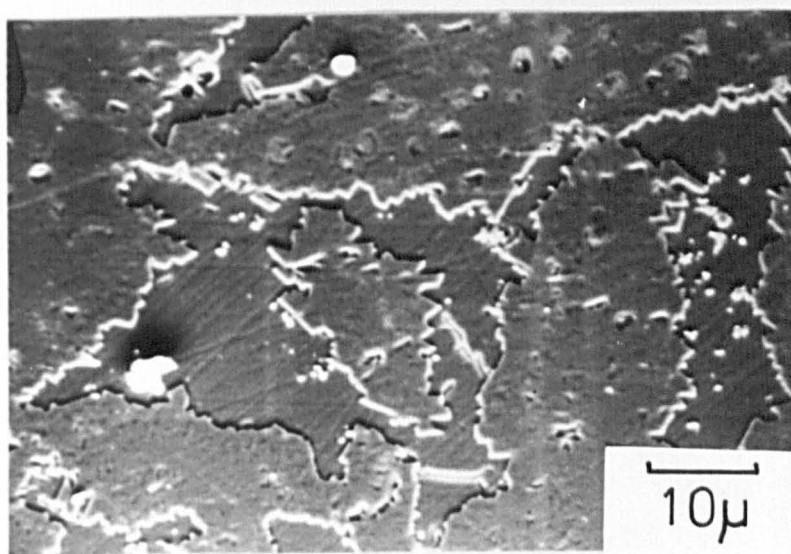
Figure VIII.2 Scanning electron micrographs of
devitrified Mg-Si-Al-O-N glasses
(28Mg:56Si:16Al)
(a) 0 e/o N
(b) 10 e/o N
(c) 18 e/o N.



(a)



(b)



(c)

Figure VIII.2(c) is the 18 e/o nitrogen glass after only 2 hours heat-treatment and crystallization is evidently not complete although X-ray diffraction shows the same phases as found on complete devitrification (N-phase, forsterite and enstatite).

VIII.1.3 Y-Si-Al-O-N glasses

Devitrification products of glasses on the 16 e/o nitrogen plane after 20 hours at 1270°C are shown in Figure VIII.3. Nitrogen-containing phases are β' -sialon, X-phase and $\text{Si}_2\text{N}_2\text{O}$. The yttrium-aluminium garnet (YAG) may also contain some nitrogen as slight changes in d-spacings from the pure oxide are observed. Lewis et al. (1980a) reported that silicon can substitute for aluminium in $\text{Y}_3\text{Al}_5\text{O}_{12}$ and concluded that nitrogen must also be present to maintain the charge balance. "C-phase" is close in composition to 'y'- $\text{Y}_2\text{Si}_2\text{O}_7$ and may contain some aluminium and possibly nitrogen (Rae & Jack, 1976).

Compositions close to the Y-Si-O-N face did not give any aluminium-containing phases although it is likely that aluminium is substituted in $\text{Si}_2\text{N}_2\text{O}$ as discussed in the previous section.

Glasses of the "standard cation composition"

Figure VIII.3 Devitrification products of glasses in the
Y-Si-Al-O-N system on the 16 e/o nitrogen plane
after treatment at 1270^oC for 20 hours.

YS - β - $\text{Y}_2\text{Si}_2\text{O}_7$

β' - β' -sialon

YAG - $\text{Y}_3\text{Al}_5\text{O}_{12}$

C - C-phase

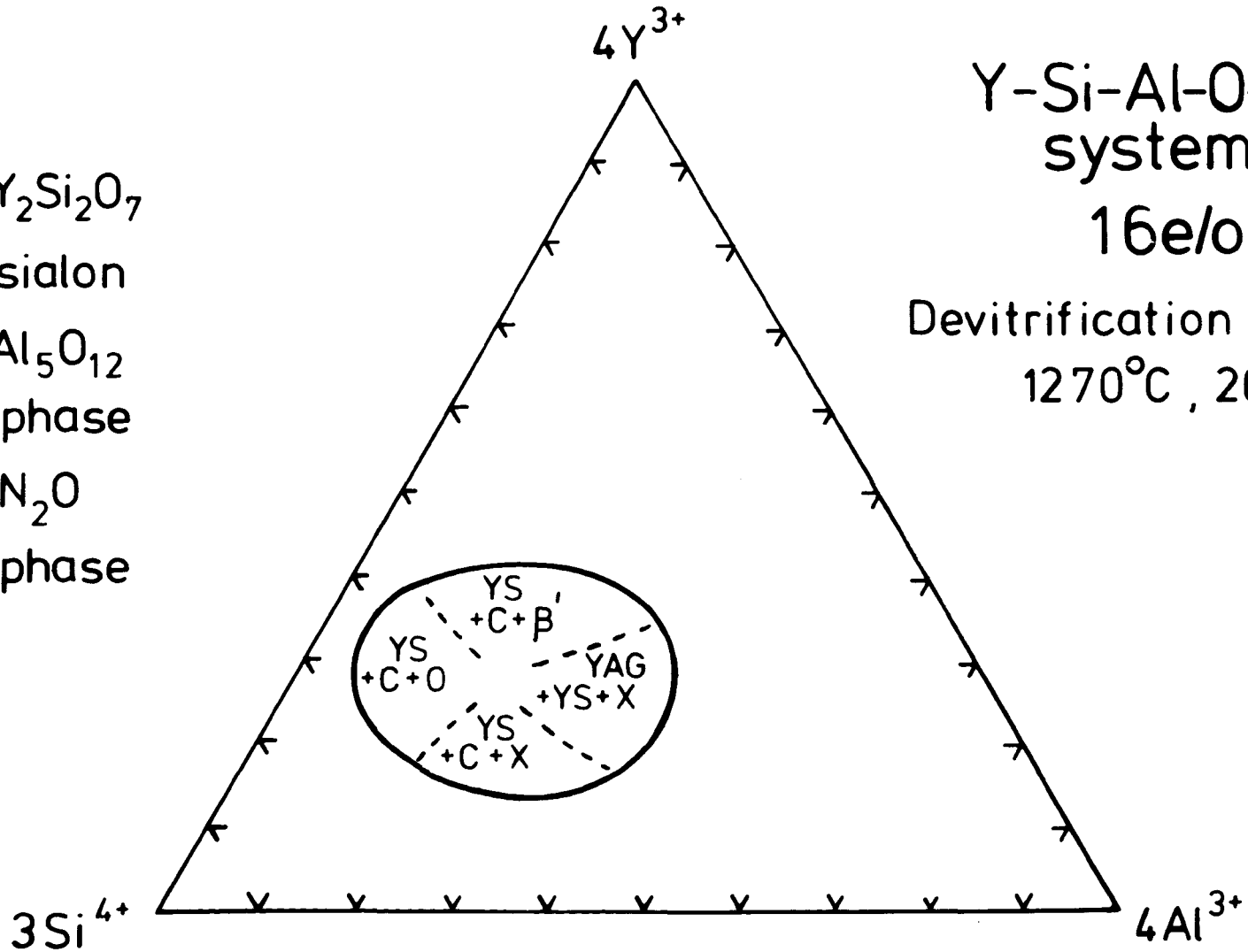
O - $\text{Si}_2\text{N}_2\text{O}$

X - X-phase

Y-Si-Al-O-N
system

16e/oN

Devitrification products
1270°C, 20 hours



containing 0, 10 and 18 e/o nitrogen that were devitrified near their crystallization temperatures gave different crystalline products. All the devitrified glasses contained $Y_2Si_2O_7$ in various modifications (Rae, 1976). The oxide glass devitrified to give mullite as the aluminium-containing phase. Both the 10 e/o N and the 18 e/o N glasses formed yttrium-aluminium garnet on heat-treatment, and the 18 e/o nitrogen glass contained another nitrogen-phase, Si_2N_2O . Figure VIII.4 shows the scanning electron micrographs of the crystallized glasses. The devitrified oxide glass had an extremely fine structure (Figure VIII.4(a)) and Figure VIII.4(b) shows fairly integrated, but simple lath-like or sometimes spherulitic crystallites on addition of 10 e/o nitrogen. Figure VIII.4(c) indicates how the 18 e/o nitrogen glass devitrifies to a more complex morphology; the dark needles are Si_2N_2O since they are not present in the 10 e/o nitrogen glass.

VIII.1.4 Ca-Si-Al-O-N glasses

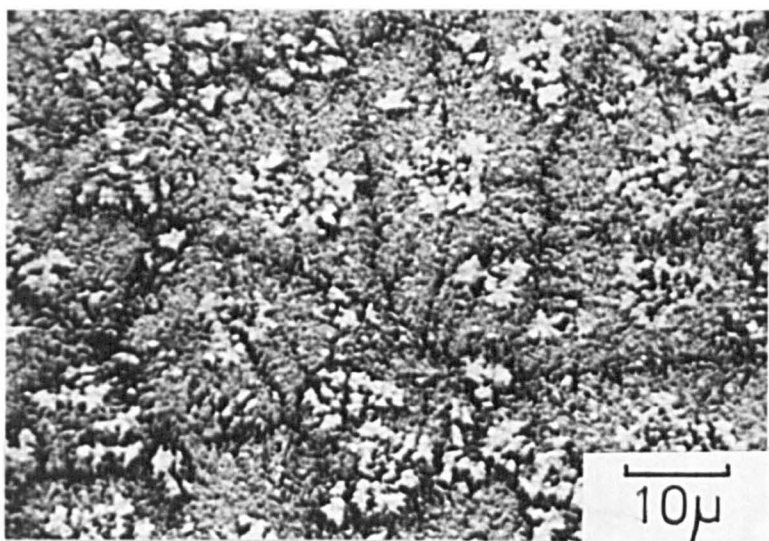
Both the oxide and nitrogen glasses devitrified to different proportions of gehlenite and wollastinite; Si_2N_2O was also present in the low aluminium, high silicon and nitrogen-containing glasses.

Figure VIII.4 Scanning electron micrographs of
devitrified Y-Si-Al-O-N glasses
(28Y:56Si:16Al)

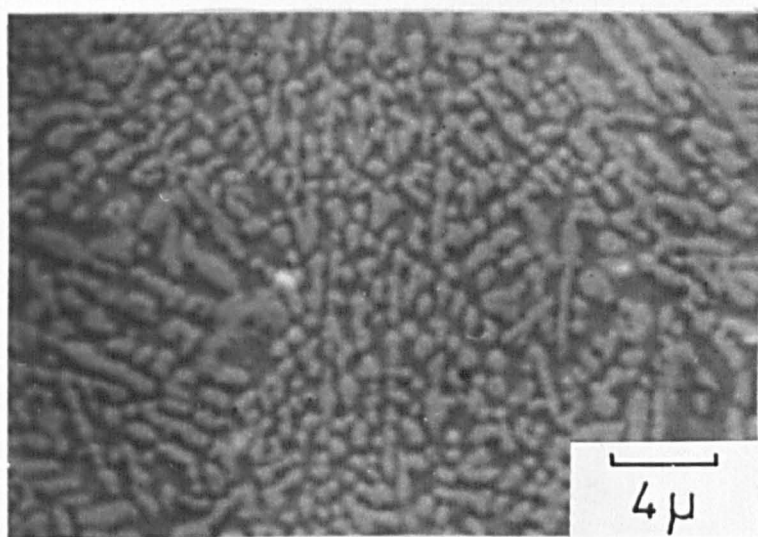
(a) 0 e/o N

(b) 10 e/o N

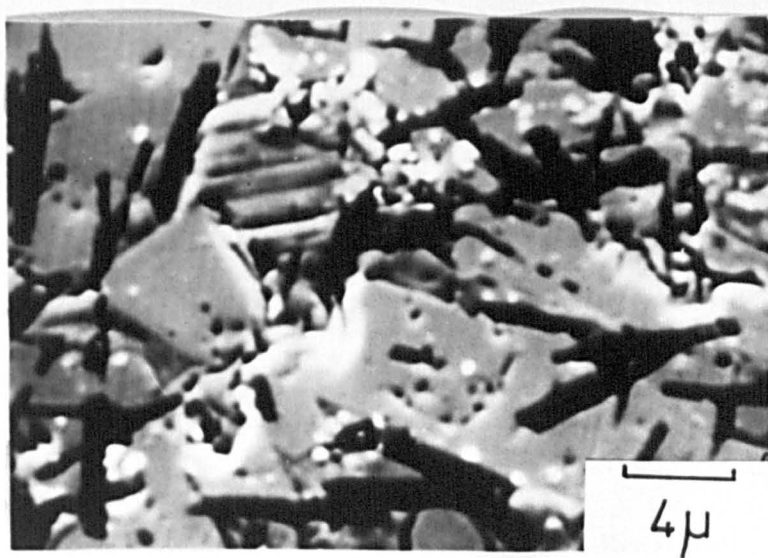
(c) 18 e/o N.



(a)



(b)



(c)

Gehlenite is a member of the melilite series of silicates. N-melilite (Rae, 1976), $Y_2Si(Si_2O_3N_4)$ is isostructural with gehlenite and forms a solid-solution with it. The incorporation of nitrogen in the gehlenite structure according to the formula $Ca_2(SiAl)_3(O,N)_7$ is not surprising and electron-probe microanalysis showed this to occur (Hampshire, 1979). Nitrogen-gehlenite is formed on devitrification of Ca-Si-Al-O-N glasses and must have a fairly wide range of homogeneity.

The scanning electron micrographs in Figure VIII.5 show that the crystalline morphology of Ca-Si-Al-O-N glasses of the standard cation composition does not change much with nitrogen substitution since the same phases are present in both.

VIII.2 Devitrification of vitreous phases present in sintered nitrogen ceramics

VIII.2.1 Introduction

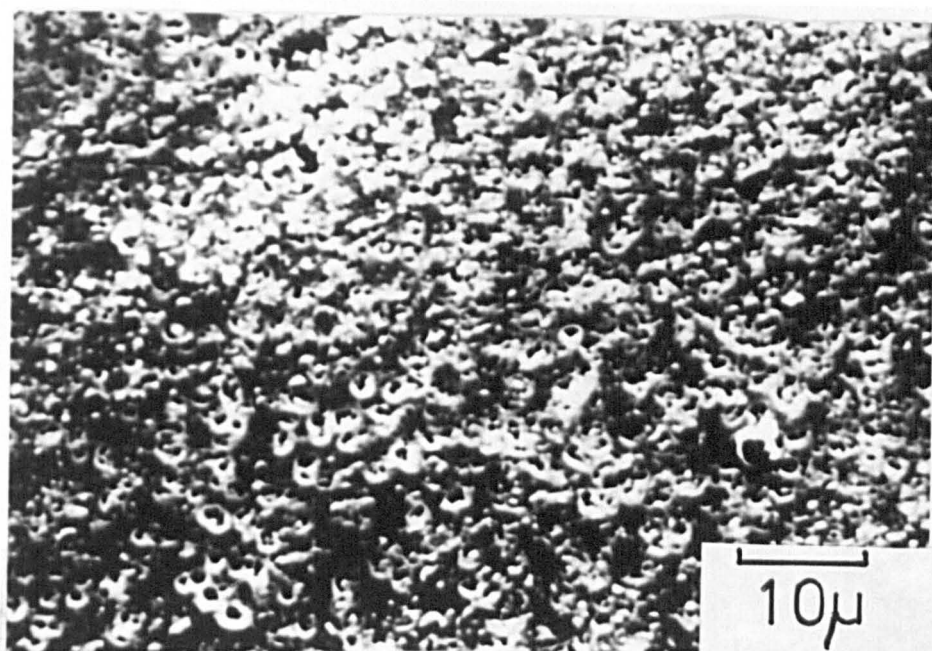
The addition of oxides such as Y_2O_3 and MgO to Si_3N_4 and β' -sialons is necessary for liquid-phase formation during pressureless sintering or hot-pressing. The liquid coats the surface of the grains (Drew & Lewis, 1974; Lewis et al., 1977) and allows the transport of material, necessary for

Figure VIII.5 Scanning electron micrographs of
devitrified Ca-Si-Al-O-N glasses

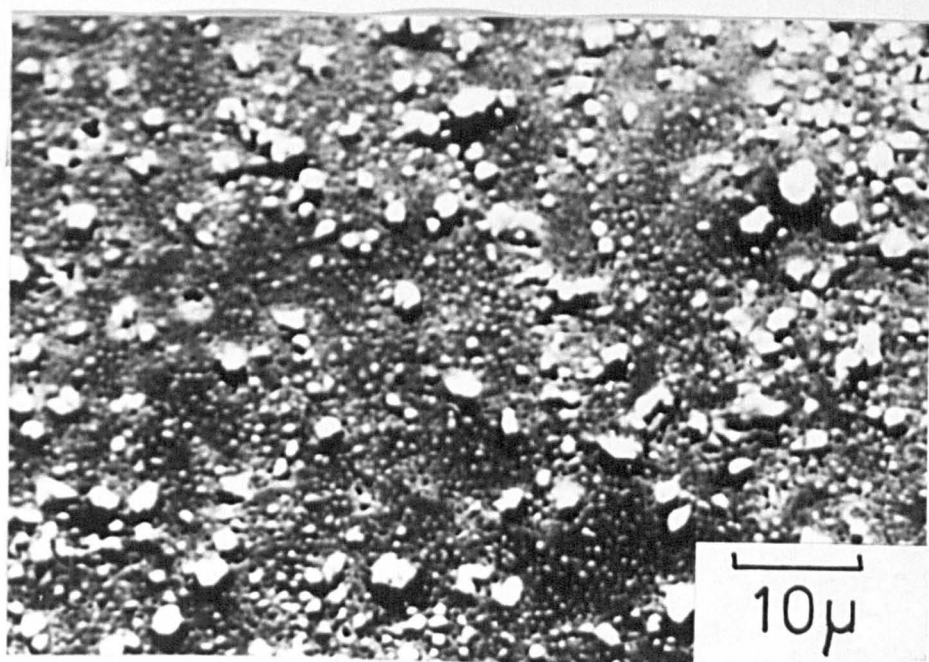
(28Ca:56Si:16Al)

(a) 10 e/o N

(b) 18 e/o N.



(a)



(b)

densification, by diffusion through the liquid; α - Si_3N_4 dissolves and β or β' -sialon is precipitated so that phase transformation also occurs during densification (Hampshire, 1980). However the oxynitride liquid cools to form a grain-boundary glass which impairs high-temperature strength, creep and oxidation resistance.

The present work has investigated the vitreous regions occurring in some M-Si-Al-O-N and M-Si-O-N systems and clearly the glassy phases formed on cooling the densified materials must have compositions within the vitreous regions examined. Any complete understanding of the high-temperature properties of nitrogen ceramics must involve a study of the viscosity and devitrification characteristics of the bulk glasses in the appropriate M-Si-Al-O-N system (Jack, 1979).

There has been little previous investigation of grain-boundary glasses in sintered nitrogen ceramics although recent work by Lewis et al. (1980a, b) and Krivanek et al. (1979) using transmission and scanning-transmission electron-microscopy made it possible to observe and analyse the grain-boundary phases.

Devitrification of the glasses gives some indication of their composition and thus should provide a clearer

idea of how improvements in the high-temperature properties of nitrogen ceramics might be achieved.

VIII.2.2 Results of heat-treatments

Table VIII.1 summarises the results of devitrification treatments on pressureless-sintered silicon nitride and β' -sialon compositions with both magnesia and yttria as densifying additives.

Si_3N_4 compositions containing MgO (1(a) and (b)) illustrate that the grain-boundary glass crystallizes to give phases found on heat-treatment of bulk Mg-Si-O-N glasses, and it is clear that the grain-boundary vitreous phase must have contained substantial amounts of nitrogen since $\text{Si}_2\text{N}_2\text{O}$ was a major devitrification product.

A Y-Si-O-N glass must be formed when Y_2O_3 is used as an additive with Si_3N_4 and the composition is probably close to that of the Y-Si-O-N glasses discussed in Chapter VI. It is well-established that impurities accumulate in the grain-boundary phases (Powell & Drew, 1974) and this may lead to greater stability because the bulk glasses were shown to be bloated and phase-separated. The devitrification products (2(a) and (b)) depend upon the heat-

Table VIII.1

Sintered material
supplied by
Dr. S. HampshirePost-preparative heat-treatment of sintered nitrogen-ceramics

No.	starting composition	original treatment		post-sintering X-ray analysis	devitrification		X-ray analysis after devitrification
		time (h)	temp. (°C)		time (h)	temp. (°C)	
1a	Si ₃ N ₄ + 5w/oMgO	0.5	1680	$\beta + \alpha$ -Si ₃ N ₄	20	1340	forsterite, Si ₂ N ₂ O, cristobalite
b	Si ₃ N ₄ + 10w/oMgO	0.5	1650	- do -	20	1340	- do -
2a	Si ₃ N ₄ + 7w/oY ₂ O ₃	2.0	1600	β -Si ₃ N ₄	20	1180	N-apatite, Y ₂ Si ₂ O ₇ , cristobalite
b	- do -	0.75	1600	- do -	45	1250	Y ₂ SiO ₅ , Si ₂ N ₂ O, cristobalite
3a	50w/oSi ₃ N ₄ , 50w/oAl ₂ O ₃ , 1w/oMgO	0.5	1680	75% β' , 25%'X' (z=2.5)	65	1300	'X' + mullite
b	β' z=3 + 5w/oMgO	0.5	1700	95% β' (z=3) 2%AlN, 3%15R	65	1300	'X', mullite, N-phase, spinel
c	53.9w/oSi ₃ N ₄ , 9.3w/o AlN, 31.6w/oAl ₂ O ₃ , 5.2w/oMgO	0.5	1680	92% β' (z=3) 8%15R	65	1300	N-phase, spinel
d	- do -	1.5	1600	94% β' (z=3) 2% α , 2% AlN	20	1270	spinel, X-phase, mullite, N-phase

continued

Table VIII.1 (continued)

Post-preparative heat-treatment of sintered nitrogen ceramics

No.	starting composition	original treatment		post-sintering X-ray analysis	devitrification		X-ray analysis after devitrification
		time (h)	temp. (°C)		time (h)	temp. (°C)	
4a	70w/oSi ₃ N ₄ , 20w/oAl ₂ O ₃ , 10w/oY ₂ O ₃	0.33	1650	95%β' (z=1.5) 3%β, 2%α	20	1270	yttrium-aluminium garnet (YAG) + C-phase
b	- do -	1.0	1600	93%β' (z=1.5) 4%β, 3%α	65	1300	Y ₂ Si ₂ O ₇ , cristobalite
c	β' z=3 mix + 3.8w/oY ₂ O ₃	0.5	1650	95%β' (z=3) 4%15R, 1%AlN	65	1300	N-apatite, Y ₂ Si ₂ O ₇
d	85w/oSi ₃ N ₄ , 5w/oAl ₂ O ₃ , 10w/oY ₂ O ₃	1.0	1600	98%β' (z=1) 2%α	65	1300	Y ₂ Si ₂ O ₇ , YAG, cristobalite

treatment temperature and time because in 2(a) the phases were N-apatite (Rae, 1976) and $Y_2Si_2O_7$ but in 2(b) these had evidently reacted together to form Si_2N_2O and Y_2SiO_5 . Assuming the original glass composition is the same in both cases it seems that Y_2SiO_5 and Si_2N_2O are the stable phase assemblage after treatment at this temperature and it is clear that the glass must contain nitrogen.

The phases found on devitrifying β' -sialon compositions sintered with MgO are similar to those found in devitrified Mg-Si-Al-O-N glasses; see Figure VIII.1. The appearance of mullite, X-phase and spinel suggest that the grain-boundary glass must have a high aluminium concentration. The proportion of magnesium-containing phases is directly related to the amount of MgO originally used. Lewis et al. (1980b) observed grain-boundary glasses only in their hot-pressed material and concluded that the majority of the magnesium was incorporated in the glass and not in the β' -phase. They also reported that increasing the MgO content led to more glass formation and consequently more Al_2O_3 was incorporated in the glass and less in the β' . It is found in the present work that even the time and temperature of the original sintering treatment affected the glass composition and, on subsequent devitrification, the final crystalline phase assemblage. This can be

clearly observed in 3(c) and (d) where the starting compositions are the same.

The β' compositions sintered with Y_2O_3 show that the glass composition must vary greatly not only with the composition of the starting mix but also, as mentioned above, with the original firing treatment. In 4(a) and (b) the devitrification products are completely different even though the starting mix is the same. It is apparent in 4(a) that the shorter devitrification time (20 hours) produces yttrium-aluminium garnet and C-phase, whereas a longer treatment (65 hours) probably allows the aluminium to be incorporated in the β' leaving only binary silicates as grain-boundary phases.

YAG and C-phase contain nitrogen, as discussed previously, and the glassy grain-boundary phases must also contain nitrogen although it is impossible to say how much without direct analysis. Jack (1977b) concluded that about 4 a/o nitrogen was incorporated in the grain boundary glass of β' -sialon hot-pressed with Y_2O_3 and it is clear from the present work that its composition falls within the Y-Si-Al-O-N glass-forming region.

VIII.2.3 Discussion

The highest viscosity bulk nitrogen glasses are in the Y-Si-Al-O-N system where softening begins around 1000°C (Chapter VII); the useful strength and oxidation resistance of β' -sialon sintered with yttria will therefore decrease above this temperature and the presence of impurities in the glass will lower the softening point still further. Suitable post-preparative heat-treatments and compositional control to obtain highly refractory phases from the grain-boundary glass offer methods of improving the high-temperature properties. However, as discussed above, the control of the grain-boundary glass composition and its devitrification products is dependant upon the many variables of densification and devitrification treatments. The devitrification of the glassy phase may also be aided by the addition of suitable nucleating-agents to the original mix. This might ensure complete crystallization during heat-treatment and avoid the retention of any glass.

The lowest solidus temperature in both the yttrium and magnesium alumino-silicate systems is approximately 1350°C and so some liquid will eventually form even in the devitrified material if this temperature is exceeded, leading to deterioration in strength and oxidation resistance. The presence of

nitrogen in silicates has been shown to cause a lowering in the solidus temperature (Hampshire, 1980). Jack (1979) pointed out that as the number of components in a particular system increases, the solidus temperatures are lowered and so in four or five component systems, even after post-preparative treatment, only a limited improvement can be made in high-temperature properties.

IX. β'' - Magnesium Sialon

IX.1 Introduction

Magnesium, beryllium and many other metal-silicon nitrides and oxynitrides have hexagonal structures based on the wurtzite-type shown by aluminium nitride. AlN is built up of AlN_4 tetrahedra whereas MgSiN_2 structure contains equal numbers of MgN_4 and SiN_4 tetrahedra and it can be regarded as an orthorhombic superlattice of the hexagonal AlN. Magnesium is therefore tetrahedrally coordinated in the nitride structure whereas it is usually octahedrally coordinated in oxides and silicates, with the exception of spinel (MgAl_2O_4) and akermanite ($\text{Ca}_2\text{MgSi}_2\text{O}_7$) where it is tetrahedrally coordinated.

Be_2SiO_4 (phenacite) is the same structural arrangement as β - Si_3N_4 but where the nitrogen atoms are replaced by oxygen atoms and two beryllium atoms substitute for two of the silicons of the β structure (see Figure II.1(a)). The beryllium atoms are therefore tetrahedrally coordinated with oxygen forming BeO_4 tetrahedra in the structure.

Mg_2SiO_4 (forsterite) is made up of isolated

SiO_4 tetrahedra in which the oxygens have a hexagonal close-packed arrangement with the magnesium cations occupying one-half of the number of octahedral holes in an ordered way and silicon occupying one eighth of the tetrahedral sites; hence magnesium is octahedrally coordinated in forsterite.

Since Be_2SiO_4 is isostructural with $\beta\text{-Si}_3\text{N}_4$, then it shows quite extensive solid-solubility in both β and β' whereas the solubility of Mg_2SiO_4 in β or β' is much lower; indeed the reaction of MgAl_2O_4 with silicon nitride indicated only 6 e/o magnesium solubility in the β' structure (Hendry et al., 1975). Gauckler et al. (1978) and Lewis et al. (1980b) reported that magnesium solubility in β' -sialon is negligible and concluded that the magnesium is incorporated in the grain-boundary glass or the spinel and polytype phases that are present after hot-pressing.

Recent work by Schneider et al. (1980) shows how a complete solid-solution can be produced between BeSiN_2 and $\beta\text{-Si}_3\text{N}_4$ and also between BeSiN_2 and AlN resulting in a single-phase material of the wurtzite structure.

The technological advantages of obtaining single-phase nitrogen ceramics is obvious since the presence

of a second phase, whether vitreous or crystalline, is the major cause of the deterioration in the high-temperature properties.

A liquid region has been reported to exist on the 3M:4X compositional plane of the Mg-Si-Al-O-N system (Jack, 1977b) close to forsterite (Mg_2SiO_4) as is shown in Figure IX.1. The existence of a phase isostructural with β - Si_3N_4 but close to a composition within this liquid region was discussed in Chapter VI. The purpose of the investigation described in the present Chapter was to study the formation of this phase, now designated as

β'' -magnesium sialon.

IX.2 Exploration of the 3M:4X plane close to forsterite

The vitreous region in the Mg-Si-Al-O-N system extends through the 3M:4X plane and slightly above it; see Chapter VI. Compositions were explored within and around the glass region on this plane and the results are presented in Figure IX.2. Peripheral compositions on the Si_3N_4 side of the glass-forming region after firing at 1700°C gave a phase with the β - Si_3N_4 structure but with unit-cell dimensions of much higher values than previously found in any β' -sialon ($z=4$). The relative changes in d-spacings are shown in

Figure IX.1 The 3M:4X plane of the Mg-Si-Al-O-N system
showing the liquid regions at 1500^o, 1600^o and 1700^oC.

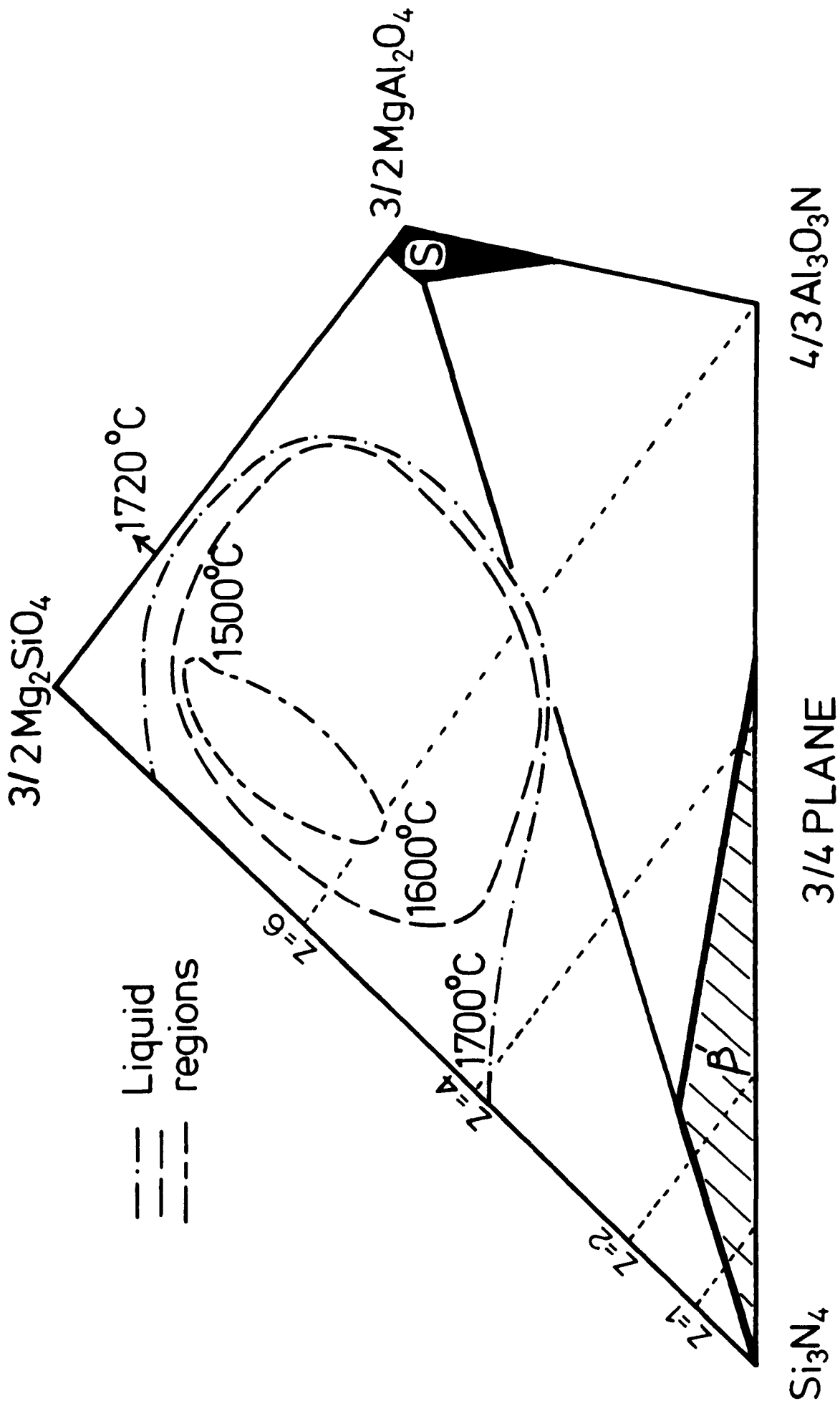


Figure IX.2 The 3M:4X plane of the Mg-Si-Al-O-N system showing the glass-forming region at 1700°C and peripheral crystalline phase fields.

Figure IX.3. The unit-cell dimensions vary depending upon the composition and, of those compositions examined, were in the range,

$$a , 7.806 - 7.930 \text{ \AA} ; \quad c , 3.069 - 3.103 \text{ \AA}$$

compared with those of a β' -sialon at the composition $z=4$ ($\text{Si}_2\text{Al}_4\text{O}_4\text{N}_4$)

$$a , 7.718 \text{ \AA} ; \quad c , 3.010 \text{ \AA} .$$

Accurate values were difficult to obtain since compositional variations give broad lines on the X-ray diffraction patterns. The new phase was designated β'' -magnesium sialon.

β'' was produced by either adding Si_3N_4 (usually in the form of high β) to a glass composition thus moving the composition outside the vitreous region to the points marked "a" and "b" on Figure IX.2, or by direct preparation from oxide and nitride powder mixes. The former method was investigated by firing glass and AME "high β - Si_3N_4 " for five minutes at 1700°C in the tungsten resistance furnace and subsequently cooling it ($250^\circ\text{C}/\text{minute}$), whereas the latter method required longer firing times, 30-60 minutes, for complete reaction.

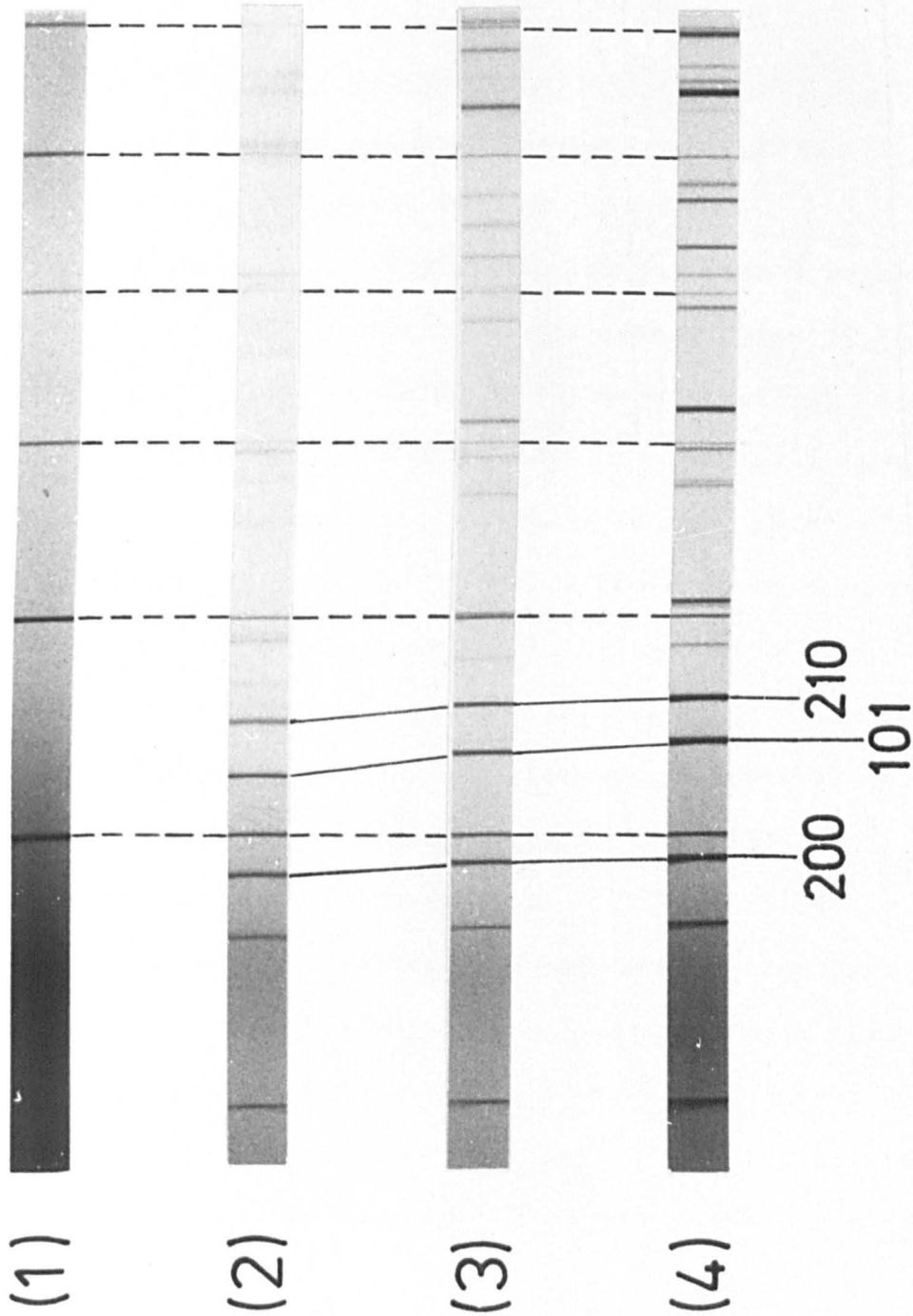
Figure IX.3 X-ray photographs showing the diffraction pattern
of β'' (2) compared with β' -sialon (3) and β -Si₃N₄ (4).

Mg-sialon
glass

Devitrified
 β''

β' -sialon
 $z=3$

β - Si_3N_4



----KCl standard

β'' was frequently found as a crystalline phase on the periphery of the glass-forming region of the Mg-Si-Al-O-N system and occurred both on and below the 3M:4X compositional plane (see Chapter VI). Trace amounts of β -Si₃N₄ were always present in conjunction with the β'' -phase.

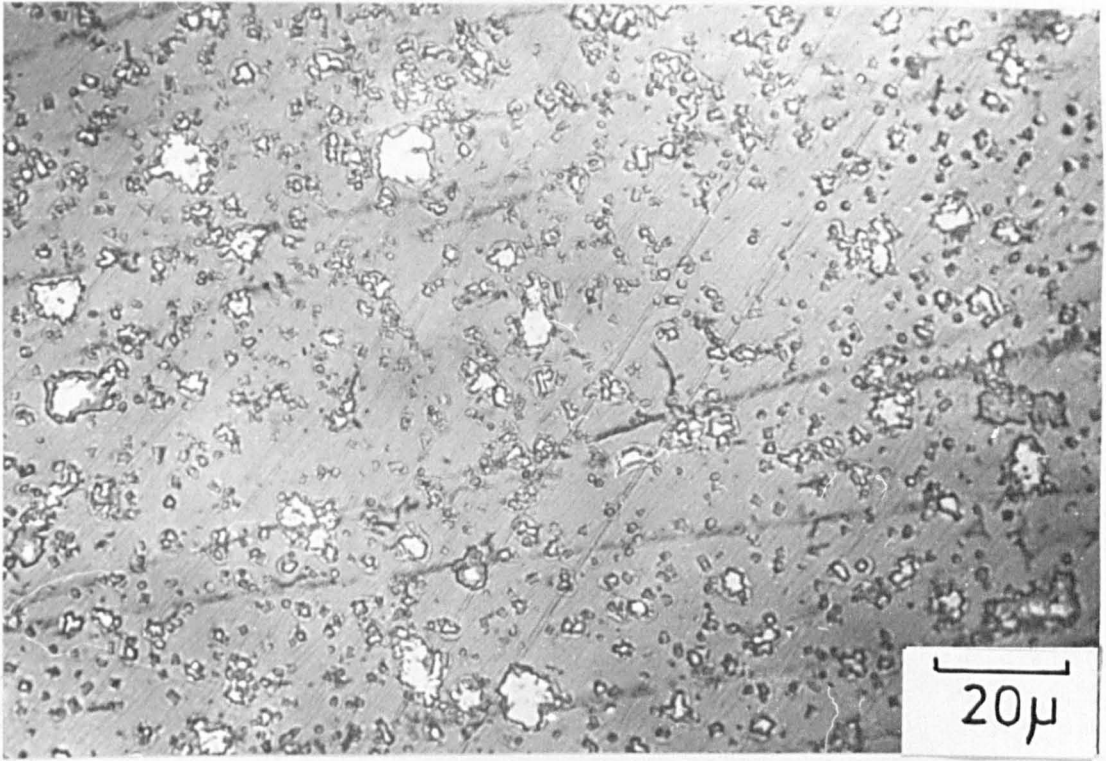
IX.3 X-ray and microscopical examination of β''

Optical and scanning electron micrographs of the composition marked "a" on Figure IX.2 ($\text{Mg}_{22}\text{Si}_{18}\text{Al}_3\text{O}_{47}\text{N}_{10}$) show small regular-shaped crystals distributed in a matrix of glass; see Figures IX.4(a) and 5(a). Heat-treatment of the same sample at 870°C for 20 hours increases the extent of crystallization around the original small crystals (Figure IX.5(b)). Further heating at 930°C for 20 hours shows that the sample is almost completely crystallized with only about 15-20% of residual glass; see Figures IX.4(b) and 5(c). X-ray diffraction showed a corresponding increase in the amount of β'' and a trace of forsterite (Mg_2SiO_4) was also detected after treatment at 930°C. Higher magnifications on the material before heat-treatment identified hexagonal crystals (Figure IX.6(a)), the electron-probe micro-analysis of which showed them to be mainly silicon nitride that had evidently precipitated from the liquid on cooling. The matrix was a homogeneous

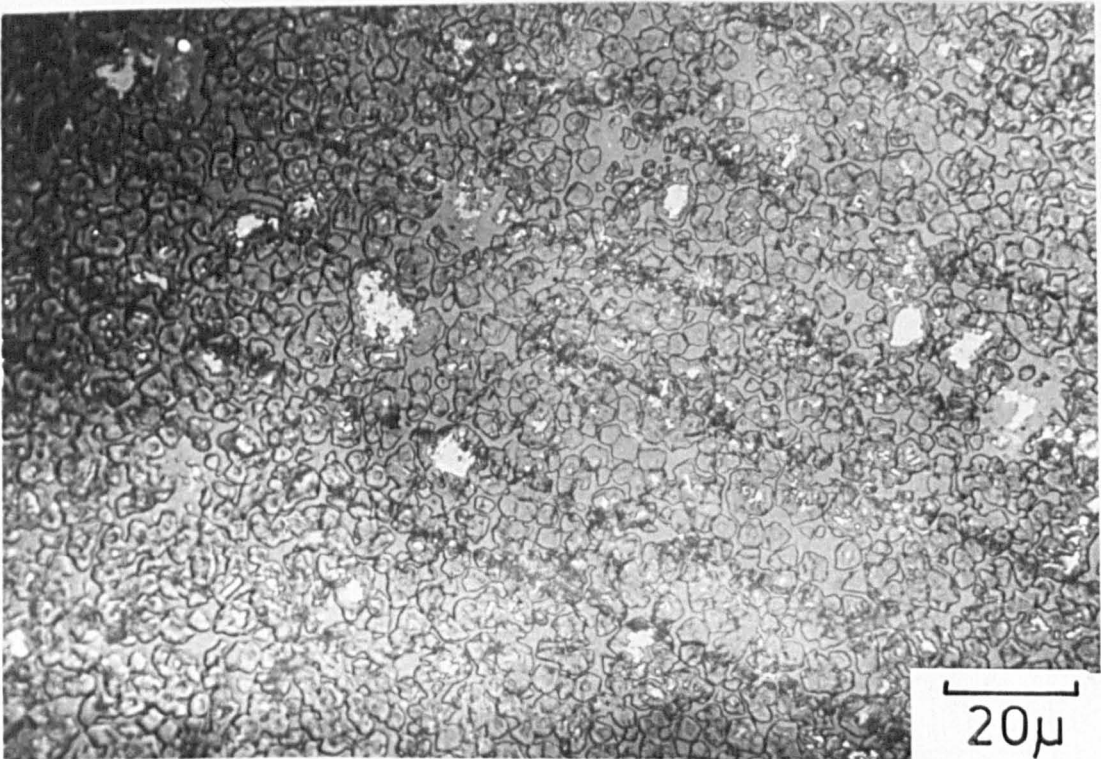
Figure IX.4 Optical micrographs of composition
 $\text{Mg}_{22}\text{Si}_{18}\text{Al}_3\text{O}_{47}\text{N}_{10}$ marked as "a" on
Figure IX.2

(a) after firing at 1700°C for 5 minutes

(b) as (a) and then devitrified at
 930°C for 20 hours.

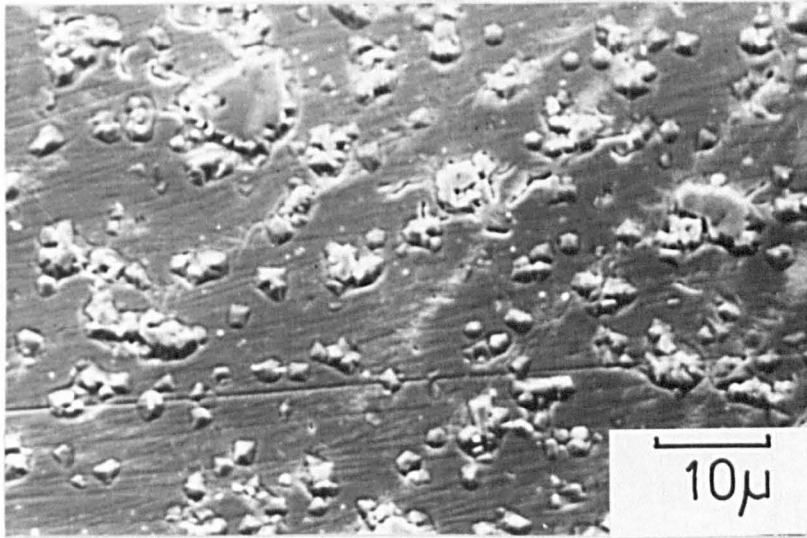


(a)

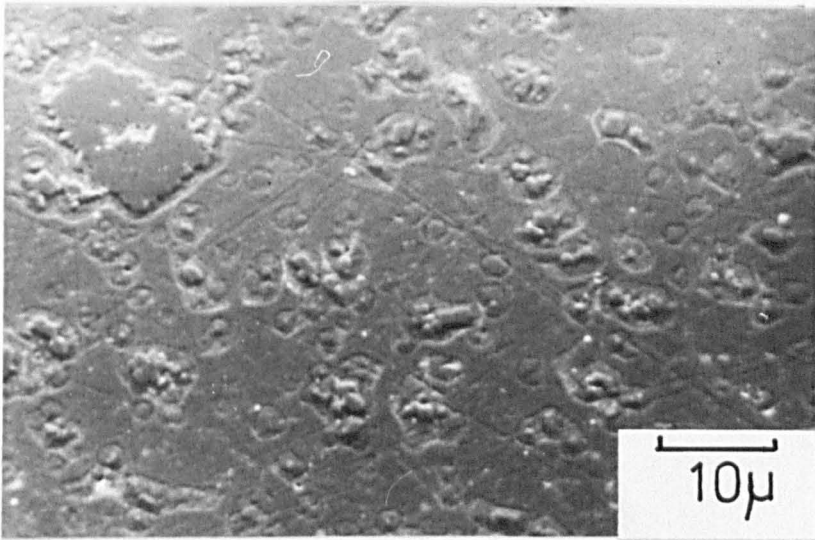


(b)

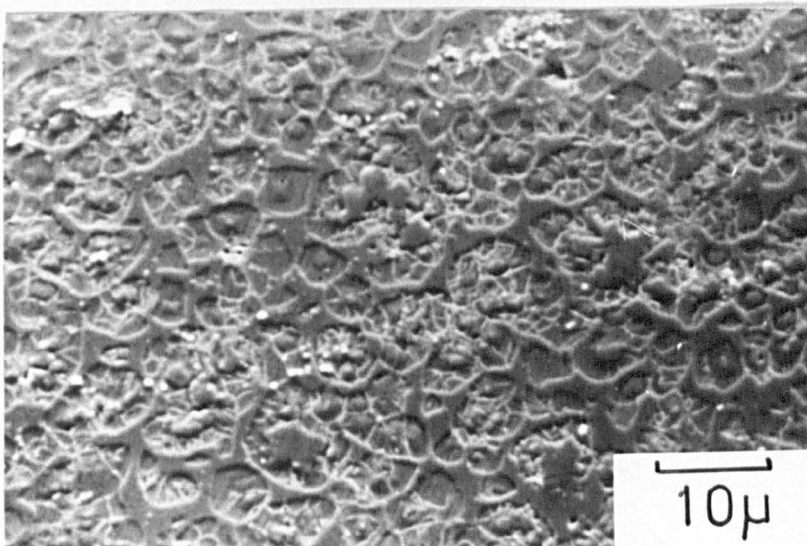
Figure IX.5 Scanning electron micrograph of
composition marked "a" on Figure IX.2
(a) after firing at 1700°C for 5 minutes
(b) as (a) and then devitrified at
 870°C for 20 hours
(c) as (a) and then devitrified at 930°C
for 20 hours.



(a)



(b)



(c)


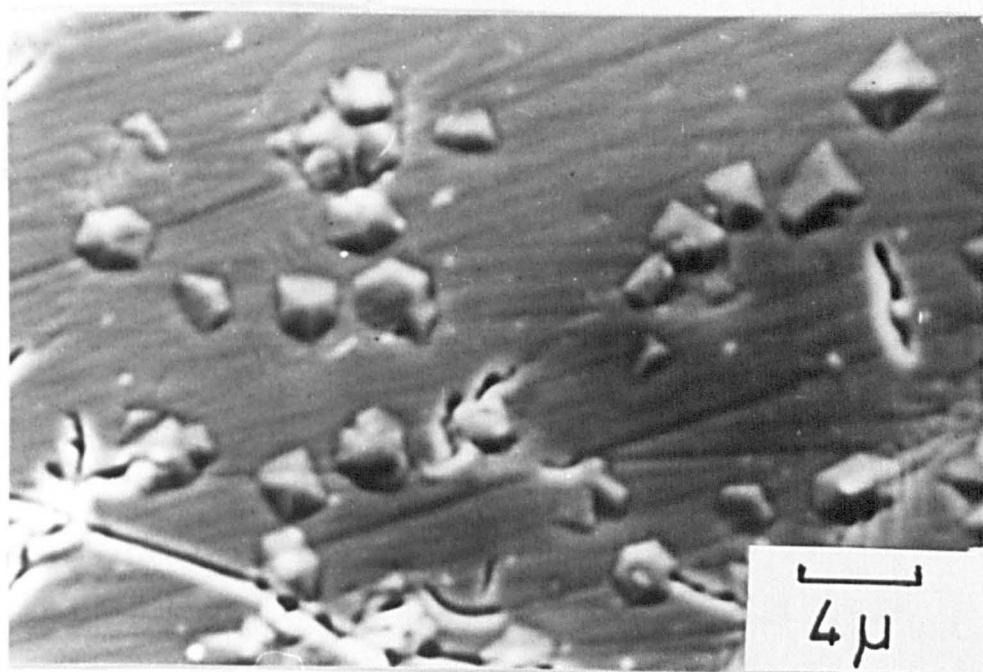
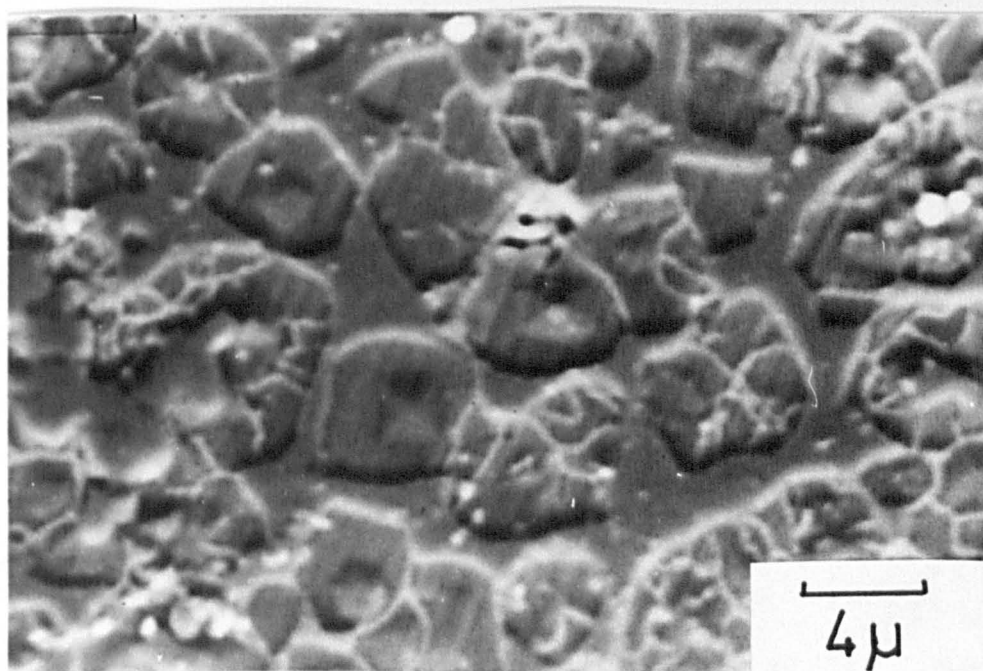


Figure IX.6 Scanning electron micrograph of
composition marked "a" on Figure IX.2
(a) after firing at 1700°C for 5 minutes
(b) as (a) and then devitrified at 930°C
for 20 hours.



(a)



(b)

glass with an analysis close to the starting composition,

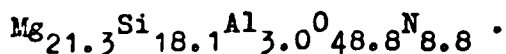


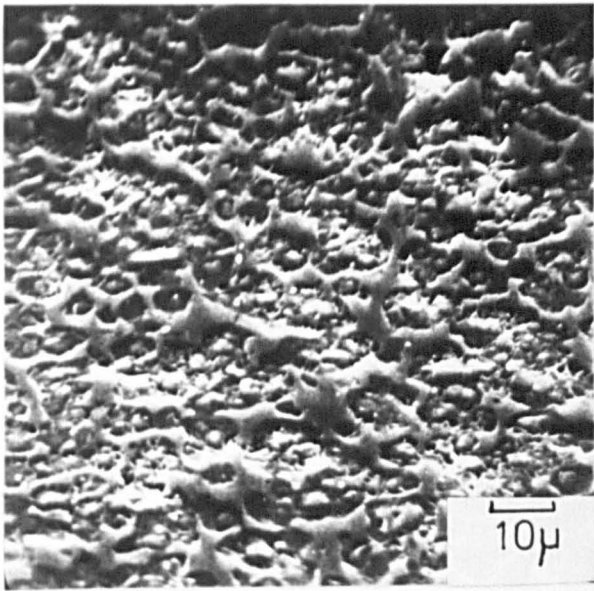
Figure IX.6(b) is a higher magnification of the sample shown by Figure IX.5(c), i.e. after treatment at 930°C for 20 hours and it is apparent that the hexagonal crystals are surrounded by equiaxed grains. Electron-probe microanalysis showed that the hexagonal crystals are again silicon nitride and the surrounding grains are of average composition, $\text{Mg}_{20.7}\text{Si}_{18.1}\text{Al}_{3.6}\text{O}_{47.9}\text{N}_{9.7}$ corresponding to the "cross" (+) marked "c" on Figure IX.2. The unit-cell dimensions of this particular β'' composition being a, 7.909 ; c, 3.100 .

The X-ray maps of the three cations obtained from EDAX (Figure IX.7) show that there is a homogeneous distribution of Mg, Si and Al around the particles of silicon nitride. It is clear from the X-ray diffraction evidence and the electron-probe microanalysis that the equiaxed crystals are the β'' -phase and have a composition $\text{Mg}_{20.7}\text{Si}_{18.1}\text{Al}_{3.6}\text{O}_{47.9}\text{N}_{9.7}$ that is very close to that of the original glass. The hexagonal crystals are evidently β - Si_3N_4 and the β'' seems to nucleate on them. Transmission electron-microscopy (Wild, 1980) has also shown this feature and epitaxial growth of the β'' on β - Si_3N_4 (or β' -sialon) seems probable since the diffraction patterns of β''

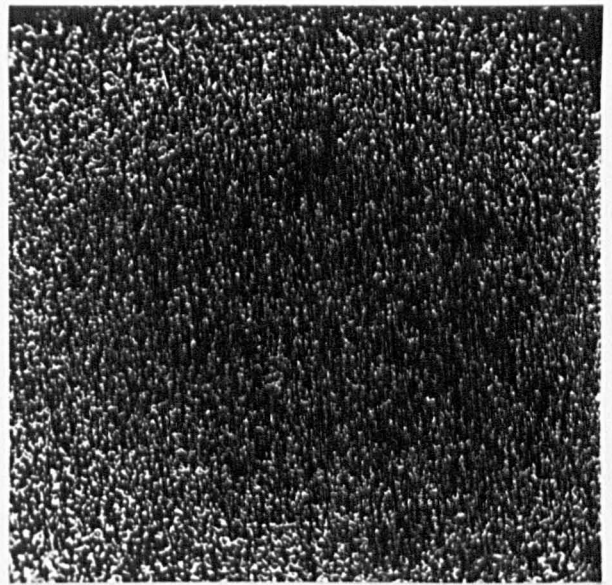
Figure IX.7 EDAX of composition marked "a" on

Figure IX.2

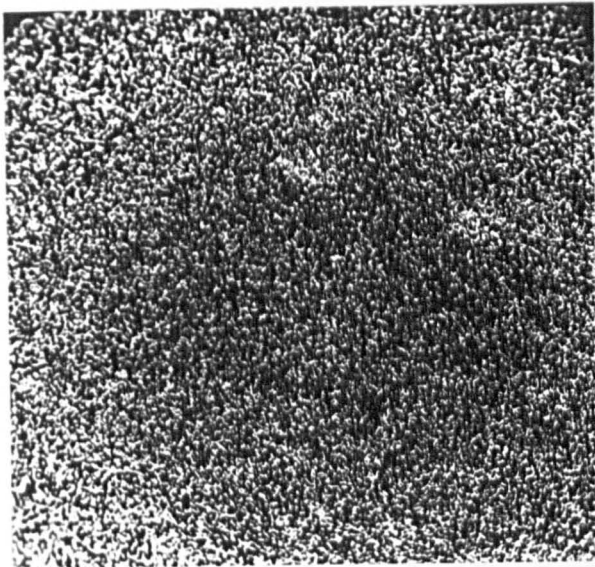
(a) secondary electron image and X-ray
maps: (b) Mg (c) Si and (d) Al.



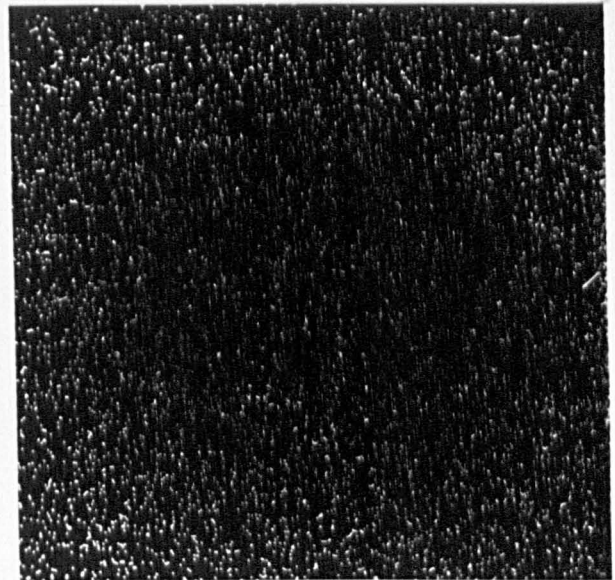
(a) Electron image



(b) Mg



(c) Si



(d) Al

and β are superimposed and have the same orientation. On shifting the composition closer to the β' -sialon phase field, β' particles act as nuclei. It is probably fortuitous that β'' is formed merely by cooling the appropriate fusion mixture since it is obviously a product of devitrification. However, under the cooling conditions employed, the sample was held sufficiently long in the correct temperature range (850° - 950° C) for crystallization to start epitaxially on β - Si_3N_4 or β' particles.

The β'' -magnesium sialon phase is not stable above 950° C and gradually transforms to forsterite, N-phase and silicon oxynitride. Heat-treatment of the sample shown in Figure IX.4(b) at 1270° C transformed it completely to the above phases.

IX.4 Discussion

The β'' -magnesium sialon phase is isostructural with β - Si_3N_4 but with highly expanded unit-cell dimensions. The only directly determined composition, $\text{Mg}_{20.7}\text{Si}_{18.1}\text{Al}_{3.6}\text{O}_{47.9}\text{N}_{9.7}$, has a metal:non-metal ratio of 3M:4X i.e. the same as for Si_3N_4 and Be_2SiO_4 , and in order to adopt the phenacite structure, and therefore maintain the requisite 3M:4X ratio, all the metal atoms must occupy tetrahedral sites in β'' .

It is clear, therefore, that magnesium cannot occupy interstitial sites in the structure, as it does in α' -sialons, $M_X(\text{Si,Al})_{12}(\text{O,N})_{24}$ where $M:X > 3:4$ (see Jack, 1976; Hampshire et al., 1978) and in the stuffed-quartz derivatives of silica (see Buerger, 1954) where Al^{3+} replaces Si^{4+} in the tetrahedral sites and the charge balance is maintained by stuffing Mg^{2+} ions into the interstitial sites (Schreyer & Schairer, 1961).

The composition of β'' is close to that of forsterite with some substitution of N^{3-} for O^{2-} and with appropriate changes in the cation ratio i.e. Si^{4+} and Al^{3+} replacing Mg^{2+} , thus maintaining a 3M:4X ratio and providing overall electroneutrality. It is clear that the change in composition enables magnesium atoms to become four-fold coordinated in the β'' -phase, rather than six-fold coordinated as in forsterite, and this change is probably due to the presence of nitrogen.

As discussed in Chapter VI there is evidence that magnesium is tetrahedrally coordinated in nitrogen glasses. It is not unreasonable, therefore, that magnesium should be tetrahedrally coordinated in a crystalline phase such as β'' which is obtained by devitrification of nitrogen glasses.

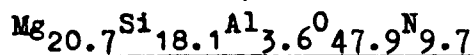
Table IX.1(a) lists the bond lengths, for tetrahedral coordination of the metal atoms that occur in the β'' -phase. For the composition $\text{Mg}_{20.7}\text{Si}_{18.1}\text{Al}_{3.6}\text{O}_{47.4}\text{N}_{9.7}$, the relative proportions of all the M-X bonds in the structure can be calculated and, using the appropriate individual bond lengths (Table IX.1(a)), an average M-X bond length of 1.825 \AA is derived. Comparison with the mean Si-N bond length of 1.74 \AA in $\beta\text{-Si}_3\text{N}_4$ indicates that the β'' -lattice is linearly expanded by 4.9% relative to β . Assuming this expansion is isotropic the unit-cell dimensions of β'' are therefore expected to be 4.9% larger than those of $\beta\text{-Si}_3\text{N}_4$.

Table IX.1(b) shows that the calculated and observed unit-cell dimensions and volumes for β'' are in reasonable agreement. The calculated a-value and c-value are respectively somewhat higher and lower than those observed but the calculated and observed cell volumes are in exact agreement. This shows that although the expansion of β'' relative to β is not isotropic, the overall volume change is accounted for by the proposed composition and structure.

Since the scattering factors of silicon, magnesium and aluminium are very similar to each another, it is not possible to detect any change in intensities or the

Table IX.1(a)

M-X bond lengths for the tetrahedral coordination of metal atoms and relative numbers of the different bonds in β'' of composition,



bond M - X	M - X bond lengths, \AA	relative numbers of M - X bonds in the β'' -phase
Mg - O	1.97	1.406
Mg - N	2.13	0.082
Si - O	1.62	0.355
Si - N	1.74	0.072
Al - O	1.75	0.071
Al - N	1.87	0.014

Table IX.1(b)

Unit-cell dimensions and volumes for β - Si_3N_4 and β'' of composition $\underline{\text{Mg}_{20.7}\text{Si}_{18.1}\text{Al}_{3.6}\text{O}_{47.9}\text{N}_{9.7}}$

	unit-cell dimensions, \AA		unit-cell volume, \AA^3
	<u>a</u>	<u>c</u>	V
β - Si_3N_4	7.61	2.91	145.9
β'' calc	7.98	3.05	168.4
β'' obs	7.92	3.10	168.4

occurrence of extra reflections in the X-ray diffraction pattern due to the presence of magnesium in the β'' structure. However it is clear from the above that magnesium must occupy tetrahedral sites in the structure.

The β'' phase crystallizes from the glass only in a limited temperature range (850° - 950° C) and in the presence of β - Si_3N_4 crystallites acting as nuclei on which it grows epitaxially. Above 950° C, diffusion rates increase and the greater structural mobility allows transformation of the β'' phase to the more stable forsterite structure with aluminium and nitrogen being accommodated in N-phase ($\text{Mg}_2\text{SiAlO}_4\text{N}$) and any excess silicon and nitrogen forming $\text{Si}_2\text{N}_2\text{O}$.

The transformation of one phase to another is not uncommon during devitrification of glasses; indeed in the Mg-Si-Al-O glass-system the formation of metastable phases such as high-quartz solid solution and magnesium-petalite occurs at low temperatures during devitrification (see Barry et al., 1978). Similarly, β'' -magnesium sialon occurs as a low-temperature devitrification product of Mg-Si-Al-O-N glasses which have compositions at or close to 3M:4X .

X. Conclusions and Suggestions for Future Work

Nitrogen-containing glasses occur in a number of M-Si-O-N and M-Si-Al-O-N systems. The M-Si-Al-O-N glass-forming regions are extensions of their corresponding M-Si-Al-O vitreous regions and occur by the substitution of oxygen by nitrogen in the glass provided that appropriate valency compensation is also made by changes in the cation composition. Initially the composition range of the glass-forming region widens up to about 10 e/o N (4 a/o) but on further substitution of oxygen by nitrogen the extent of the vitreous region is gradually reduced. The maximum nitrogen solubility is in the range 10-12.5 a/o depending upon the particular system. The highest nitrogen-containing glasses so far obtained are in the Y-Si-Al-O-N system.

Viscosity and refractive index in all the nitrogen-glass systems increase with nitrogen concentration. These observations are of possible technological significance since replacement of oxygen by nitrogen in glasses provides a means of changing glass properties.

The study of viscosity, and devitrification of nitrogen glasses is necessary for the understanding of the high-temperature properties of nitrogen ceramics. Eventual improvements may be made in these materials by compositional control of the grain-boundary vitreous phases and post-preparative devitrification heat-treatments to obtain refractory second phases compatible with the matrix.

The β'' -magnesium sialon phase is isostructural with β - Si_3N_4 and has a composition close to that of forsterite (Mg_2SiO_4) but with some substitution of Mg^{2+} by Si^{4+} and Al^{3+} and also O^{2-} by N^{3-} . The phase is obtained by devitrification of 3M:4X glasses and must be nucleated by β - Si_3N_4 or β' -sialon. The possible stabilization of this phase to higher temperatures is worth further exploration since single-phase nitrogen ceramics densified with magnesia additions might then be possible.

Appendix

The Dielectric Properties of Selected Nitrogen Glasses

Initial measurements of dielectric constant on some calcium and magnesium sialon glasses are discussed (Thorp & Kenmuir, 1980). The glasses were of the standard cation composition, 28 e/o M : 56 e/o Si : 16 e/o Al , (see Chapter VII), and are given in Table A.1. The measurements were carried out at Durham University on specimens prepared at Newcastle.

Values of the real (ϵ') and imaginary (ϵ'') parts of the dielectric constant and the a.c. conductivity (σ_{ac}) were obtained at room temperature over a frequency range 10^3 Hz to 10^4 Hz using bridge techniques. The experimental methods are described in detail by Thorp & Rad (1980) and Rad (1980). Specimens of 1 cm diameter and a thickness of 0.05 cm were prepared from the bulk glasses by cutting and polishing and transparent discs similar to those shown in Figure VII.15 were obtained. Circular gold electrodes were evaporated onto the surfaces of the discs to provide good electrical contact with the electrodes of the measuring jig. Careful estimation

Table A.1 Composition of the glasses investigated and their dielectric constants

sample number		composition						ϵ' 1600 Hz	ϵ_{∞}	refractive index ($\epsilon_{\infty}^{1/2}$)
		Mg	Ca	Si	Al	O	N			
1	e/o	28	-	56	16	100	0	6.8	2.46	1.567
	a/o	16.8	-	16.8	6.4	60.0	0			
2	e/o	28	-	56	16	82	18	8.3	2.71	1.645
	a/o	17.4	-	17.4	6.7	51.0	7.5			
3	e/o	-	28	56	16	100	0	8.8	2.59	1.609
	a/o	-	16.8	16.8	6.4	60.0	0			
4	e/o	-	28	56	16	88	12	9.7	2.77	1.664
	a/o	-	17.2	17.2	6.5	54.2	4.9			
5	e/o	-	28	56	16	86	14	10.1	2.80	1.673
	a/o	-	17.3	17.3	6.5	53.1	5.8			

of edge effects enabled an accuracy of $\pm 6\%$ to be achieved.

Table A.1 shows the values of ϵ' and the variations of $\log (\epsilon' - \epsilon_{\infty})$ with $\log \omega$ are illustrated in Figure A.1. The value of ϵ_{∞} was estimated from the optical refractive index measurements discussed in Chapter VII. The data obtained for each composition fit well with the Universal dielectric response law

$$(\epsilon' - \epsilon_{\infty}) = \omega^{(n-1)}$$

and the slopes of the individual plots give a value of $n = 0.99 \pm 0.02$ for all the glasses. It is clear that substitution of nitrogen for oxygen increases for both the magnesium and calcium glasses at any frequency in the range examined. The value of ϵ' also increases when changing the modifying cation from magnesium to calcium in both the oxide and nitrogen glasses. As discussed in Chapter VII, the values of refractive index are altered in a similar way by the same compositional changes (see Table A.1).

The conductivity data are shown in Figure A.2 and the curves for each glass composition fit well with the variation expected for a hopping mechanism

Figure A.1 Dependence of $(\epsilon' - \epsilon_{\infty})$ on frequency and composition.

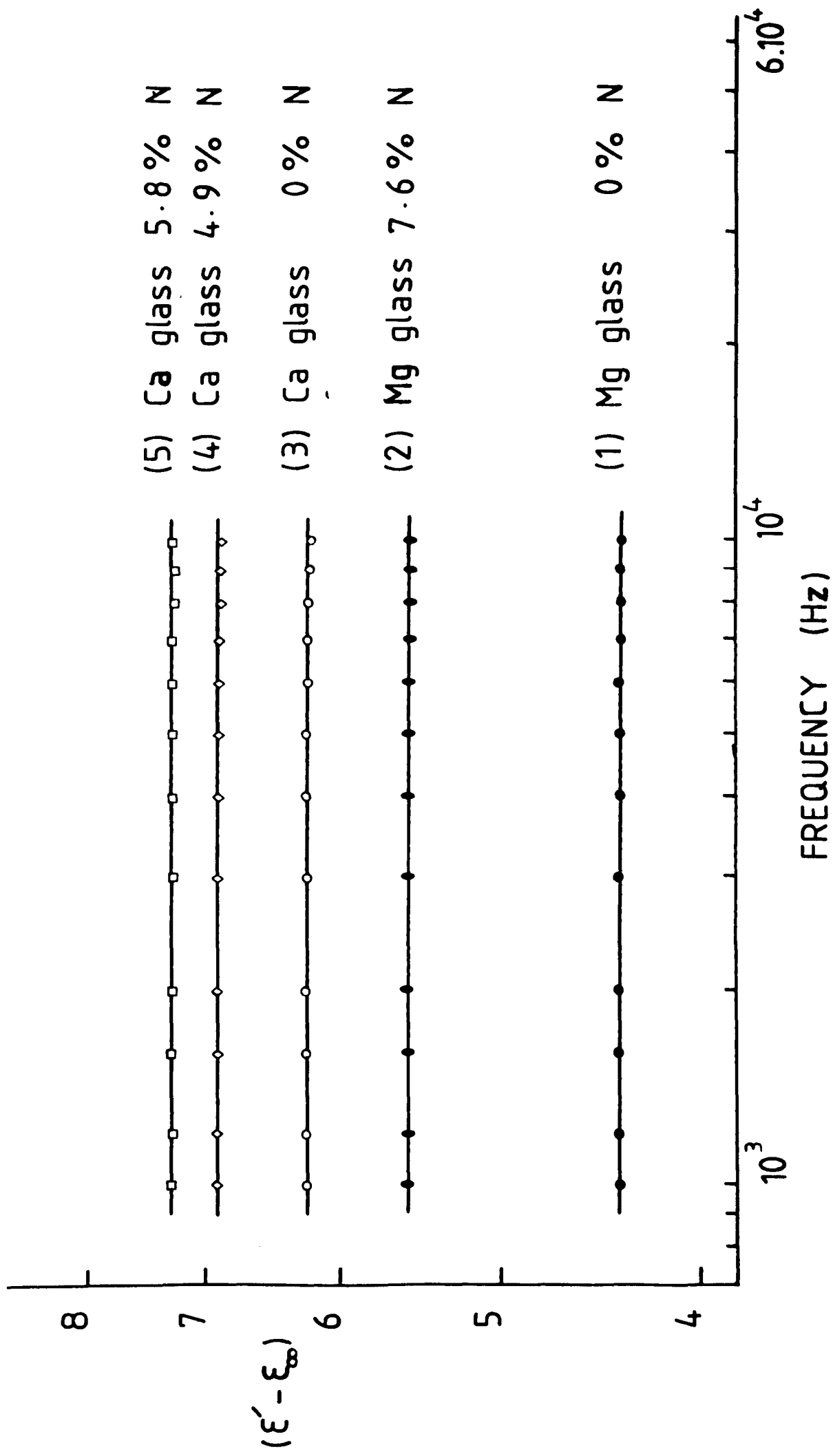
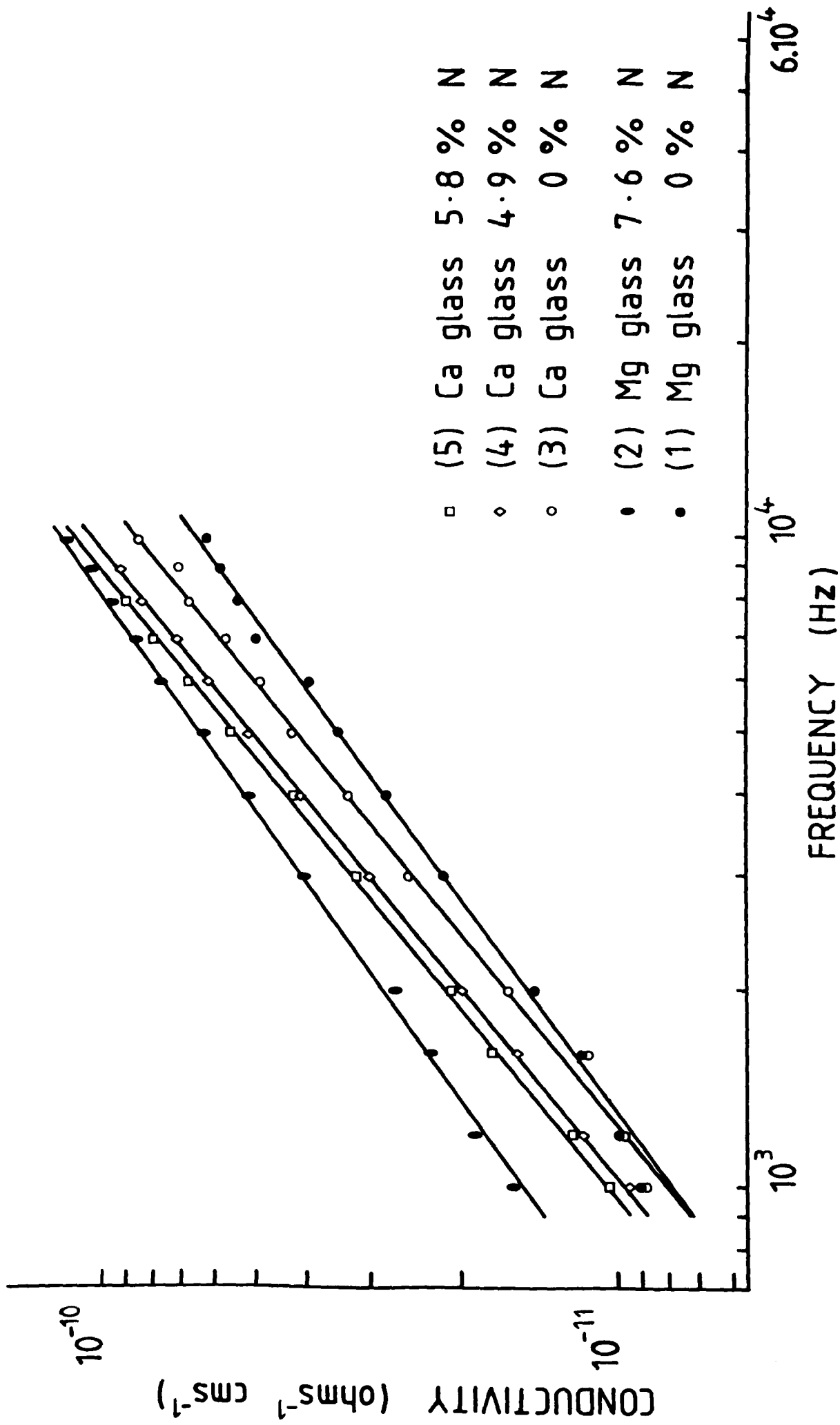


Figure A.2 Dependence of conductivity on frequency and composition.



of conductivity where $\sigma_{ac} \propto \omega^n$. The data give a value of $n = 1.0 \pm 0.1$ for the calcium glasses which is in good agreement with that found from the $(\epsilon' - \epsilon_{\infty})$ curves. In the case of the magnesium glasses the values of n derived from the conductivity measurements are rather lower than those obtained from the dielectric plots. It must be pointed out that it is more difficult to measure accurately the values of σ_{ac} than ϵ' and this might explain the discrepancy.

Conductivities for Y-Si-Al-O-N glasses reported by Leedecke & Loehman (1980) at 100 kHz and elevated temperatures are of a similar order to those discussed here in the kHz range but measured at room temperature. The above authors also reported an increase in ϵ' , at room temperature, with nitrogen addition.

Acknowledgements

I wish to thank Dr. J.S. Thorp and Miss S.V.J. Kenmuir of the Department of Applied Physics and Electronics, the University of Durham for providing the results of their measurements of electrical properties and for their helpful discussions.

Appendix references

- Thorp, J.S. & Kenmuir, S.V.J. (1980) Paper submitted to J. Mat. Sci.
- Thorp, J.S. & Enayati-Rad, N. (1980) Paper submitted to J. Mat. Sci.
- Enayati-Rad, N. (1980) Ph.D. Thesis, University of Durham.
- Leedecke, C.J. & Loehman, R.E. (1980) J. Am. Ceram. Soc. 63, 190.

References

- Barry, T.I., Cox, J.M. & Morrell, R. (1978).
J. Mat. Sci. 13, 594.
- Berry, M. (1979). Internal Report, Department of
Metallurgy and Engineering Materials, University
of Newcastle upon Tyne.
- Briggs, J. (1975). Glass and Ceramic Bulletin
(India) 22, 73.
- Briggs, J. & Carruthers, T.G. (1976). Phys. Chem.
Glasses 17, 30.
- Buang, K. (1979). Ph.D. Thesis, University of
Newcastle upon Tyne.
- Buerger, M.J. (1954). Am. Min. 39, 600.
- Chyung, K. & Wusirika, R.R. (1978). U.S. Patent
No. 4,070,198.
- Davies, M.W. & Meherali, S.G. (1971). Met. Trans.
2, 2729.
- Dodsworth, J. (1980). Ph.D. Thesis, University of
Newcastle upon Tyne.
- Doremus, R.H. (1973). "Glass Science".
John Wiley & Sons (New York).
- Drew, P. & Lewis, M.H. (1974). J. Mat. Sci. 9, 261.
- Elmer, T.H. & Nordberg, M.E. (1965). Proceedings of the
7th International Congress on Glass, Brussels, p. 30.
- Elmer, T.H. & Nordberg, M.E. (1967). J. Am. Ceram. Soc.
50, 6, 275.
- Findley, A. (1927). "The Phase Rule and its Applications",
6th ed., Longmans Green (London).

- Gauckler, L.J., Lukas, H.L. & Petzow, G. (1975).
J. Am. Ceram. Soc. 58, 346.
- Gauckler, L.J., Lukas, H.L. & Tien, T.Y. (1976).
Mat. Res. Bull. 11, 503.
- Gauckler, L.J., Weiss, J. & Tien, T.Y. (1978).
J. Am. Ceram. Soc. 61, 397.
- Gazza, G.E. (1975). Bull. Am. Ceram. Soc. 54, 778.
- Hagy, H.E. (1963). J. Am. Ceram. Soc. 46, 93.
- Hampshire, S., Park, H.K., Thompson, D.P. & Jack, K.H.
(1978). Nature 274, 880.
- Hampshire, S. (1978 & 1979) Internal Reports
Crystallography laboratory, University of Newcastle
upon Tyne.
- Hampshire, S. (1980). Ph.D. Thesis, University of
Newcastle upon Tyne.
- Hardie, D. & Jack, K.H. (1957). Nature 180, 332.
- Harding, F.L. & Ryder, R.J. (1970). Glass Tech. 11, 54.
- Hendry, A., Perera, D.S., Thompson, D.P. & Jack, K.H.
(1975). "Special Ceramics" (P. Popper ed.) Vol. 6,
p. 321.
- Hetherington, G., Jack, K.H. & Kennedy, J.C. (1964).
Phys. Chem. Glasses 5, 5.
- Holmquist, S.B. (1963). Zeits. Krist. 118, 477.
- Indrestedt, I. & Brosset, C. (1964). Acta Chem. Scand.
18, 1879.
- Jack, K.H. & Wilson, W.I. (1972). Nature, 231, 28.
- Jack, K.H. (1973). Trans. J. Brit. Ceram. Soc. 72, 376.
- Jack, K.H. (1974). "Ceramics for High-Performance
Applications", 265 (ed. Burke, J.J., Corum, A.E. &
Katz, R.N.) -Proc. 2nd Army Mat. Tech. Conf.,
Brook Hill Pub. Co. (Chestnutt Hill, Mass.).
- Jack, K.H. (1976)b. J. Mat. Sci. 11, 1135.
- Jack, K.H. (1977)a. Proc. NATO Adv. Study Inst., "Nitrogen

- Ceramics" (Riley ed.) p. 257 (Noordhof, Leyden).
- Jack, K.H. (1977)b. Final Technical Report, European Research Office, United States Army, Grant No. DAERO-76-9-067.
- Jack, K.H. (1979). Materials Science Monographs, 6, "Energy and Ceramics" (ed. Vincenzini, P.) p. 534. Elsevier Pub. Co. (Amsterdam, Oxford, New York).
- Kelen, T. & Mulfinger, H.O. (1968). Glasstechn. Ber. 41, 230.
- Krivanek, O.L., Shaw, T.M. & Thomas, G. (1979). J. Am. Ceram. Soc., 62, 585.
- Lang, J., Verdier, P. & Marchand, R. (1979). Journées d'Etude sur les Nitrures, Jens 4. University of Limoges, France.
- Leedecke, C.J. & Loehman, R.E. (1980). J. Am. Ceram. Soc. 63, 190.
- Lewis, M.H., Powell, B.D., Drew, P., Lumby, R.J., North, B. & Taylor, A.J. (1977). J. Mat. Sci. 12, 61.
- Lewis, M.H., Bhatti, A.R., Lumby, R.J. & North, B. (1980)a. J. Mat. Sci. 15, 103.
- Lewis, M.H., Bhatti, A.R., Lumby, R.J. & North, B. (1980)b. J. Mat. Sci. 15, 438.
- Loehman, R.E. (1978). J. Am. Ceram. Soc. 62, 491.
- Loehman, R.E. (1979). Prog. Report 1, for Metallurgy & Mat. Sci. Div. U.S. Army Research Office.
- Lumby, R.J., North, B. & Taylor, A.J. (1975) "Special Ceramics 6", 283 (ed. Popper, P.) Brit. Ceram. Res. Assn. (Stoke-on-Trent).
- Makishima, A., Yoshiaki, T. & Sakaino, T. (1978). J. Am. Ceram. Soc. 61, 247.
- McMillan, P.W. (1964). "Glass-Ceramics". Academic Press (London & New York).

- Mozzi, R.L. & Warren, B.E. (1969). J. Appl. Cryst. 2, 164.
- Mulfinger, H.O. & Meyer, H. (1963). Glastech. Ber. 36, 481.
- Mulfinger, H.O. & Franz, H. (1965). Glastech. Ber. 38, 235.
- Mulfinger, H.O. (1966). J. Am. Ceram. Soc. 49, 462.
- Nuttall, K. & Thompson, D.P. (1974). J. Mat. Sci. 9, 850.
- Oyama, Y. & Kamigaito, O. (1971). Japan J. Appl. Phys. 10, 1637.
- Perera, D.S. (1976). Ph.D. Thesis, University of Newcastle upon Tyne.
- Powell, B.D. & Drew, P. (1974). J. Mat. Sci. 9, 261.
- Rae, A.W.J.M., Thompson, D.P., Pipkin, N.J. & Jack, K.H. (1975). "Special Ceramics 6" (ed. Popper, P.) p. 347, The Brit. Ceram. Res. Assn., Stoke-on-Trent.
- Rae, A.W.J.M. (1976). Ph.D. Thesis, University of Newcastle upon Tyne.
- Rae, A.W.J.M. & Jack, K.H. (1976). Technical Report submitted to J. Lucas Ltd.
- Rae, A.W.J.M. (1977). Internal Report, Crystallography laboratory, University of Newcastle upon Tyne.
- Rae, A.W.J.M., Thompson, D.P. & Jack, K.H. (1977). "Ceramics for High-performance Applications II" 1039 (ed. Burke, J.J., Lence, E.N. & Katz, R.N.) Proc. 5th Army Mat. Tech. Comp., Brook Hill Pub. Co. (Chestnut Hill, Mass.).
- Revesz, A.G. (1970). J. Non-Cryst. Sol. 4, 347.
- Roebuck, P.H.A. (1978). Ph.D. Thesis, University of Newcastle upon Tyne.

- Roebuck, P.H.A. & Thompson, D.P. (1977). "High Temperature Chemistry of Inorganic and Ceramic Materials", 222, (ed. Glasser, F.P. & Popper, P.) The Chemical Society (London).
- Schneider, G., Gauckler, L.J. & Petzow, G. (1980). J. Am. Ceram. Soc. 63, 32.
- Schreyer, W. & Schairer, J.F. (1961). Zeits. Krist. 116, 60.
- Spacie, C.J. (1980). Internal Report, Department of Metallurgy and Engineering Materials, University of Newcastle upon Tyne.
- Swarts, E.L. (1968). Proceedings of the 8th International Congress on Glass (London) p. 472.
- Terwilliger, G.R. & Lange, F.F. (1974). J. Am. Ceram. Soc. 57, 25.
- Thompson, D.P. (1977). "Nitrogen Ceramics" 129 (ed. Riley, F.L.) Proc. NATO Adv. Study Inst. E23, Noordhoff (Leyden).
- Warren, B.E. & Bischof, J. (1938). J. Am. Ceram. Soc. 21, 259.
- Wild, S., Grieveson, P. & Jack, K.H. (1968). "The crystal chemistry of phases in the Si-N-O and related systems". Prog. Report No. 1, M.O.D. Contract No. N/CP.61/9411/67/4B/MP387.
- Wild, S., Grieveson, P., Jack, K.H. & Latimer, M.J. (1972)a. Special Ceramics 5, 377 (ed. Popper, P.) Brit. Ceram. Res. Assn. (Stoke-on-Trent).
- Wild, S., Grieveson, P. & Jack, K.H. (1972)b. Special Ceramics 5, 385 (ed. Popper, P.) Brit. Ceram. Res. Assn. (Stoke-on-Trent).
- Wild, S. (1980). Private Communication.
- Yamamoto, A. (1965). Analyst (Japan) 14, 692.

Zachariasen, W.H. (1932). Amer. Chem. Soc.
54, 3841.

Zernicke, J. (1955). "Chemical Phase Theory"
Kluwer, Deventer, Netherlands.